Nucleon-nucleon scattering in covariant chiral effective field theory

Yang Xiao

université PARIS-SACLAY

Beihang University

Nucleon-nucleon scattering in covariant chiral effective field theory

Diffusion nucléon-nucléon dans la théorie des champs effective chirale covariante

Thèse de doctorat de l'université Paris-Saclay et de l'université Beihang

École doctorale n°576 Particules, hadrons, énergie et noyau : instrumentation, imagerie, cosmos et simulation (PHENIICS)
Spécialité de doctorat : Structure et réactions nucléaires
Graduate School : Physique. Référent : Faculté des sciences d'Orsay

Thèse préparée dans l'unité de recherche **IJCLab** (Université Paris-Saclay, CNRS), sous la direction d'**Ubirajara VAN KOLCK**, Professeur, et la co-direction de **Lisheng GENG**, Professeur

Thèse soutenue à Pékin, le 3 juin 2022, par

Yang XIAO

Composition du jury

Jie MENG Professeur, Peking University	Président
Norbert KAISER Professeur, Technical University of Munich	Rapporteur
Bingwei LONG Professeur, Sichuan University	Rapporteur & Examinateur
Shangui ZHOU Chercheur, University of Chinese Academy of Sciences	Examinateur
Shilin ZHU Professeur, Peking University	Examinateur
Yujie ZHANG Professeur, Beihang University	Examinateur
Ubirajara VAN KOLCK Professeur, Université Paris-Saclay	Directeur de thèse

THESE DE DOCTORAT

NNT : 2022UPASP051

université PARIS-SACLAY

ÉCOLE DOCTORALE
Particules, hadrons, énergie et noyau : instrumentation, imagerie, cosmos et simulation (PHENIICS)

Titre : Diffusion nucléon-nucléon dans la théorie des champs effective chirale covariante

Mots clés : interaction nucléaire, théorie des champs chirale covariante, théorie des perturbations chirale, théorie des champs de baryon lourd, résonance de Roper

Résumé : L'étude de la structure et des réactions nucléaires sur la base d'interactions nucléaires microscopiques est un sujet central de la physique nucléaire depuis ses débuts. Cependant, des problèmes délicats ancrés dans les interactions nucléaires microscopiques conventionnelles – par exemple, l de diffusion neutron-deutéron A_y qui n'a pas été décrit de manière cohérente même avec l'inclusion des forces à trois nucléons — exigent des études supplémentaires de l'interaction nucléaire dans une approche modèle-indépendant. Ces dernières années, de nombreuses études concernant la structure, les réactions et l'astrophysique nucléaires dans un cadre covariant — telles que la théorie de la fonctionnelle de la densité covariante, la méthode de Dirac-Bruckner-Hartree-Fock et la phénoménologie de Dirac — ont connu un grand succès, soulignant l'importance de l'invariance de Lorentz dans les systèmes nucléaires. Cependant, en raison de l'absence de forces nucléaires chirales covariantes de haute précision, le potentiel CD-Bonn est largement utilisé dans les méthodes relativistes actuels du traitement du problème à N-corps, ce qui peut être considéré comme un compromis satisfaisant.

Cela motive l'étude de l'interaction nucléaire dans le cadre de la théorie des champs effectifs chiraux covariants afin de fournir des informations supplémentaires sur les schémas mentionnés précédemment et d'explorer si l'interaction nucléaire chirale covariante peut surmonter des problèmes de longue date. En outre, la plupart des interactions nucléaires chirales actuelles ne prennent en compte que l'état fondamental des nucléons, les contributions des états excités baryoniques étant reléguées aux constantes de basse énergie (LEC) d'ordre supérieur. Il a été prouvé que l'inclusion explicite du $\Delta(1232)$ améliore la convergence de l'interaction nucléaire chirale. Cependant, par rapport aux études exhaustives de l'interaction nucléaire chirale Δ, le rôle de la résonance de Roper ($N(1440)$) est encore inconnu. Puisque la masse de Roper n'est que d'environ 200 MeV plus importante que celle de $\Delta(1232)$, sa contribution à l'interaction nucléaire doit également être étudiée.

Dans cette thèse, nous dérivons les paramètres d'entrées critiques pour la construction des interactions nucléaires chirales covariantes de haute précision et quantifions les contributions de la résonance de Roper à la force nucléaire chirale :

On adopte ici une version covariante de l'analyse dimensionnelle naïve et construisons un lagrangien de contact à deux nucléons contraint par les symétries de Lorentz, la parité, la conjugaison de charges et la conjugaison hermitienne.

À l'aide de la théorie des perturbations chirale baryonique covariante, nous calculons les contributions d'échange à deux pions (TPE) au premier ordre et à l'ordre suivant à l'interaction nucléon-nucléon (NN) jusqu'à l'ordre $\mathcal{O}(q^3)$. Les corrections relativistes jouent un rôle important dans les ondes F, en particulier l'onde partielle ${}^3F_2$.

Nous dérivons les composantes à longue portée du potentiel TPE NN avec une résonance intermédiaire de Roper. Nous montrons que la contribution de Roper est importante pour les ondes D et améliore légèrement la description des déphasages pour toutes les ondes partielles.

Le travail présenté dans cette thèse représente un élément essentiel pour la construction d'interactions nucléaires chirales covariantes de haute précision, ainsi que d'interaction nucléaire chirale avec des résonances baryoniques explicites.

université PARIS-SACLAY

ÉCOLE DOCTORALE
Particules, hadrons, énergie et noyau : instrumentation, imagerie, cosmos et simulation (PHENIICS)

Title : Nucleon-nucleon scattering in covariant chiral effective field theory
Keywords : nuclear force, covariant chiral effective field theory, chiral perturbation theory, heavy baryon effective field theory, Roper resonance

Abstract : Studying nuclear structure and nuclear reactions based on the microscopic nuclear forces has been a central topic in nuclear physics since its inception. However, tricky puzzles rooted in conventional microscopic nuclear forces — for example, the neutron-deuteron scattering analyzing power A_y which has not been described consistently even with the inclusion of three-nucleon forces — demand further studies of the nuclear force in a model-independent approach. In recent years, countless studies of nuclear structure, reactions, and astrophysics in a covariant framework — such as covariant density functional theory, the Dirac-Bruckner-Hartree-Fock method, and Dirac phenomenology — have achieved great success, highlighting the importance of Lorentz invariance in nuclear systems. However, due to lack of high-precision covariant chiral nuclear forces, the CD-Bonn potential is widely used in present nuclear relativistic many-body methods, which can be regarded as a compromise. This motivates the study of the nuclear force in covariant chiral effective field theory to provide further insights to the aforementioned schemes, and to explore whether the covariant chiral nuclear force can overcome longstanding problems. In addition, most of the present chiral nuclear forces contain only the ground-state nucleon, with the contributions from baryon excited states relegated to higher-order low-energy constants (LECs). The explicit inclusion of the $\Delta(1232)$ has been proven to improve the convergence of the chiral nuclear force. However, compared with the comprehensive studies of the Δ-full chiral nuclear force, the role of Roper resonance ($N(1440)$) is still unknown. Since the Roper mass is only about 200 MeV larger than the $\Delta(1232)$'s, its contribution to the nuclear force also needs to be studied.

In this thesis, we derive the critical input to the construction of high-precision covariant chiral nuclear forces and quantify the contributions to the chiral nuclear force from the Roper resonance :

We adopt a covariant version of naive dimensional analysis and construct the two-nucleon contact Lagrangian constrained by Lorentz, parity, charge conjugation, and hermitian conjugation symmetries.

Employing the covariant baryon chiral perturbation theory, we calculate the leading- and next-to-leading-order two-pion exchange (TPE) contributions to nucleon-nucleon (NN) interaction up to order $\mathcal{O}(q^3)$. The relativistic corrections play an important role in F waves, especially the ${}^3F_2$ partial wave.

We derive the long-range components of the NN TPE potential with an intermediate Roper resonance. Leading-order interactions in heavy baryon chiral perturbation theory are considered. We show that the Roper contribution is sizeable for D waves and improves slightly the description of phase shifts for all the partial waves.

The work presented in this thesis is an essential building block for the construction of high-precision covariant chiral nuclear forces, as well as the chiral nuclear force with explicit baryon resonances.

Acknowledgements

My great-grandparents were buried deep in the hill. When I was a child, every time worshiping ancestors, my mother always burned joss paper while murmuring, "May you bless your great-grandson be admitted to a good university".

Where thoughts arise from My interest in physics started in the middle school textbook, in which the editors introduced the history of modern physics briefly in the *To My Classmates*. I was inspired by those wise minds immediately and was interested in physics. More than ten years have passed since then, and with the completion of my doctoral thesis, I am entering a new phase of my academic career. Through everything, physics was and still is my favorite subject. Preparing the thesis itself is not technically challenging, just a summary of the works done during the doctoral period, but those memories of student days are worth remembering anyway.

About family My hometown Lingling locates in the southwest of Hunan province. Hunan people are attached to education which is also well evidenced in my family. Like all other parents, my parents expected me to have a bright future, so they were strict with me in my studies, especially my mother, who was a meticulous person. When I was in high school, there was a time when I was addicted to video games, and every night after my parents fell asleep, I gently took my father's laptop from the study and went to my room to play video games until 2-3 a.m., and then put it back. Not a bad plan, right ? However, my mother noticed the trick from my tired demeanor when I woke up every morning, and I was caught in a few days. Instead of rebuking me, my mother reasoned with me kindly and patiently. This was engraved in my memory, and I have entirely dropped the lousy habit. In contrast to being strict with me at home, my parents never hesitated to praise me in front of my relatives and friends. Their education and care are responsible for my progress step by step. Of course, my grandparents, aunts and uncles, and other relatives have also been very caring to me. First, I would like to thank them sincerely for their dedication and commitment.

About Beihang Studying at university is very different from primary and middle schools in China. In primary and middle schools, the study is usually teacher-led, while in universities, students have to rely mainly on self-study. Since there is no pressure on the promotion rate, university teachers typically do not care about students' grades as much as primary and middle school teachers. Prof. Lisheng Geng is not a typical university teacher. I first met Prof. Lisheng Geng in atomic physics class. Unlike other teachers who teach in a "laissez-faire" style, Prof. Lisheng Geng emphases interacting with students and often calls us to answer questions in class. Once again, after I failed to recite the exact values of *magic numbers*, Prof. Lisheng Geng instructed me about the necessity of studying hard seriously. From then on, I realized that he was earnest about everything, so I also devoted myself to learning. In many cases, it is not the enthusiasm that drives persistence, but persistence begets enthusiasm. Such an attitude has deeply influenced me until now. I would like to express my gratitude to my supervisor Prof. Lisheng Geng.

I would also like to thank all my current and former teachers and colleagues at the Beihang nuclear theory group, particularly Prof. Huaxing Chen, Prof. Manuel Pavon Valderrama, Dr. Xiulei Ren, Dr. Kaiwen Li, Dr. Dan Zhou, Dr. Erliang Cui, Dr, Rong An, Dr. Ying Huang, Dr. Maojun Yan, Dr. Xiaopeng Zhou, Dr. Junxu Lu, Dr. Ruixiang Shi, Dr. Tianwei Wu, Jing Song, Dr. Mingzhu Liu, Chunxuan Wang, Xizhe Ling, Qianqian Bai, Qianqian Wang, Xiaoxu Dong, Yujing Tian, Guofan Sheng, Taiwan Zhen, Fanzheng Peng, Zhiwei Liu, Qinlong Yao, Weiguang Li, Xueying Yang, Haonan Feng, Yawen Pan, Shuangyi Li, Jiaming Xie, Ziying Yang, Tianchen Wu, Xinyu Hu, Ruyou Zhen, Yuying Ying for the enjoyable work atmosphere and the help and guidance in the past years. I would like to wish you all the best of luck.

About Paris-Saclay Although I spent more time in my apartment than in the lab due to the pandemic, living in France was still a fantastic experience. I would like to express my gratitude to my co-supervisor Ubirajara van Kolck for his guidance, for many enlightening discussions in physics and many constructive comments and suggestions in thesis writing. I would like to thank Prof. Bachir Moussallam and Prof. Michael Urban for their help in all aspects of my life in France.

Last, special thanks to Prof. Norbert Kaiser, Prof. Bingwei Long, Prof. Jie Meng, Prof. Jiangming Yao, Prof. Lihua Zhu, Prof. Shangui Zhou, Prof. Shilin Zhu, and Prof. Yujie Zhang [1] for reviewing my thesis and attending my thesis defense.

1. List in no particular order.

Table des matières

1 - Introduction

The nuclear force is the most essential ingredient of nuclear physics, and a microscopic understanding of it has long been the central topic in nuclear physics. In 1932, the discovery of the neutron by Chadwick [1] opened the doors for the studies of the nuclear force. Since then, understanding the nature of the interactions between nucleons has always been one of the most important problems in nuclear physics. The first attempt was made by Yukawa [2]. In 1935, Yukawa proposed that the interactions between nucleons can be mediated by particles whose mass is about 200 times that of an electron called mesons [1], and his theory is the famous meson-exchange theory. Although Yuakwa's theory has been proved not enough for the description of the nuclear force, the main idea of the meson-exchange theory, that the nuclear force is mediated by mesons, is still instructive today. In the following years, it was suggested by some physicists that other mesons should also be considered [3, 4]. However, because of the complicated operators' structures therein, such theories are not widely used. As a matter of fact, at that time, most physicists believed that the nature of the nuclear force would eventually be expressed in a simple form like the Coulomb force and gravity. But this idea was proved to be wrong by experiments. The nuclear force then was found to be almost impossible to be described by a simple theory [5].

The main problem with Yukawa's theory is that much heavier mesons should be included in order to describe the behaviour of the nuclear force at its core part ($r \lesssim 1$ fm). Based on Yuwaka's pioneering work, Taketani, Nakamura and Sasaki proposed a new theory of the nuclear force [6]. The main idea is to divide the nuclear force into three parts based on the force range. The one-pion exchange (OPE) accounts for the long-range part ($r \gtrsim 3$ fm) of the nuclear force, the two-pion exchange is responsible for the medium-range part ($1 \lesssim r \lesssim 3$ fm) of the nuclear force, while the multi-pion exchange contributes to the short-range part ($r \lesssim 1$ fm) of the nuclear force. This concept is instructive since it is the first time that the nuclear force is realized to consist of different behaviours at different force ranges. However, the difficulties in deriving the multi-pion exchange potential constrain its further application.

Another way to construct the nuclear force emerged in 1950$\sim$60s : phenomenologically, based on the abundant nucleon-nucleon (NN) scattering data. The general form of the short-range part of such forces is usually obtained by various invariance analyses. For example, the Paris potential is expressed in terms of the usual nonrelativistic invariants with five components (central, spin-spin, tensor, spin-orbit, and quadratic spin-orbit) for each isospin state [7]. At the same time,

1. As a matter of fact, the particles in Yukawa's theory turn out to be pseudoscalar pions.

the long-range part is obtained by considering dispersion theory. By the 1970s, the widely used phenomenological nuclear forces included the Hamada Johnston potential [8], the Reid potential [9], and the Paris potential [7]. These phenomenological nuclear forces are in overall agreement with nucleon-nucleon scattering data. However, their forms are somewhat arbitrary and they contain many adjustable parameters.

In the 1970s, the meson-exchange theory experienced a breakthrough due to the discovery of heavy mesons. The corresponding theory is known as the one-boson-exchange (OBE) model [10, 11, 12]. According to the OBE model, the long-range part of the nuclear force is still dominated by one-pion exchange, the medium-range part of the nuclear force can be derived by the exchange of mesons with masses of $500 \sim 550$ MeV [2], while the short-range part of the nuclear force can be obtained by the exchange of heavier mesons, whose masses are around $720 \sim 1000$ MeV. Utilizing the OBE model, a strong repulsive interaction is obtained in the core part of the nuclear force, accounting for the appearance of a repulsive core. Since the OBE potential contains some coupling constants, which are fixed by the experimental data, the theory is still semi-phenomenological.

Apart from these models, in the 1980s, Oka, Faessler and Shimizu [13, 14, 15] proposed to study the nuclear force in quark models. It is the first time that the repulsive core of the nuclear force can be well explained by the effective one-gluon exchange. Although these early quark models do well in the explanation of the short-range part of the nuclear force, the attractive nature of the medium- and long-range part of the nuclear force cannot be described at quark level. Meson exchange must be included in such theories to generate these parts of the nuclear force, and such mixed theories are known as quark-meson mixed models. After years of improvements, the well-known quark models include the coupled-channel chiral quark model [16], constituent quark model [17, 18], chiral quark model [19, 20], quark delocalization color screening model [21, 22, 23, 24, 25], and SU(6) quark model [26, 27, 28, 29].

A high-precision nuclear force is needed in order to obtain the accurate nuclear structure and reaction calculations. Motivated by this, various high-precision phenomenological nuclear forces [30, 31, 32, 33] were proposed by the late 1990s. These forces can be classified into two categories : those based on invariance under parity, charge conjugation, time reversal, and hermitian conjugation, such as the Reid93 potential [34] and the AV18 potential [31], and those based on the OBE model, such as the Nijmegen potential [30] and the CD-Bonn potential [33]. The nucleon-nucleon scattering data and the properties of the deuteron can be well explained by these high-precision models. For example, the CD-Bonn potential could describe about 6000 pp and np scattering data below 300 MeV with χ^2/datum ≈ 1, much more precise than any other nuclear force and partial-wave analysis

2. η and σ mesons exchange are responsible for the medium-range part of nuclear force according to Refs. [11, 12].

till then. The cost of such high precision is around 30-50 adjustable parameters introduced in these theories. Still, these high-precision nuclear forces indeed serve as high quality inputs to nuclear structure and reaction calculations.

The wide applications of the aforementioned high-precision phenomenological nuclear forces do not satisfy physicists since they are all phenomenological. The ideal nuclear force should be not only of high precision but also model independent. Since the 1970s, Quantum Chromodynamics (QCD) has been known to be the fundamental theory of strong interactions, describing the interactions among quarks by gluon exchange. Moreover, the nuclear force is realized to be a residual strong interaction. However, a direct study of the nuclear force based on QCD is impossible because of the non-perturbative nature of QCD in the low-energy regime. Two possible ways to derive the nuclear force in QCD are : 1) perform Lattice QCD simulations in super computers and 2) develop low-energy effective theories of QCD. The former has made considerable progress recently [35, 36, 37, 38, 39, 40, 41, 42, 43, 44, 45, 46, 47], but the calculations are performed in the unphysical region due to the massive computational resources needed, and results are contradictory. In recent years, considerable efforts have been made to establish the relation between the nuclear force and QCD within the framework of effective field theory (EFT). The work in this direction has made remarkable achievements and high-precision nuclear forces were constructed from heavy baryon chiral perturbation theory (HBChPT) more recently [48, 49, 50, 51].

In 1979, Weinberg suggested that a model independent and systematic expansion for the S-matrix can be obtained by the consideration of QCD's approximate SU(2)$_L\times$ SU(2)$_R$ chiral symmetry [52]. Chiral symmetry is spontaneously broken and leads to the existence of light pseudoscalar bosons, which are identified as pions. This theory was first applied in the $\pi\pi$ sector [53, 54]. When extended to the one-baryon sector, it encounters the so-called power counting breaking problem (PCB) because of the large non-zero nucleon mass in the chiral limit [55]. This problem can be solved within the framework of HBChPT [56] by making the extreme non-relativistic limit assumption, that the momentum transfer between nucleons is much smaller than the nucleon mass, which implies an expansion in powers of a small momentum over the nucleon mass. Different from $\pi\pi$ and πN systems, a two-nucleon bound state (deuteron) exists, showcasing the non-perturbative nature of the NN interaction. In order to accommodate it, in the 1990s, Weinberg suggested calculating the NN potential perturbatively in the chiral expansion and then iterating it to all orders in a Schrödinger or Lippmann-Schwinger equation to obtain the amplitude [57, 58].

The first application of Weinberg's scheme in the NN sector by Ordóñez, Ray, and van Kolck [59, 60] yielded a reasonable description of NN data at $\mathcal{O}((Q/\Lambda_\chi)^3)$ [3] with explicit Deltas and a Gaussian regulator, where there are seven independent short-range interactions. The benefits of such a local regulator include

3. In this thesis, $\Lambda_\chi \sim 4\pi f_\pi \approx 1$ GeV.

the conservation of analytical structure of the T-matrix close to the pion threshold and the fact that no spectral function regularization is needed, while a drawback is that it leads to a mixing of different partial-wave channels due to the dependence of $\vec{q}$ over the scattering angle. The peripheral NN phase shifts in Δ-less and Δ-full chiral perturbation theory were obtained by Brockmann, Gerstendorfer, Kaiser and Weise [61, 62]. The Δ-less chiral nuclear force was rederived by Epelbaum, Glöckle, and Meißner [63]. The so-called high precision chiral nuclear force with a nonlocal, super-Gaussian exponential regulator was constructed at $\mathcal{O}((Q/\Lambda_\chi)^4)$ by Entem and Machleidt [64]. The description of the NN data by this chiral nuclear force is comparable to that of high-precision phenomenological potentials, but with fewer parameters. A series of high-quality chiral nuclear forces have been derived since then [64, 65, 66, 67, 48, 68, 49, 50, 51]. State-of-the-art chiral nuclear forces have been constructed at $\mathcal{O}((Q/\Lambda_\chi)^5)$ [48, 49, 50] and $\mathcal{O}((Q/\Lambda_\chi)^6)$ [51].

However, some problems are rooted in the nuclear forces obtained in Weinberg's power counting. For example, a consistent description of the neutron-deuteron scattering analysis power A_y has not been achieved even when the chiral three-nucleon force is considered [69] [4]. Possible solutions are either including subleading $3N$ contact terms, which implies a slower convergence of χEFT than expected, or realizing that proper renormalization of the theory requires a new power counting [71, 72, 73, 74]. Besides, the non-relativistic nature of the forces also constrains their applications in many-body studies in relativistic frameworks. Motivated by the need for a better chiral nuclear force with faster convergence and nuclear structure and reaction calculations in a relativistic framework, a relativistic chiral nuclear force [5] was proposed in 2018 [75]. It exhibits a faster convergence compared to the conventional chiral nuclear force. Special relativity is one of the two pillars of modern physics. In molecular/atomic, nuclear, and on- baryon systems, a relativistic framework shows unique advantages and can accurately explain the relevant experimental phenomena . It is obvious that the scale of the two-nucleon system is between the scale of nuclear system and the scale of one-baryon system. Therefore, one would naturally expect that relativity effects are also sizeable in the NN interaction. Motivated by this, a relativistic chiral nuclear force was constructed at leading order in Ref. . Such an approach keeps the complete form of the nucleon field. Moreover, the effective potential V, obtained by calculating the relevant Feynman diagrams, is inserted into the Kadyshevsky equation instead of the Lippmann-Schwinger equation. Therefore, more relativistic effects are maintained in this approach compared to the HB formalism from the beginning [6]. As a result,

4. Notice in Ref. [69], the truncation error is roughly estimated by a variation of cut-off from 500 MeV to 600 MeV, a modern error estimate method [70] may yield more convincing results.

5. The "relativistic" here refers to the nucleon field being defined by Dirac spinors instead of Pauli spinors.

6. One should notice that the two approaches are equivalent if the calculations are performed up to sufficient high order.

one can observe in Fig. 3 and Fig. 4 of Ref. [75] that the leading-order relativistic chiral nuclear force is comparable to the next-to-leading-order non-relativistic chiral nuclear force for the description of the S- and P-waves NN scattering phase shifts with only five parameters, implying a faster convergence inside the theory.

Nevertheless, the leading-order relativistic chiral nuclear force is still far from enough for nuclear structure and reaction calculations. The discrepancies between the leading-order relativistic chiral nuclear force and the NN scattering phase-shift analysis [34] imply the necessity of higher-order calculations. As shown in Fig. 1.1, in order to perform beyond-leading-order calculations, the relevant high-order contact vertices and two-pion exchange contributions are needed.

The aforementioned chiral nuclear forces mainly contain only the ground-state nucleon, with the contributions from baryon excited states relegated to higher-order LECs. Although already of high precision, these chiral nuclear forces still encounter some problems, e.g., convergence with respect to the components of the TPE potential. It has long been realized [61] that the formally subleading component of TPE is comparable to or even larger than the presumably leading TPE, which challenges the power counting underlying χEFT. The convergence issues of chiral nuclear forces can be ameliorated by the explicit inclusion of baryon resonances. If the effects of a resonance are relegated to LECs, non-analytic contributions are lost which limits the expansion range of the theory. Including a low-lying resonance explicitly as a low-energy degree of freedom not only extends the validity of the EFT but also reorganizes the multipion-exchange contributions and improves the order-by-order convergence. The lowest nucleon excitation is the Delta isobar, $\Delta(1232)$, whose mass m_Δ is only $\delta \equiv m_\Delta - m_N \simeq 300$ MeV higher than the nucleon's. Its contribution to NN [59, 60, 62, 76, 77, 78, 79, 80, 81] and three-nucleon [82, 83, 84, 85, 86] chiral forces has attracted increasing attention. However, the role of the second nucleon excitation, the Roper resonance $N(1440)$ which has been proved necessary for the description of πN scattering in the P_{11} channel, is so far still unknown in the nucleon-nucleon interaction. Since the NN system can be regarded as an extension of the πN system, and the $N(1440)$'s mass m_R is $\rho \equiv m_R - m_\Delta \simeq 500$ MeV higher than the nucleon's, it is interesting to study the contributions from the Roper resonance to the nuclear force.

In this thesis, we follow closely the aforementioned discussion, study the necessary input to the construction of a high-precision relativistic nuclear force, and investigate the role of Roper resonance in the nucleon-nucleon interaction in chiral effective field theory (ChEFT [7]). Specifically, we construct the relativistic nucleon-nucleon contact Lagrangian up to order $\mathcal{O}(q^4)$ ($q \sim Q/\Lambda_\chi$ is a small expansion parameter) based on a covariant version of naive dimensional analysis. A self-consistent check is made by performing the non-relativistic reduction of the relativistic Lagrangian. In addition to this, we also calculate the two-pion exchange contributions to the nucleon-nucleon interaction in the relativistic ChPT and com-

7. In this thesis, "ChEFT" and "χEFT" are used interchangeably.

pare our results with those obtained in the HBChPT. Overall better descriptions of the NN scattering spherical partial waves are found in our method. The two works provide crucial input to construct a high-precision nuclear force in relativistic ChPT. At last, we also for the first time quantify the contributions to the nucleon-nucleon interaction from the Roper resonance $N(1440)$.

The thesis is organized as follows. In Chapter 2, we give a concise introduction of chiral perturbation theory. Starting from the principle of effective field theory, we introduce chiral symmetry and its breaking. The concept of power counting rules is introduced later. Aiming at constructing a high-precision chiral nuclear force, a relativistic power counting is proposed and the detailed steps to construct the corresponding chiral Lagrangians are laid out in Chapter 3. In Chapter 4, we quantify the relativistic effects in the TPE of the nucleon-nucleon interaction. Note that the works presented in Chapter 3 and Chapter 4 are necessary ingredients to construct a high-precision chiral nuclear force. The role of the Roper resonance $N(1440)$ in the nucleon-nucleon interaction is discussed in Chapter 5, followed by a summary and outlook in Chapter 6. Non-relativistic NN contact Lagrangian up to order $\mathcal{O}(q^4)$ is shown in Appendix A.

The thesis is based on Refs. [87, 88, 89] . In addition, these and similar ideas have been exploited in other papers [90, 91, 92, 93, 94, 95, 96].

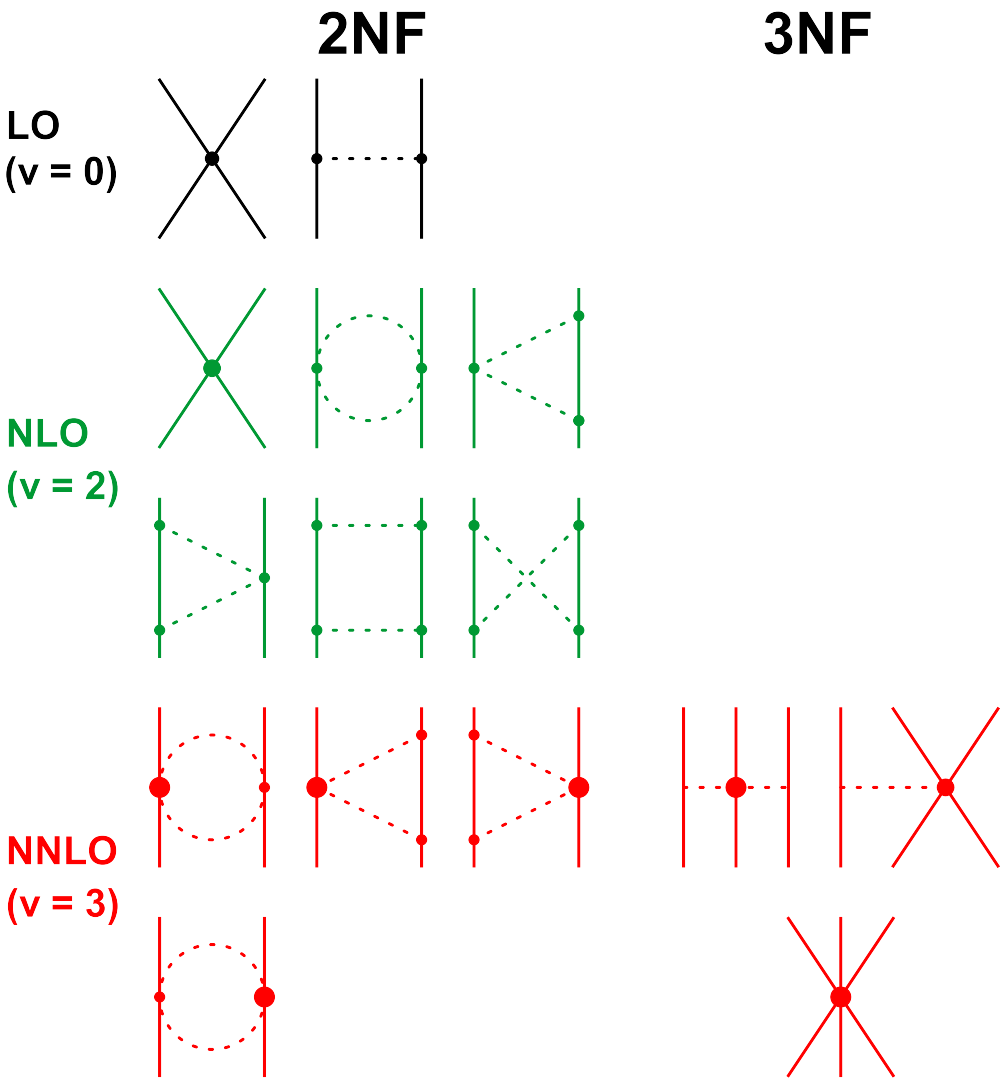

Figure 1.1 – The hierarchy of chiral nuclear potentials with Weinberg's power counting scheme. The solid lines refer to the nucleons, the dashed lines denote the pions, while the small, medium and heavy dots represent vertices of order $\Delta_i = 0, 1, 2$ respectively.

2 - Chiral effective field theory

As the framework unifying the three fundamental interactions except for gravity, the standard model (SM) of particle physics has been proved to be extremely successful in explaining physical phenomena governed by the electromagnetic, weak, and strong interactions, while accommodating all known elementary particles. In a nucleus, the interactions between nucleons are expected to be the residual effects of the more fundamental strong interaction, thus they should be well described in the framework of the standard model by QCD. However, because of two characteristics of QCD, namely color confinement and asymptotic freedom, in nuclear physics, the basic degrees of freedom are nucleons and pions instead of quarks. Moreover, the coupling constant is much larger than 1 in the low-energy regime, hence it cannot be regarded as a small expansion parameter. Therefore, the perturbative method is invalid, implying the necessity of developing a more efficient approach for describing the interactions between nucleons. As already discussed in Chapter 1, state-of-the-art nuclear forces are already of high precision both phenomenologically and microscopically, and one of the most widely used microscopic nuclear forces is based on chiral effective field theory.

In this chapter, we start with the principle of effective field theory. The basic degrees of freedom involved in the study of the nuclear force are introduced next. Then, the symmetries of ChEFT, especially chiral symmetry and its breaking, are emphasized. At last, we briefly introduce the systematic method to identify the relative importance of terms in ChEFT. In principle, renormalization-group (RG) invariance, which indicates observables should not depend on the value of cut-off (Λ), should also be stressed in an EFT. But since it is not the focus point of our work, we do not discuss about it in detail in this thesis.

2.1 . Effective field theory

A systematic low-energy approximation to an underlying theory is referred to as effective field theory. The word "effective" implies that only the physics of interest is maintained. In contrast, the details of the higher-energy physics are ignored, reflecting the philosophy "low-energy physics is independent of the details of the high-energy physics". This idea is very important, and in a sense, it is the reason why physics itself can be understood in the approximate theory. For example, we can obtain the energy levels of hydrogen in quantum mechanics without knowing any details of the nucleus. Of course, describing physics in the fundamental theory is always reasonable. But in most cases, mathematics is rather complex. Effective field theory is an efficient method to describe physics then. For example, when describing the motion of macroscopic objects, such as projectiles and parts of machinery, it is convenient to utilize Newtonian mechanics instead of special relativity. In this

case, Newtonian mechanics can be regarded as an effective field theory of special relativity (underlying theory).

There are two distinct ways to utilize EFTs [97]. One is the so-called "top-bottom" way [97]. It refers to the case that the underlying theory is known but it is useful to have a simpler theory at low-energies. In order to design such a simpler theory, one needs to "integrate out" high-energy degrees of freedom of the underlying theory and match onto a low-energy theory. The "simpler theory" agrees with the underlying theory in the infrared regime, while differs in the ultraviolet regime. There are several EFTs motivated by this idea, such as the heavy quark effective field theory (HQEFT), non-relativistic quantum electrodynamics (NRQED), non-relativistic QCD (NRQCD) and soft-collinear EFT (SCEFT). If the underlying theory is unknown or the "integration" of the high-energies degrees of freedom is difficult, EFT can be developed in the "bottom-top" way [97]. That is, one starts from the determination of soft scale and hard scale and identifies all degrees of freedom relevant in the physical phenomena of interest. Then, write down the most general Lagrangian that incorporates all the symmetries existing or necessary for the description of physics in this energy regime, e.g., Lorentz symmetry and gauge symmetry. At last, pick out the relatively important terms in the Lagrangian with a systematic rule, namely the power counting rule. As a matter of fact, the standard model and the chiral effective field theory are formulated in this philosophy. In the following sections, we briefly introduce the general steps to construct the second kind of EFT with special attention to chiral effective field theory.

2.2 . Degrees of freedom

The first step is to identify soft and hard scales and the appropriate degrees of freedom. The degrees of freedom involved in the study of the nuclear forces are obviously nucleons and pions. However, the choice of soft and hard scales is a little bit ambiguous. In the pure pionic system, because the pion mass is about 139 MeV and much smaller than the vector meson mass, e.g., ρ meson mass 770 MeV, the physics involves in the vector mesons is relatively insignificant for the physics of the pions. Therefore, the pion mass and its momentum are obviously possible choices for the soft scale Q, while the vector meson mass is the hard scale Λ. The situation becomes a little complex when including the nucleons. Since the nucleon mass is around 939 MeV, which is very close to the chiral symmetry breaking scale $\Lambda_\chi \approx 1$ GeV, if we regard the nucleon mass as the soft scale, it suggests the expansion parameter $O\left(m_n/\Lambda_\chi\right) \approx 1$ and the convergence of the theory is totally ruined. This problem can be solved both non-relativistically in HB EFT [56, 98] and relativistically in infrared (IR) EFT [99] and Extended-on-mass-shell (EOMS) EFT [100, 101] by regarding the nucleon mass as a hard scale. Notice that although the soft and hard scales between the three approaches are the same, the ways to deal with the so-called high-order terms are rather different, which further result in

different descriptions of physical observables. Here we do not focus too much on the difference of the three methods; one can refer to Ref. [102] for more details. To summarize, in the baryon chiral EFT, the soft scales denote the pion mass m_π, the four momentum of pion q^μ and the three momentum of nucleon $\vec{p}$, while the hard scales collect the nucleon mass m_n and the chiral symmetry breaking scale Λ_χ.

2.3 . Chiral symmetry and its breaking

The next step is to construct the most general Lagrangian incorporating all the relevant symmetries of the underlying theory. For a nucleus, the relevant symmetries contain the parity $\mathcal{P}$, charge $\mathcal{C}$, time reversal $\mathcal{T}$, hermitian conjugation $\mathcal{H}$ and chiral symmetries. In this section, we start with the QCD Lagrangian and introduce briefly chiral symmetry and its breaking [1]. Detailed discussions can be found in Ref. [67].

QCD is a non-abelian gauge theory with SU(3) symmetry. At the typical hadronic mass scale ~ 1 GeV, which is of our interest, the EFT contains strong interactions, electromagnetic interactions and even weak interactions. In this work, we focus mainly on the strong interaction in the nucleon-nucleon scattering, while the electromagnetic and weak interactions are neglected for simplicity. The QCD Lagrangian in the SU(3) flavor space then reads,

$$\mathcal{L}_{QCD} = \bar{q}\left(i\gamma^\mu D_\mu - \mathcal{M}\right) q - \frac{1}{4} G^\alpha_{\mu\nu} G^{\mu\nu}_\alpha . \tag{2.1}$$

where $q = (u, d, s)^{\mathrm{T}}$ is the quark field, γ^μ is the Dirac matrix, D_μ refers to the gauge covariant derivative,

$$D_\mu = \partial_\mu - igA^\alpha_\mu T_\alpha, \tag{2.2}$$

with g the coupling constants, A^α_μ denotes the gluon field and $T_\alpha = \lambda_\alpha/2$ with $\alpha = 1...8$ refers to the SU(3) generators. The gauge invariant gluon field strength tensor $G^\alpha_{\mu\nu}$ is defined as,

$$G^\alpha_{\mu\nu} = \partial_\mu A^\alpha_\nu - \partial_\nu A^\alpha_\mu + g f^a_{bc} A^b_\mu A^c_\nu, \tag{2.3}$$

with f^a_{bc} the SU(3) structure constants. Since the focus of this work is to study the interactions between the nucleons, it is natural to consider up and down quarks only. In this case, the quark field reduces to $q = (u, d)^{\mathrm{T}}$, the quark mass matrix $M = diag(m_u, m_d)$, where $m_u = 2.5\pm0.8$ MeV and $m_d = 5\pm0.9$ MeV [103] refers to the up and down quark mass respectively [2]. Moreover, the large gap between the light quark masses and the hadronic mass scale ~ 1 GeV suggests that it is interesting to study QCD by taking the light quark masses to zero, namely the chiral

1. The constraints from other symmetries are discussed in detail in Chapter 3.
2. The u- and d-quark masses are estimates of so-called "current-quark masses," in a mass-independent subtraction scheme such as MS at a scale $\mu \approx 2$ GeV.

limit, at the relatively low-energy regime of our interest. The QCD Lagrangian then reads,

$$\mathcal{L}^0_{QCD} = i\bar{q}\gamma^\mu D_\mu q - \frac{1}{4}G^\alpha_{\mu\nu}G^{\mu\nu}_\alpha. \tag{2.4}$$

If we define the left- and right-handed projection operators as,

$$P_L = \frac{1}{2}(1-\gamma_5), \qquad P_R = \frac{1}{2}(1+\gamma_5), \tag{2.5}$$

with $\gamma_5 = i\,\gamma_0\gamma_1\gamma_2\gamma_3$, and separate the quark field into left- and right-handed components,

$$q_L = P_L\, q, \qquad q_R = P_R\, q, \tag{2.6}$$

the QCD Lagrangian can be rewritten in the chiral limit as,

$$\mathcal{L}^0_{QCD} = i\,\bar{q}_L\gamma^\mu D_\mu q_L + i\,\bar{q}_R\gamma^\mu D_\mu q_R - \frac{1}{4}G^\alpha_{\mu\nu}G^{\mu\nu}_\alpha. \tag{2.7}$$

Defining unitary transformations,

$$L = \exp\left(-i\Theta^L_i\frac{\tau_i}{2}\right), \qquad R = \exp\left(-i\Theta^R_i\frac{\tau_i}{2}\right), \tag{2.8}$$

where τ_i with $i = 1, 2, 3$ denotes the SU(2) generators and is known as Pauli spin matrix. The chiral limit QCD Lagrangian $\mathcal{L}^0_{QCD}$ is invariant under gobal transformations,

$$q_L \mapsto L\, q_L, \qquad q_R \mapsto R\, q_R. \tag{2.9}$$

Thus, the left- and right-handed quark fields can be isolated by introducing such projection operators. The symmetry that originates from such invariance is SU(2)$_L$ $\times$ SU(2)$_R$ symmetry, which is called chiral symmetry. According to Noether's Theorem, there are six conserved currents corresponding to the six SU(2) generators; three left-handed currents,

$$L^\mu_i = \bar{q}_L\gamma^\mu\frac{\tau_i}{2}q_L, \quad \text{with} \quad \partial_\mu L^\mu_i = 0, \tag{2.10}$$

and three right-handed currents,

$$R^\mu_i = \bar{q}_R\gamma^\mu\frac{\tau_i}{2}q_R, \quad \text{with} \quad \partial_\mu R^\mu_i = 0. \tag{2.11}$$

Recombining these conserved currents to the vector and axial-vector currents,

$$V^\mu_i = R^\mu_i + L^\mu_i = \bar{q}\gamma^\mu\frac{\tau_i}{2}q, \quad \text{with} \quad \partial_\mu V^\mu_i = 0, \tag{2.12}$$

$$V^\mu = R^\mu + L^\mu = \bar{q}\gamma^\mu q, \tag{2.13}$$

$$A^\mu_i = R^\mu_i - L^\mu_i = \bar{q}\gamma^\mu\gamma_5\frac{\tau_i}{2}q, \quad \text{with} \quad \partial_\mu A^\mu_i = 0, \tag{2.14}$$

$$A^\mu = R^\mu - L^\mu = \bar{q}\gamma^\mu\gamma_5 q. \tag{2.15}$$

Defining vector transformation,

$$V = \exp\left(-\Theta_i^V \frac{\tau_i}{2}\right), \tag{2.16}$$

the chiral limit QCD Lagrangian $\mathcal{L}^0_{QCD}$ is invariant under vector transformation,

$$q \mapsto V\, q. \tag{2.17}$$

The symmetry implied in such invariance is isospin symmetry. The vector current V_μ originates from rotations of the left- and right-handed quark fields with the same phase and the corresponding conserved charge is the quark number. However, the conservation of the axial-vector current A^μ is broken after quantization of the Dirac fermions (Adler-Bell-Jackiw anomaly) [104, 105]. Therefore, a larger symmetry group $\mathrm{SU}(2)_L \times \mathrm{SU}(2)_R \times \mathrm{U}(1)_V$ can be observed for massless u and d quarks.

So far all the discussions are based on the assumptions that $m_u = m_d = 0$. The situation becomes much different once we take into account the quark mass term,

$$\mathcal{L}_M = -\bar{q}\mathcal{M}q = -(\bar{q}_R\mathcal{M}q_L + \bar{q}_L\mathcal{M}q_R). \tag{2.18}$$

The total Lagrangian $\mathcal{L}_{QCD} = \mathcal{L}^0_{QCD} + \mathcal{L}_M$ is no longer invariant under the left- and right-handed transformations, and the chiral symmetry breaks explicitly. Nevertheless, such explicit symmetry breaking is insignificant because of the large gap between the light quark masses and the hadronic mass. Apart from the explicit chiral symmetry breaking, chiral symmetry also breaks spontaneously, which can be observed by referring to the hadron spectrum. The isospin triplet pions are suggested to exist due to the spontaneous chiral symmetry breaking according to the Goldstone's theorem.

The above discussions are for the QCD Lagrangian. Our goal is to obtain Lagrangians that collect the degrees of freedom necessary for describing nucleon-nucleon interaction. Such mapping can be realized in the standard non-linear realization of chiral symmetry [106, 107] and is introduced in the following.

The isospin triplet pions behave under transformation $\mathrm{SU}(2)_L \times \mathrm{SU}(2)_R$ as a unitary matrix $U(x)$ that fulfills,

$$U \mapsto RUL^\dagger, \quad U^\dagger U = 1, \quad \det U = 1. \tag{2.19}$$

A popular choice for the U is the exponential parametrization $U(x) = \exp\left(i\boldsymbol{\tau}\cdot\boldsymbol{\pi}/f_\pi\right)$, with the pion fields are defined as,

$$\boldsymbol{\pi} = \sum_{i=1}^{3} \tau_i\phi_i(x) = \begin{pmatrix} \phi_3 & \phi_1 - i\phi_2 \\ \phi_1 + i\phi_2 & -\phi_3 \end{pmatrix} \equiv \begin{pmatrix} \pi^0 & \sqrt{2}\pi^+ \\ \sqrt{2}\pi^- & -\pi^0 \end{pmatrix}, \tag{2.20}$$

and f_π is the pion decay constant. For a transformation of the subgroup $\mathrm{SU}(2)_V$ with $L = R = V$, U transforms as,

$$U \mapsto VUV^\dagger. \tag{2.21}$$

The nucleon field ψ is defined as $\psi = (p, n)^T$. But in order to describe its behaviour under the aforementioned transformations, it is convenient to introduce the octet baryons represented in traceless 3×3 matrix $B(x)$ in flavor space,

$$B = \sum_{i=1}^{8} \frac{B_i \lambda_i}{\sqrt{2}} = \begin{pmatrix} \frac{1}{\sqrt{2}}\Sigma^0 + \frac{1}{\sqrt{6}}\Lambda & \Sigma^+ & p \\ \Sigma^- & -\frac{1}{\sqrt{2}}\Sigma^0 + \frac{1}{\sqrt{6}}\Lambda & n \\ \Xi^- & \Xi^0 & -\frac{2}{\sqrt{6}}\Lambda \end{pmatrix}, \tag{2.22}$$

where λ_i with $i = 1, 2, 3, 4, 5, 6, 7, 8$ refers to the SU(3) generators. The non-linear realization of chiral symmetry for the baryons leads to the transformation of $B(x)$ under chiral symmetry group SU(3)$_L\times$ SU(3)$_R$ as,

$$B \mapsto KBK^\dagger, \tag{2.23}$$

with K the SU(3)-valued compensator field,

$$K(L, R, U) = \sqrt{LU^\dagger R^\dagger} R \sqrt{U}. \tag{2.24}$$

The square root of the matrix U, $u = \sqrt{U}$ transforms as,

$$u \mapsto \sqrt{RUL^\dagger} = RuK^\dagger = KuL^\dagger. \tag{2.25}$$

For the transformation of the subgroup SU(3)$_V$,

$$B \mapsto VBV^\dagger. \tag{2.26}$$

Now that we have obtained the degrees of freedom in the chiral Lagrangian, namely the pion and nucleon fields, the explicit form of the chiral Lagrangians incorporating all the relevant symmetries of QCD can be deduced then. Since part of this thesis is about the construction of the relativistic chiral NN contact Lagrangians, we do not give an introduction about it in this chapter to avoid unnecessary duplication of content. One can refer to Chapter 3 and Chapter 4 for detailed discussions on the NN and πN Lagrangians [3] .

2.4 . Power counting rule

Once the Lagrangians are constructed, one can in principle use them to calculate the Feynman diagrams and obtain the consequent physical observables. However, EFT Lagrangians contain an infinite number of terms allowed by the symmetries. Hence it is important to have a method to identify the relatively most important terms in the effective Lagrangians, namely the power counting rule. In this section, we introduce Weinberg's power counting rule. The effective Lagrangian takes the general form,

$$\mathcal{L} = \sum_i c_i \left(Q, \Lambda\right) O_i(\{\psi\}), \tag{2.27}$$

3. The chiral Lagrangians for $\pi\pi$ system are not given in this thesis because they are not involved in our study.

where Q is the soft scale, Λ is the hard scale, $c_i\,(Q,\Lambda)$ are constants, whose values are fixed by the physical observables, $O_i(\{\psi\})$ refer to operators containing field ψ. The summation of the repeating index i from zero to infinity is implied.

From Eq. (2.27) we observe that the most general effective Lagrangian contains an infinite number of terms, which implies the Feynman diagrams to be calculated for a physical observable of interest are also infinite. The theory is totally inapplicable without a rule to identify which terms are important and which ones are not. Such a rule is called power counting rule. Utilizing the power counting rule, the T matrix from Eq. (2.27) can further be decomposed into,

$$\mathcal{T}(Q)=\sum_{\nu=0}^{\infty}\left(\frac{Q}{\Lambda}\right)^{\nu}F^{(\nu)}\left[\frac{Q}{\Lambda};c_i^{(\nu)}\left(\frac{Q}{\Lambda}\right)\right], \tag{2.28}$$

where ν is a counting index, $F^{(\nu)}$ refer to the polynomials generated by the dynamics of field ψ, and $c_i^{(\nu)}$ are constants. As long as the expansion parameter $\mathcal{O}(Q/\Lambda)<1$, the contributions from terms with relatively large ν are insignificant compared to those with small ν due to the exponential suppression. Thus the number of Feynman diagrams needed to be calculated is finite for a physical observable of interest to a given accuracy. Notice the power counting rule refers to the relation between the index ν in Eq. (2.28) and the label i in Eq. (2.27).

Then we discuss the power counting rules in ChEFT in detail. As we stated in Sec. 2.1, in constructing the nucleon-nucleon interaction, Q contains the pion mass m_π, the four momentum of the pion q^μ and the three momentum of the nucleon $\vec{p}$, while Λ refers to the chiral symmetry breaking scale Λ_χ or the nucleon mass m_n. Combining these energy scales with the Feynman rules, which indicate that the pion propagator is in form of $\frac{1}{q^2-m_\pi^2}$, the nucleon propagator is in form of $\frac{1}{\not{p}-m_n}$, and each loop in the Feynman diagrams implies an integration over the four momentum, it is natural to identify that the pion propagator is of order Q^{-2}, the nucleon propagator is of order Q^{-1}, the derivative of the pion/nucleon field is of order Q^1 and the integration over the four momentum is of order Q^4. Such a way to count the order is the well-known naive dimensional analysis. Utilizing topology, Weinberg proposed a simple relation to count the chiral order of an irreducible Feynman diagram [57, 58, 108],

$$\nu=4-A-2C+2L+\sum_i v_i\Delta_i, \qquad \Delta_i=d_i+\frac{1}{2}n_i-2, \tag{2.29}$$

where ν refers to the chiral order, A refers to the number of nucleon fields, C represents the number of separately connected pieces, L denotes the number of loops and v_i is the number of vertices with order of Δ_i, d_i refers to the number of derivatives and n_i is the number of internal nucleon lines connected to the vertex.

Eq. (2.29) works well for systems with $A\leq 2$. However, it encounters a difficulty when applied to systems with $A\geq 3$. The problem can be illustrated in

a straightforward way. For example, consider the simplest case, that is no loops ($L = 0$), all vertices of zero order ($\Delta_i = 0$) and $C = C_{max} = A - 1$. For the two nucleon system, the chiral order $\nu = 4 - 2 - 2 + 0 + 0 = 0$, while for the three nucleon system, the chiral order $\nu = 2 - 3 - 2 + 0 + 0 = -3 \leq 0$. This suggests that an unnatural expansion at this order in form of $(\Lambda/Q)^3$. This problem come from the normalization of the nucleon states, and can be solved by an redefinition of the chiral order $\nu' = \nu + 3A - 6$, the new power counting rule then is,

$$\nu' = -2 + 2A - 2C + 2L + \sum_i v_i \Delta_i. \tag{2.30}$$

An alternative power counting to Eq. (2.29) proposed by Friar [109] under the different assumption of disconnected piece scales is,

$$\nu'' = -1 + A - C + 2L + \sum_i \nu_i + \Delta_i. \tag{2.31}$$

With Weinberg's power counting rule (Eq. (2.29)) and the redefined one (Eq. (2.30)), one could calculate any physical process to a desired accuracy. Since we mainly pay attention to the nucleon-nucleon system in this work, Eq. (2.30) can be reduced to,

$$v' = 2L + \sum_i v_i \Delta_i. \tag{2.32}$$

Note at very low energies, i.e., for momenta $Q \ll m_\pi$, it is possible to describe the few-nucleon systems with short-range interactions alone. A modern systematic framework based on this idea is known as pionless EFT. For a review, see Ref. [110]. The chiral order $\nu(\not{\pi})$ in pionless EFT is different from Eq. (2.32) and is in the form of [110],

$$\nu(\not{\pi}) = \sum_i V_i \mu_i, \tag{2.33}$$

where V_i is the number of vertices with f_i nucleon lines and μ is the counting index for the potential.

Eq. (2.32) leads to the hierarchy of chiral nuclear potentials in Weinberg's scheme as shown in Fig. 1.1. The most important leading order (LO, $\nu = 0$) is consists of one-pion exchange term, which is responsible for the long-range part of the nuclear force, and the nucleon-nucleon contact term with order zero vertex, which mainly contributes to the short-range part of the nuclear force. The next-to-leading order contributes to order two (NLO, $\nu = 2$) instead of order one because of the constrains from parity. At the next-to-leading order, the so-called two-pion exchange term emerges and the contact term with vertex of order two also contributes. In the chiral nuclear force, the two-pion-exchange contributions are important for the medium-range of the nuclear force. And it has been found in Ref. [61] that the order-two two-pion exchange together with the order-three two-pion exchange are necessary for the description of D-, F- and G-waves

nucleon-nucleon phase shifts. At next-to-next-to leading order (NNLO, $\nu = 3$), for the two-nucleon force, only two-pion exchange terms exist, the contact terms vanish because of the same reason as at order $\nu = 1$. Moreover, the three-nucleon force starts to contribute at this order. At the next-to-next-to-next-to-leading order (N^{3}LO, $\nu = 4$), the two-pion exchange with two loops, three-pion exchange and the contact terms with vertex of order $\nu = 4$ appear for the two-nucleon force. In addition to this, three-nucleon forces still exist and a four-nucleon force emerges. For the sake of simplicity, the Feynman diagrams show up at this order and higher orders are not given completely.

Based on the discussions above, we can start to calculate the beyond-leading-order contributions to the nuclear force in the relativistic chiral EFT. Our efforts in this direction are explained in detail in Chapter 3 and Chapter 4.

3 - Covariant chiral nucleon-nucleon contact Lagrangian

To construct the relativistic high-precision chiral nuclear force, the relevant nucleon-nucleon contact Lagrangians are needed. In this chapter, We propose a covariant [1] power counting scheme and construct the chiral two-nucleon contact Lagrangians constrained by Lorentz, parity, charge conjugation, hermitian conjugation, and chiral symmetries. We show that at $\mathcal{O}(q^0)$, $\mathcal{O}(q^2)$, $\mathcal{O}(q^4)$, where q denotes the three-momentum of the nucleon, there are 4, 13, and 23 terms, respectively. We find that by performing $1/m_n$ expansions, the covariant Lagrangians reduce to the conventional non-relativistic ones, which include 2, 7, and 15 terms at each corresponding order.

This chapter is organized as follows. In Sec. 3.1, we explain the general principles to construct a covariant nucleon-nucleon Lagrangian, list the approximate equalities derived from the equation of motion and use them to eliminate redundant terms, and write down the covariant nucleon-nucleon contact Lagrangian up to order $\mathcal{O}(q^4)$. In Sec. 3.2, we compare our results with those of earlier studies and perform the non-relativistic reduction, which is followed by a short summary in Sec. 3.3. A concise derivation of the non-relativistic nucleon-nucleon contact Lagrangian up to order $\mathcal{O}(q^4)$ is given in Appendix A.

3.1 . Relativistic chiral NN Lagrangians up to $\mathcal{O}(q^4)$

The relativistic chiral NN contact Lagrangian should fulfill the following requirements. First of all, the Lagrangian must be a Lorentz scalar. Second, it has to be invariant under chiral transformations, parity ($\mathcal{P}$), charge conjugation ($\mathcal{C}$), hermitian conjugation, and time reversal. Third, it needs to satisfy a proper power counting so that one can determine the relative importance of each term and have limited terms at each order in the chiral expansion.

The general expression of a covariant nucleon-nucleon contact Lagrangian [2] reads,

$$\frac{1}{(2m_n)^{N_d}}\left(\bar{\psi} i\overleftrightarrow{\partial}^{\alpha} i\overleftrightarrow{\partial}^{\beta} ... \Gamma_A \psi\right) \partial^{\lambda}\partial^{\mu} ... \left(\bar{\psi} i\overleftrightarrow{\partial}^{\sigma} i\overleftrightarrow{\partial}^{\tau} ... \Gamma_B \psi\right), \tag{3.1}$$

where ψ and $\bar{\psi}$ denote the relativistic nucleon field, $\overleftrightarrow{\partial}^{\alpha} = \overrightarrow{\partial}^{\alpha} - \overleftarrow{\partial}^{\alpha}$, and $\Gamma \in$

1. In the present thesis, "relativistic" and "covariant" are used interchangeably in most cases except for the discussions involving the Roper resonance, where the calculations are performed in the non-relativistic covariant framework (covariant HB EFT).

2. In the present work, to simplify the derivation, we do not consider the interaction of external fields and the pion with the nucleon.

$\{\mathbb{1}, \gamma_5, \gamma^\mu, \gamma_5\gamma^\mu, \sigma^{\mu\nu}, g^{\mu\nu}, \epsilon^{\mu\nu\rho\sigma}\}$. In the above equation, N_d refers to the number of four-derivatives (both $\overleftrightarrow{\partial}$ and ∂) in the Lagrangian, m_n refers to the nucleon mass in the chiral limit, and the factor $1/(2m_n)^{N_d}$ has been introduced so that all the contact terms have the same dimension [111].

For the construction of effective Lagrangians, symmetry constraints are the most important. In our present case, apart from the invariance under Lorentz transformation, the covariant nucleon-nucleon contact Lagrangian has to be invariant under local chiral, parity, charge conjugation, hermitian conjugation, and time reversal transformations. The Lorentz indices α, β... have to be contracted among themselves to fulfill Lorentz invariance. The local chiral symmetry can be trivially fulfilled because the nucleon field ψ transforms under chiral rotation $\psi \to K\psi$, where $K \in$SU(2)$_V$. The hermitian conjugation symmetry does not impose any constraint since to fulfill it one can always multiply the Lagrangian with a proper choice of factor i. According to the CPT (charge, parity, and time reversal) theorem, time reversal symmetry is also automatically fulfilled if parity symmetry and charge conjugation symmetry are fulfilled. Therefore, one only needs to make sure that parity and charge conjugation symmetries are fulfilled.

Table 3.1 – Chiral dimensions and properties of fermion bilinears, derivative operators, Dirac matrices, and Levi-Civita tensor, under parity ($\mathcal{P}$), charge conjugation ($\mathcal{C}$), and hermitian conjugation transformations.

	$\mathbb{1}$	γ_5	γ_μ	$\gamma_5\gamma_\mu$	$\sigma_{\mu\nu}$	$\epsilon_{\mu\nu\rho\sigma}$	$\overleftrightarrow{\partial}_\mu$	∂_μ
$\mathcal{P}$	$+$	$-$	$+$	$-$	$+$	$-$	$+$	$+$
$\mathcal{C}$	$+$	$+$	$-$	$+$	$-$	$+$	$-$	$+$
h.c.	$+$	$-$	$+$	$+$	$+$	$+$	$-$	$+$
dim	0	1	0	0	0	$-$	0	1

To construct the NN Lagrangian, one has to specify a proper power counting. In our present case, we need to specify the chiral dimensions of all the building blocks. In the covariant case, the power counting is more involved, compared to the non-relativistic case (see the Appendix. A). The chiral dimensions and properties of fermion bilinears, derivative operators, Dirac matrices, and Levi-Civita tensor under parity, charge conjugation, and hermitian conjugation transformations are listed in Table 3.1. The derivative ∂ acting on the whole bilinear is of order $\mathcal{O}(q^1)$, while the derivative $\overleftrightarrow{\partial}$ acting inside a bilinear is of $\mathcal{O}(q^0)$ due to the presence of the nucleon mass, where q denotes a generic small momentum, such as the nucleon three-momentum. The bilinear $\bar{\psi}\gamma_5\psi$ is of order $\mathcal{O}(q^1)$ because it mixes the large and small components of the Dirac spinor. The Levi-Civita tensor $\epsilon_{\mu\nu\rho\sigma}$ contracting with n derivatives acting inside a bilinear raises the chiral order by $n-1$. If a derivative $\overleftrightarrow{\partial}$ is contracted with one of the Dirac matrices $\gamma_5\gamma^\mu$ or $\sigma^{\mu\nu}$ in a different bilinear, the matrix element is of $\mathcal{O}(q^1)$, as can be explicitly checked by

means of the equation of motion (EOM). Therefore, at each order in the powering counting, only a finite number of ∂ and $\epsilon_{\mu\nu\rho\sigma}$ appear. However, in principle, any numbers of pairwise contracted $i\overleftrightarrow{\partial}$ of the form

$$\begin{aligned}\widetilde{\mathcal{O}}^{(n)}_{\Gamma_A\Gamma_B} = \frac{1}{(2m_n)^{2n}} \quad & \left(\bar{\psi} i\overleftrightarrow{\partial}^{\mu_1} i\overleftrightarrow{\partial}^{\mu_2} ... i\overleftrightarrow{\partial}^{\mu_n} \Gamma^\alpha_A \psi\right) \\ \times \quad & \left(\bar{\psi} i\overleftrightarrow{\partial}_{\mu_1} i\overleftrightarrow{\partial}_{\mu_2} ... i\overleftrightarrow{\partial}_{\mu_n} \Gamma_{B\alpha} \psi\right),\end{aligned} \tag{3.2}$$

is allowed, since it is of $\mathcal{O}(q^0)$. Such a term gives $N(p_1)+N(p_2) \mapsto N(p_3)+N(p_4)$. On the other hand, such structures as

$$\frac{[(p_1+p_3)\cdot(p_2+p_4)]^n}{(2m_n)^{2n}}, \quad \frac{[(p_1+p_4)\cdot(p_2+p_3)]^n}{(2m_n)^{2n}}, \tag{3.3}$$

can be rewritten as

$$\left[1+\frac{(s-4m_n^2)-u}{4m_n^2}\right]^n, \quad \left[1+\frac{(s-4m_n^2)-t}{4m_n^2}\right]^n, \tag{3.4}$$

with $s-4m_n^2 = -(p_1-p_2)^2 = -(p_3-p_4)^2 \sim \mathcal{O}(q^2)$ and $u=(p_1-p_4)^2 \sim \mathcal{O}(q^2)$, and $t=(p_1-p_3)^2 \sim \mathcal{O}(q^2)$. [3] Therefore, at $\mathcal{O}(q^0)$, only the terms with $n=0,1,2$ are needed, at $\mathcal{O}(q^2)$ only the terms with $n=0,1$ are needed, and at $\mathcal{O}(q^4)$ only the terms with $n=0$ are needed since no new structure will be included for n larger than those specified above.

Following the general principles of constructing effective Lagrangians and guided by Table 3.1, one can write down all the terms of $\mathcal{O}(q^0)$, $\mathcal{O}(q^2)$, and $\mathcal{O}(q^4)$. As we show in the following part, not all of them are independent up to the order we are interested, and one can use the EOM to eliminate the nonindependent or redundant terms.

Table 3.2 – Decomposition of the Dirac matrix products $\Gamma\gamma_\lambda$ into charge conjugation even and charge conjugation odd parts.

Γ	Γ'_λ	Γ''_λ
$\mathbb{1}$	γ_λ	0
γ_μ	$g_{\mu\lambda}1$	$-i\sigma_{\mu\lambda}$
γ_5	0	$\gamma_5\gamma_\lambda$
$\gamma_5\gamma_\mu$	$\frac{1}{2}\epsilon_{\mu\lambda\rho\tau}\sigma^{\rho\tau}$	$g_{\mu\lambda}\gamma_5$
$\sigma_{\mu\nu}$	$\epsilon_{\mu\nu\lambda\tau}\gamma_5\gamma^\tau$	$-i\left(g_{\mu\lambda}\gamma_\nu - g_{\nu\lambda}\gamma_\mu\right)$
$\epsilon_{\mu\nu\rho\tau}\gamma^\tau$	$\epsilon_{\mu\nu\rho\lambda}1$	$g_{\mu\lambda}\gamma_5\sigma_{\nu\rho} + g_{\rho\lambda}\gamma_5\sigma_{\mu\nu} + g_{\nu\lambda}\gamma_5\sigma_{\rho\mu}$
$\epsilon_{\mu\nu\rho\tau}\gamma_5\gamma^\tau$	$g_{\mu\lambda}\sigma_{\nu\rho} + g_{\rho\lambda}\sigma_{\mu\nu} + g_{\nu\lambda}\sigma_{\rho\mu}$	$\epsilon_{\mu\nu\rho\lambda}\gamma_5$
$\epsilon_{\mu\nu\rho\alpha}\sigma^\alpha_\tau$	$\gamma_5\gamma_\rho\left(g_{\lambda\nu}g_{\mu\tau} - g_{\lambda\mu}g_{\nu\tau}\right) + \gamma_5\gamma_\nu\left(g_{\lambda\mu}g_{\rho\tau} - g_{\lambda\rho}g_{\mu\tau}\right) + \gamma_5\gamma_\mu\left(g_{\lambda\rho}g_{\nu\tau} - g_{\lambda\nu}g_{\rho\tau}\right)$	$ig_{\lambda\tau}\epsilon_{\mu\nu\rho\alpha}\gamma^\alpha - i\epsilon_{\mu\nu\rho\lambda}\gamma_\tau$
$\frac{i}{2}\epsilon_{\mu\nu\rho\tau}\sigma^{\rho\tau} = \gamma_5\sigma_{\mu\nu}$	$\frac{1}{i}\left(g_{\mu\lambda}\gamma_5\gamma_\nu - g_{\nu\lambda}\gamma_5\gamma_\mu\right)$	$\epsilon_{\mu\nu\lambda\rho}\gamma^\rho$

The equation of motion for the nucleon refers to the well-known Dirac equation at LO

$$\not{\partial}\psi = \gamma^\mu\partial_\mu\psi = -im_n\psi + \mathcal{O}(q)\,, \tag{3.5}$$

3. This can be easily checked by noting that in the center-of-mass frame $p_1^\mu = m_n + \mathcal{O}(q)$ and $p_2^\mu = m_n - \mathcal{O}(q)$ because of momentum conservation.

and its hermitian conjugate. Up to higher order corrections one can replace $\not{\partial}\psi$ by $-im_n\psi$ and $\bar{\psi}\overleftarrow{\not{\partial}}$ by $im_n\bar{\psi}$. To fully utilize this EOM, one needs to transform terms that do not contain $\not{\partial}$ into a form that contains it. Such a technique has been extensively discussed in the construction of the πN Lagrangian [112] and baryon-baryon Lagrangian [113]. The details can be found in Refs. [112, 113]. The master formula is

$$-2im_n\left(\bar{\psi}\Gamma\psi\right) \approx 2(\bar{\psi}\Gamma\times\gamma_\lambda\partial^\lambda\psi) = \left(\bar{\psi}\Gamma'^\lambda\overleftrightarrow{\partial}_\lambda\psi\right) + \partial_\lambda\left(\bar{\psi}\Gamma''^\lambda\psi\right), \tag{3.6}$$

where Γ, Γ' and Γ'' are Dirac matrices listed in Table 3.2 [113] and $\approx$ indicates equal up to higher orders. Using the EOM together with the decomposition of Dirac matrices, one can obtain the following linear relations :

$$\partial^\mu\left(\bar{\psi}\gamma_\mu\psi\right) \approx 0, \tag{3.7.1}$$

$$\partial^\mu\left(\bar{\psi}\overleftrightarrow{\partial}_\mu\psi\right) \approx 0, \tag{3.7.2}$$

$$\partial^\mu\left(\bar{\psi}\gamma_5\gamma_\mu\psi\right) \approx -2m_n\left(\bar{\psi}i\gamma_5\psi\right), \tag{3.7.3}$$

$$\partial^\mu\left(\bar{\psi}\sigma_{\mu\nu}\psi\right) \approx \left(\bar{\psi}i\overleftrightarrow{\partial}_\nu\psi\right) - 2m_n\left(\bar{\psi}\gamma_\nu\psi\right), \tag{3.7.4}$$

$$\left(\bar{\psi}\gamma^\mu i\overleftrightarrow{\partial}_\mu\psi\right) \approx 2m_n\left(\bar{\psi}\psi\right), \tag{3.7.5}$$

$$\left(\bar{\psi}\overleftrightarrow{\partial}^2\psi\right) \approx -4m_n^2\left(\bar{\psi}\psi\right) - \partial^2\left(\bar{\psi}\psi\right), \tag{3.7.6}$$

$$\left(\bar{\psi}\gamma_5\gamma^\mu i\overleftrightarrow{\partial}_\mu\psi\right) \approx 0, \tag{3.7.7}$$

$$\left(\bar{\psi}i\overleftrightarrow{\partial}_\mu\sigma^{\mu\nu}\psi\right) \approx -\partial^\nu\left(\bar{\psi}\psi\right), \tag{3.7.8}$$

$$-2im_n\left(\bar{\psi}\gamma_5\gamma^\mu\psi\right) \approx \left(\bar{\psi}\frac{1}{2}\epsilon^{\mu\lambda\rho\tau}\sigma_{\rho\tau}\overleftrightarrow{\partial}_\lambda\psi\right) + \partial^\mu\left(\bar{\psi}\gamma_5\psi\right), \tag{3.7.9}$$

$$-2im_n\left(\bar{\psi}\sigma^{\mu\nu}\psi\right) \approx \left(\bar{\psi}\epsilon^{\mu\lambda\rho\tau}\gamma_5\gamma_\tau\overleftrightarrow{\partial}_\lambda\psi\right) + \partial_\lambda\left(\bar{\psi} - i\left(g^{\mu\lambda}\gamma^\nu - g^{\nu\lambda}\gamma^\mu\right)\psi\right), \tag{3.7.10}$$

$$-2im_n\left(\bar{\psi}\epsilon_{\mu\nu\rho\tau}\gamma^\tau\psi\right) \approx \left(\bar{\psi}\epsilon_{\mu\nu\rho\lambda}\overleftrightarrow{\partial}^\lambda\psi\right) + \partial^\lambda\left(\bar{\psi}\left(g_{\mu\lambda}\gamma_5\sigma_{\nu\rho} + g_{\rho\lambda}\gamma_5\sigma_{\mu\nu} + g_{\nu\lambda}\gamma_5\sigma_{\rho\mu}\right)\psi\right), \tag{3.7.11}$$

$$-2im_n\left(\bar{\psi}\epsilon_{\mu\nu\rho\tau}\gamma_5\gamma^\tau\psi\right) \approx \left(\bar{\psi}\left(\sigma_{\nu\rho}\overleftrightarrow{\partial}_\mu + \sigma_{\mu\nu}\overleftrightarrow{\partial}_\rho + \sigma_{\rho\mu}\overleftrightarrow{\partial}_\nu\right)\psi\right) + \partial^\lambda\left(\bar{\psi}\epsilon_{\mu\nu\rho\lambda}\gamma_5\psi\right), \tag{3.7.12}$$

$$-2im_n\left(\bar{\psi}\epsilon_{\mu\nu\rho\alpha}\sigma^\alpha{}_\tau\psi\right) \approx \left(\bar{\psi}\gamma_5\gamma_\rho\left(\overleftrightarrow{\partial}_\nu g_{\mu\tau} - \overleftrightarrow{\partial}_\mu g_{\nu\tau}\right)\psi\right) + \left(\bar{\psi}\gamma_5\gamma_\nu\left(\overleftrightarrow{\partial}_\mu g_{\rho\tau} - \overleftrightarrow{\partial}_\rho g_{\mu\tau}\right)\psi\right) \tag{3.7.13}$$

$$+\left(\bar{\psi}\gamma_5\gamma_\mu\left(\overleftrightarrow{\partial}_\rho g_{\nu\tau} - \overleftrightarrow{\partial}_\nu g_{\rho\tau}\right)\psi\right) + \partial^\lambda\left(\bar{\psi}\left(ig_{\lambda\tau}\epsilon_{\mu\nu\rho\alpha}\gamma^\alpha - i\epsilon_{\mu\nu\rho\lambda}\gamma_\tau\right)\psi\right),$$

$$m_n\left(\bar{\psi}\epsilon_{\mu\nu\rho\tau}\sigma^{\rho\tau}\psi\right) \approx \left(\bar{\psi}\left(\gamma_5\gamma_\mu i\overleftrightarrow{\partial}_\nu - \gamma_5\gamma_\nu i\overleftrightarrow{\partial}_\mu\right)\psi\right) + \partial^\lambda\left(\bar{\psi}\epsilon_{\mu\nu\lambda\rho}\gamma^\rho\psi\right), \tag{3.7.14}$$

$$\left(\bar{\psi}\epsilon_{\mu\nu\alpha\beta}i\overleftrightarrow{\partial}^\mu i\overleftrightarrow{\partial}^\nu\cdots\psi\right) = 0. \tag{3.7.15}$$

The set of relations in Eq. (3.7) lead to the following four simplification rules :

1. Terms with $\epsilon_{\mu\nu\rho\tau}$ can always be transformed into those without it, so no terms with $\epsilon_{\mu\nu\rho\tau}$ are needed,
2. The derivative ∂_μ acting on the whole fermion bilinear cannot be contracted with any elements of the Clifford algebra except for $\sigma^{\mu\nu}$,
3. The derivative $i\overleftrightarrow{\partial}^\mu$ cannot be contracted with any elements of the Clifford algebra inside the same fermion bilinear,
4. Terms with γ^μ can be transformed into terms with $i\overleftrightarrow{\partial}^\mu$ except for the cases where it is contracted with $\sigma^{\mu\nu}$.

Table 3.3 – A complete set of relativistic NN contact Lagrangian up to $\mathcal{O}(q^4)$.

$\widetilde{O}_1$	$(\bar{\psi}\psi)\,(\bar{\psi}\psi)$	$\widetilde{O}_{21}$	$\frac{1}{16m_n^4}\left(\bar{\psi}i\overleftrightarrow{\partial}^\mu\psi\right)\partial^2\partial^\nu\left(\bar{\psi}\sigma_{\mu\nu}\psi\right)$
$\widetilde{O}_2$	$(\bar{\psi}\gamma^\mu\psi)\,(\bar{\psi}\gamma_\mu\psi)$	$\widetilde{O}_{22}$	$\frac{1}{16m_n^4}\left(\bar{\psi}\sigma^{\mu\alpha}\psi\right)\partial^2\partial_\alpha\partial^\nu\left(\bar{\psi}\sigma_{\mu\nu}\psi\right)$
$\widetilde{O}_3$	$(\bar{\psi}\gamma_5\gamma^\mu\psi)\,(\bar{\psi}\gamma_5\gamma_\mu\psi)$	$\widetilde{O}_{23}$	$\frac{1}{16m_n^4}\left(\bar{\psi}\sigma^{\mu\nu}i\overleftrightarrow{\partial}^\alpha\psi\right)\partial^\beta\partial_\nu\left(\bar{\psi}\sigma_{\alpha\beta}i\overleftrightarrow{\partial}_\mu\psi\right)$
$\widetilde{O}_4$	$(\bar{\psi}\sigma^{\mu\nu}\psi)\,(\bar{\psi}\sigma_{\mu\nu}\psi)$	$\widetilde{O}_{24}$	$\frac{1}{16m_n^4}\left(\bar{\psi}\psi\right)\partial^4\left(\bar{\psi}\psi\right)$
$\widetilde{O}_5$	$(\bar{\psi}\gamma_5\psi)\,(\bar{\psi}\gamma_5\psi)$	$\widetilde{O}_{25}$	$\frac{1}{16m_n^4}\left(\bar{\psi}\gamma^\mu\psi\right)\partial^4\left(\bar{\psi}\gamma_\mu\psi\right)$
$\widetilde{O}_6$	$\frac{1}{4m_n^2}\left(\bar{\psi}\gamma_5\gamma^\mu i\overleftrightarrow{\partial}^\alpha\psi\right)\left(\bar{\psi}\gamma_5\gamma_\alpha i\overleftrightarrow{\partial}_\mu\psi\right)$	$\widetilde{\mathcal{O}}_{26}$	$\frac{1}{16m_n^4}\left(\bar{\psi}\gamma_5\gamma^\mu\psi\right)\partial^4\left(\bar{\psi}\gamma_5\gamma_\mu\psi\right)$
$\widetilde{O}_7$	$\frac{1}{4m_n^2}\left(\bar{\psi}\sigma^{\mu\nu}i\overleftrightarrow{\partial}^\alpha\psi\right)\left(\bar{\psi}\sigma_{\mu\alpha}i\overleftrightarrow{\partial}_\nu\psi\right)$	$\widetilde{O}_{27}$	$\frac{1}{16m_n^4}\left(\bar{\psi}\sigma^{\mu\nu}\psi\right)\partial^4\left(\bar{\psi}\sigma_{\mu\nu}\psi\right)$
$\widetilde{O}_8$	$\frac{1}{4m_n^2}\left(\bar{\psi}i\overleftrightarrow{\partial}^\mu\psi\right)\partial^\nu\left(\bar{\psi}\sigma_{\mu\nu}\psi\right)$	$\widetilde{O}_{28}$	$\frac{1}{4m_n^2}\left(\bar{\psi}\gamma_5 i\overleftrightarrow{\partial}^\alpha\psi\right)\left(\bar{\psi}\gamma_5 i\overleftrightarrow{\partial}_\alpha\psi\right)-\widetilde{O}_5$
$\widetilde{O}_9$	$\frac{1}{4m_n^2}\left(\bar{\psi}\sigma^{\mu\alpha}\psi\right)\partial_\alpha\partial^\nu\left(\bar{\psi}\sigma_{\mu\nu}\psi\right)$	$\widetilde{O}_{29}$	$\frac{1}{16m_n^4}\left(\bar{\psi}\gamma_5\gamma^\mu i\overleftrightarrow{\partial}^\alpha i\overleftrightarrow{\partial}^\beta\psi\right)\left(\bar{\psi}\gamma_5\gamma_\alpha i\overleftrightarrow{\partial}_\mu i\overleftrightarrow{\partial}_\beta\psi\right)-\widetilde{O}_6$
$\widetilde{O}_{10}$	$\frac{1}{4m_n^2}\left(\bar{\psi}\psi\right)\partial^2\left(\bar{\psi}\psi\right)$	$\widetilde{O}_{30}$	$\frac{1}{16m_n^4}\left(\bar{\psi}\sigma^{\mu\nu}i\overleftrightarrow{\partial}^\alpha i\overleftrightarrow{\partial}^\beta\psi\right)\left(\bar{\psi}\sigma_{\mu\alpha}i\overleftrightarrow{\partial}_\nu i\overleftrightarrow{\partial}_\beta\psi\right)-\widetilde{O}_7$
$\widetilde{O}_{11}$	$\frac{1}{4m_n^2}\left(\bar{\psi}\gamma^\mu\psi\right)\partial^2\left(\bar{\psi}\gamma_\mu\psi\right)$	$\widetilde{O}_{31}$	$\frac{1}{16m_n^4}\left(\bar{\psi}i\overleftrightarrow{\partial}^\mu i\overleftrightarrow{\partial}^\beta\psi\right)\partial^\alpha\left(\bar{\psi}\sigma_{\mu\alpha}i\overleftrightarrow{\partial}_\beta\psi\right)-\widetilde{O}_8$
$\widetilde{O}_{12}$	$\frac{1}{4m_n^2}\left(\bar{\psi}\gamma_5\gamma^\mu\psi\right)\partial^2\left(\bar{\psi}\gamma_5\gamma_\mu\psi\right)$	$\widetilde{O}_{32}$	$\frac{1}{16m_n^4}\left(\bar{\psi}\sigma^{\mu\alpha}i\overleftrightarrow{\partial}^\beta\psi\right)\partial_\alpha\partial^\nu\left(\bar{\psi}\sigma_{\mu\nu}i\overleftrightarrow{\partial}_\beta\psi\right)-\widetilde{O}_9$
$\widetilde{O}_{13}$	$\frac{1}{4m_n^2}\left(\bar{\psi}\sigma^{\mu\nu}\psi\right)\partial^2\left(\bar{\psi}\sigma_{\mu\nu}\psi\right)$	$\widetilde{O}_{33}$	$\frac{1}{16m_n^4}\left(\bar{\psi}i\overleftrightarrow{\partial}^\alpha\psi\right)\partial^2\left(\bar{\psi}i\overleftrightarrow{\partial}_\alpha\psi\right)-\widetilde{O}_{10}$
$\widetilde{O}_{14}$	$\frac{1}{4m_n^2}\left(\bar{\psi}i\overleftrightarrow{\partial}^\alpha\psi\right)\left(\bar{\psi}i\overleftrightarrow{\partial}_\alpha\psi\right)-\widetilde{O}_1$	$\widetilde{O}_{34}$	$\frac{1}{16m_n^4}\left(\bar{\psi}\gamma^\mu i\overleftrightarrow{\partial}^\alpha\psi\right)\partial^2\left(\bar{\psi}\gamma_\mu i\overleftrightarrow{\partial}_\alpha\psi\right)-\widetilde{O}_{11}$
$\widetilde{O}_{15}$	$\frac{1}{4m_n^2}\left(\bar{\psi}\gamma^\mu i\overleftrightarrow{\partial}^\alpha\psi\right)\left(\bar{\psi}\gamma_\mu i\overleftrightarrow{\partial}_\alpha\psi\right)-\widetilde{O}_2$	$\widetilde{O}_{35}$	$\frac{1}{16m_n^4}\left(\bar{\psi}\gamma_5\gamma^\mu i\overleftrightarrow{\partial}^\alpha\psi\right)\partial^2\left(\bar{\psi}\gamma_5\gamma_\mu i\overleftrightarrow{\partial}_\alpha\psi\right)-\widetilde{O}_{12}$
$\widetilde{O}_{16}$	$\frac{1}{4m_n^2}\left(\bar{\psi}\gamma_5\gamma^\mu i\overleftrightarrow{\partial}^\alpha\psi\right)\left(\bar{\psi}\gamma_5\gamma_\mu i\overleftrightarrow{\partial}_\alpha\psi\right)-\widetilde{O}_3$	$\widetilde{O}_{36}$	$\frac{1}{16m_n^4}\left(\bar{\psi}\sigma^{\mu\nu}i\overleftrightarrow{\partial}^\alpha\psi\right)\partial^2\left(\bar{\psi}\sigma_{\mu\nu}i\overleftrightarrow{\partial}_\alpha\psi\right)-\widetilde{O}_{13}$
$\widetilde{O}_{17}$	$\frac{1}{4m_n^2}\left(\bar{\psi}\sigma^{\mu\nu}i\overleftrightarrow{\partial}^\alpha\psi\right)\left(\bar{\psi}\sigma_{\mu\nu}i\overleftrightarrow{\partial}_\alpha\psi\right)-\widetilde{O}_4$	$\widetilde{O}_{37}$	$\frac{1}{16m_n^4}\left(\bar{\psi}i\overleftrightarrow{\partial}^\alpha i\overleftrightarrow{\partial}^\beta\psi\right)\left(\bar{\psi}i\overleftrightarrow{\partial}_\alpha i\overleftrightarrow{\partial}_\beta\psi\right)-2\widetilde{O}_{14}-\widetilde{O}_1$
$\widetilde{O}_{18}$	$\frac{1}{4m_n^2}\left(\bar{\psi}\gamma_5\psi\right)\partial^2\left(\bar{\psi}\gamma_5\psi\right)$	$\widetilde{O}_{38}$	$\frac{1}{16m_n^4}\left(\bar{\psi}\gamma^\mu i\overleftrightarrow{\partial}^\alpha i\overleftrightarrow{\partial}^\beta\psi\right)\left(\bar{\psi}\gamma_\mu i\overleftrightarrow{\partial}_\alpha i\overleftrightarrow{\partial}_\beta\psi\right)-2\widetilde{O}_{15}-\widetilde{O}_2$
$\widetilde{O}_{19}$	$\frac{1}{16m_n^4}\left(\bar{\psi}\gamma_5\gamma^\mu i\overleftrightarrow{\partial}^\nu\psi\right)\partial^2\left(\bar{\psi}\gamma_5\gamma_\nu i\overleftrightarrow{\partial}_\mu\psi\right)$	$\widetilde{O}_{39}$	$\frac{1}{16m_n^4}\left(\bar{\psi}\gamma_5\gamma^\mu i\overleftrightarrow{\partial}^\alpha i\overleftrightarrow{\partial}^\beta\psi\right)\left(\bar{\psi}\gamma_5\gamma_\mu i\overleftrightarrow{\partial}_\alpha i\overleftrightarrow{\partial}_\beta\psi\right)-2\widetilde{O}_{16}-\widetilde{O}_3$
$\widetilde{O}_{20}$	$\frac{1}{16m_n^4}\left(\bar{\psi}\sigma^{\mu\nu}i\overleftrightarrow{\partial}^\alpha\psi\right)\partial^2\left(\bar{\psi}\sigma_{\mu\alpha}i\overleftrightarrow{\partial}_\nu\psi\right)$	$\widetilde{O}_{40}$	$\frac{1}{16m_n^4}\left(\bar{\psi}\sigma^{\mu\nu}i\overleftrightarrow{\partial}^\alpha i\overleftrightarrow{\partial}^\beta\psi\right)\left(\bar{\psi}\sigma_{\mu\nu}i\overleftrightarrow{\partial}_\alpha i\overleftrightarrow{\partial}_\beta\psi\right)-2\widetilde{O}_{17}-\widetilde{O}_4$

Using the four rules listed above, we obtain a minimal and complete set of relativistic NN contact Lagrangian terms $\widetilde{O}_i(i=1,...,40)$, which are summarized in Table 3.3.

3.2 . Discussions

3.2.1 . Comparison with previous works

The Lagrangian listed in Table 3.3 is different from those of Refs. [111, 114, 113]. Moreover, the results of Refs. [111, 114, 113] can be reduced to ours using the approximate equalities listed in the last section. Compared with the results of Refs. [111, 114], in our case all the terms with $\epsilon_{\mu\nu\alpha\beta}$ are eliminated using the EOM. In Ref. [113], their results contain at most two pairwise contracted $i\overleftrightarrow{\partial}$ of the form

$$\frac{1}{(2m_n)^{2n}}\left(\bar{\psi}i\overleftrightarrow{\partial}^{\mu_1}i\overleftrightarrow{\partial}^{\mu_2}...i\overleftrightarrow{\partial}^{\mu_n}\Gamma_A^{\alpha}\psi\right)\left(\bar{\psi}i\overleftrightarrow{\partial}_{\mu_1}i\overleftrightarrow{\partial}_{\mu_2}...i\overleftrightarrow{\partial}_{\mu_n}\Gamma_{B\alpha}\psi\right) \tag{3.8}$$

up to $\mathcal{O}(q^2)$, while we only include at most one, which is consistent with Ref. [111]. We note that the terms with $\partial^{\mu}\left(\bar{\psi}\sigma_{\mu\nu}\psi\right)$ are included in our Lagrangian but are not in those of Refs. [111, 114, 113]. This is just a different choice of independent terms, because $\partial^{\mu}\left(\bar{\psi}\sigma_{\mu\nu}\psi\right) = \left(\bar{\psi}\sigma_{\mu\nu}\overrightarrow{\partial}^{\mu}\psi\right) + \left(\bar{\psi}\overleftarrow{\partial}^{\mu}\sigma_{\mu\nu}\psi\right) \approx \left(\bar{\psi}i\overleftrightarrow{\partial}_{\nu}\psi\right) - 2m_n\left(\bar{\psi}\gamma_{\nu}\psi\right)$. In Refs. [111, 114], terms containing $\left(\bar{\psi}i\overleftrightarrow{\partial}^{\mu}\psi\right)\left(\bar{\psi}\gamma_{\mu}\psi\right)$ are included, while in our case, we replace them with $\left(\bar{\psi}i\overleftrightarrow{\partial}^{\mu}\psi\right)\partial^{\nu}\left(\bar{\psi}\sigma_{\mu\nu}\psi\right)$ using the EOM. Note further that in Ref. [113], the terms with $\partial^{\mu}\left(\bar{\psi}\sigma_{\mu\nu}\psi\right)$ are not included because such terms are argued to be of higher order. However, we prefer to keep these terms because they are of unique Lorentz structure which satisfy our power counting rule. The Γ_i's in our work are also different from those in Ref. [113]. In our work, we take $\Gamma_i \in \{\mathbb{1}, \gamma_5, \gamma^{\mu}, \gamma_5\gamma^{\mu}, \sigma^{\mu\nu}, g^{\mu\nu}, \epsilon^{\mu\nu\rho\sigma}\}$ to keep the complete Dirac Algebra. While in Ref. [113], $\Gamma_i' \in \{\mathbb{1}, \gamma_5\gamma^{\mu}, \sigma^{\mu\nu}, g^{\mu\nu}, \epsilon^{\mu\nu\rho\sigma}\}$ by means of the EOM. Nevertheless, these are simply different choices and can be transformed into each other using the EOM. Note that $-2im\left(\bar{\psi}\gamma_5\psi\right) \approx \partial^{\mu}\left(\bar{\psi}\gamma_5\gamma_{\mu}\psi\right)$ and $2m\left(\bar{\psi}\gamma^{\mu}\psi\right) \approx \left(\bar{\psi}i\overleftrightarrow{\partial}^{\mu}\psi\right)$. The two structures on the left-hand-side of the above equations are contained in our work while the structures on the right-hand-side are included in Ref. [113].

As in the one-baryon sector, one encounters also in the two-baryon sector the problem that nominally higher order terms contain lower order terms that break the power counting [55]. For instance, according to our criteria listed above, we should include $\widetilde{O}'_{14} = \frac{1}{4m_n^2}\left(\bar{\psi}i\overleftrightarrow{\partial}^{\mu}\psi\right)\left(\bar{\psi}i\overleftrightarrow{\partial}_{\mu}\psi\right)$ at order $\mathcal{O}(q^2)$. However, this term actually starts to contribute at $\mathcal{O}(q^0)$ so that it breaks our power counting. Therefore, we redefine $\widetilde{O}_{14} = \frac{1}{4m_n^2}\left(\bar{\psi}i\overleftrightarrow{\partial}^{\mu}\psi\right)\left(\bar{\psi}i\overleftrightarrow{\partial}_{\mu}\psi\right) - \left(\bar{\psi}\psi\right)\left(\bar{\psi}\psi\right)$ to recover the power counting. The same also applies to $\widetilde{O}_{14-17}$ and $\widetilde{O}_{28-40}$. Notice that this procedure is very similar to the EOMS scheme [101, 100] [4], except in the one baryon sector, power counting breaking terms only appear in the loop calculation with propagating baryons. In the nucleon-nucleon sector, they already appear at tree level because the nucleon momentum is involved to increase the chiral order.

3.2.2 . Non-relativistic reductions

4. For a related discussion in the NN sector, see, e.g., Ref [115].

The relativistic results, when reduced to the non-relativistic ones in the heavy baryon limit, should recover the well-known $2+7+15$ linear independent non-relativistic terms up to $\mathcal{O}(q^4)$ [65]. We checked that indeed this is the case.

To perform the non-relativistic reduction of the covariant chiral Lagrangian constructed in our present work, one has to replace the relativistic nucleon field operator ψ with the non-relativistic nucleon field operator N and then expand the relativistic Lagrangian in terms of $1/m_n$. The relativistic nucleon field operator $\psi(x)$ is [5]

$$\psi(x) = \sum_{s=\pm 1/2} \int \frac{d\boldsymbol{p}}{(2\pi)^3} \frac{m_n}{E_p} \widetilde{b}_s(\boldsymbol{p})\, u^{(s)}(\boldsymbol{p})\, \mathrm{e}^{-ip\cdot x}, \tag{3.9}$$

with the following normalization :

$$\left[\widetilde{b}_s(\boldsymbol{p}), \widetilde{b}^\dagger_{s'}(\boldsymbol{p}')\right]_+ = \frac{E_p}{m}(2\pi)^3 \delta(\boldsymbol{p}-\boldsymbol{p}')\delta_{ss'}, \quad \bar{u}^{(s)}(\boldsymbol{p}) u^{(s')}(\boldsymbol{p}) = \delta_{ss'}, \tag{3.10}$$

where $\widetilde{b}_s(\boldsymbol{p})$ and $\widetilde{b}^\dagger_{s'}$ are annihilation and creation operators for a nucleon in spin state s and s'. A sum over the repeated index $s(s') = \pm\frac{1}{2}$ is implied. The Dirac spinors of u and $\bar{u}$ have the following form

$$\bar{u}_i = \sqrt{\frac{E_i + m_n}{2m_n}} \left(\mathbb{1}\ ,\ -\frac{\boldsymbol{\sigma}\cdot\boldsymbol{p}'}{E_i + m_n} \right) \chi_s\,, u_j = \sqrt{\frac{E_j + m_n}{2m_n}} \begin{pmatrix} \mathbb{1} \\ \frac{\boldsymbol{\sigma}\cdot\boldsymbol{p}}{E_j+m_n} \end{pmatrix} \chi_s\,, \tag{3.11}$$

with

$$E_i = \sqrt{{m_n}^2 + \boldsymbol{p}'^2}\,, \quad E_j = \sqrt{{m_n}^2 + \boldsymbol{p}^2}\,. \tag{3.12}$$

The non-relativistic nucleon filed $N(x)$ is

$$N(x) = \sum_{s=\pm 1/2} \int \frac{d\boldsymbol{p}}{(2\pi)^3}\, b_s(\boldsymbol{p})\, \chi_s\, \mathrm{e}^{-ip\cdot x}\ . \tag{3.13}$$

Here, the isospin indices have been suppressed by using the Fierz rearrangement [111]. Note that $b_s(\boldsymbol{p}) = \sqrt{m_n/E_p}\, \widetilde{b}_s(\boldsymbol{p})$. To order $\mathcal{O}(q^4)$ at which we are working, the relativistic nucleon field operator ψ can be expanded in terms of the non-relativistic field $N(x)$, defined in Eq. (3.13), as

$$\begin{aligned} \psi(x) \;=\; & \left[\begin{pmatrix} 1 \\ 0 \end{pmatrix} - \frac{i}{2m_n} \begin{pmatrix} 0 \\ \boldsymbol{\sigma}\cdot\boldsymbol{\nabla} \end{pmatrix} + \frac{1}{8m_n^2} \begin{pmatrix} \boldsymbol{\nabla}^2 \\ 0 \end{pmatrix} \right. \\ & \left. - \frac{3i}{16m_n^3} \begin{pmatrix} 0 \\ \boldsymbol{\sigma}\cdot\boldsymbol{\nabla}\boldsymbol{\nabla}^2 \end{pmatrix} + \frac{11}{128m_n^4} \begin{pmatrix} \boldsymbol{\nabla}^4 \\ 0 \end{pmatrix} \right] N(x) + \mathcal{O}(q^5)\ . \end{aligned} \tag{3.14}$$

The Dirac matrices are defined as,

$$\gamma^0 = \begin{pmatrix} 1 & 0 \\ 0 & -1 \end{pmatrix}, \gamma^5 = \begin{pmatrix} 0 & 1 \\ 1 & 0 \end{pmatrix}, \boldsymbol{\gamma} = \begin{pmatrix} 0 & \boldsymbol{\sigma} \\ -\boldsymbol{\sigma} & 0 \end{pmatrix}, \sigma^{\mu\nu} = \frac{i}{2}\left[\gamma^\mu, \gamma^\nu\right]. \tag{3.15}$$

5. Following Ref. [111], its antiparticle component has been dropped for simplicity.

with the $\boldsymbol{\sigma} = (\sigma_1, \sigma_2, \sigma_3)$ the Pauli spin matrices.

Using these relations and the properties of Pauli matrices, one can perform the non-relativistic expansion of the covariant Lagrangian of Table 3.3. The results are summarized in Table 3.4. They are presented as linear combinations of the non-relativistic Lagrangian O_i defined in Table A.1. One can easily check that there are 24 linear independent terms, consistent with the well-known $2 + 7 + 15$ non-relativistic terms shown in Table A.1 in the Appendix.

3.3 . Summary

We have constructed a complete set of relativistic NN contact Lagrangians up to order $\mathcal{O}(q^4)$. Using the EOM to eliminate the redundant terms, we find only 4 terms of $\mathcal{O}(q^0)$, 13 terms of $\mathcal{O}(q^2)$, and 23 terms of $\mathcal{O}(q^4)$. We compared with previous studies and identified the differences and the reasoning behind them. In addition, we checked that by performing $1/m_n$ expansions, one can recover the corresponding non-relativistic chiral Lagrangians, which has 24 terms up to $\mathcal{O}(q^4)$. The covariant Lagrangian constructed in the present work can be of use in building covariant nuclear forces as well as studying relativistic corrections.

It should be emphasized that the completeness and minimality of the set of covariant Lagrangians derived in the present work should be understood with respect to the power counting rules we chose and the choice we made regarding how to use the equation of motion to remove redundant terms and to limit the number of available terms. More precisely, they may better be referred to as an economical set of covariant Lagrangians that can recover those of the heavy baryon. We hope that the present work can motivate more studies in this direction.

Table 3.4 – The non-relativistic expressions corresponding to the contact interactions of Table 3.3.

$\tilde{O}_1$	$O_S + \frac{1}{4m_n^2}(O_1 - 2O_2 + 2O_3) + \frac{1}{16m_n^4}(3O_8 - 4O_9 + O_{10} + O_{11} + 4O_{12} - 2O_{13} - O_{16} + O_{17} - O_{21} - O_{22})$
$\tilde{O}_2$	$O_S + \frac{1}{4m_n^2}(4O_2 - 6O_3 + O_4 + 2O_5 + O_6 + 2O_7) + \frac{1}{16m_n^4}(8O_9 - O_{10} + O_{11} - 12O_{12} - 2O_{13} + 3O_{14} + 4O_{15} + O_{16} + O_{17} + 3O_{18} + 4O_{19} - O_{22})$
$\tilde{O}_3$	$-O_T + \frac{1}{4m_n^2}(-2O_3 - O_4 + 2O_5 - O_6 + 6O_7) + \frac{1}{16m_n^4}(O_{10} - O_{11} - 4O_{12} + 2O_{13} - 3O_{14} + 4O_{15} - O_{16} - O_{17} - 3O_{18} + 12O_{19} - 2O_{22})$
$\tilde{O}_4$	$2O_T + \frac{1}{4m_n^2}(2O_1 + 4O_2 - 12O_3 + 8O_5 - 2O_6 + 12O_7) + \frac{1}{16m_n^4}(6O_8 + 8O_9 + 2O_{10} + 2O_{11} - 24O_{12} - 4O_{13} + 16O_{15} - 2O_{16} + 2O_{17} - 6O_{18} + 24O_{19} - 4O_{21} + 4O_{22})$
$\tilde{O}_5$	$-\frac{1}{4m_n^2}(O_6 + 2O_7) - \frac{1}{16m_n^4}(3O_{18} + 4O_{19} + O_{21})$
$\tilde{O}_6$	$\frac{1}{4m_n^2}(-4O_6 + 8O_7) + \frac{1}{16m_n^4}(-4O_{18} + 4O_{21})$
$\tilde{O}_7$	$\frac{1}{4m_n^2}(O_1 + 2O_2 - 8O_3 - 4O_4 + 8O_5 - 4O_6 + 8O_7) + \frac{1}{16m_n^4}(-4O_{10} + 4O_{11} + 2O_{12} - 12O_{13} - 4O_{14} + 8O_{17} - 4O_{18} - 4O_{21} - 8O_{22})$
$\tilde{O}_8$	$\frac{1}{4m_n^2}(O_1 + 2O_2 - 4O_3) + \frac{1}{16m_n^4}(-2O_{12} + 4O_{13} + 4O_{16} - 4O_{17} + 4O_{21} + 4O_{22})$
$\tilde{O}_9$	$\frac{1}{4m_n^2}(-O_4 - 2O_5 - O_6 - 2O_7) + \frac{1}{16m_n^4}(-O_8 - 4O_9 - 2O_{10} - 4O_{11} + 6O_{12} + 12O_{13} - O_{14} - 4O_{15} + 2O_{16} - 8O_{17} - O_{18} - 4O_{19} + 5O_{21} + 8O_{22})$
$\tilde{O}_{10}$	$\frac{1}{4m_n^2}(-O_1 - 2O_2) + \frac{1}{16m_n^4}(-2O_8 + 4O_{11} - 2O_{12} - 4O_{13})$
$\tilde{O}_{11}$	$\frac{1}{4m_n^2}(-O_1 - 2O_2) + \frac{1}{16m_n^4}(-O_8 - 4O_9 + 2O_{10} - 8O_{11} + 6O_{12} + 12O_{13} - O_{14} - 4O_{15} - 2O_{16} - 4O_{17} - O_{18} - 2O_{19} - 2O_{20} - O_{21} - 4O_{22})$
$\tilde{O}_{12}$	$\frac{1}{4m_n^2}(O_4 + 2O_5) + \frac{1}{16m_n^4}(2O_{12} + 4O_{13} + 2O_{14} - 4O_{17} + O_{18} - 6O_{19} + 2O_{20} + O_{21} - 12O_{22})$
$\tilde{O}_{13}$	$\frac{1}{4m_n^2}(-2O_4 - 4O_5) + \frac{1}{16m_n^4}(-2O_8 - 8O_9 - 4O_{10} - 8O_{11} + 12O_{12} + 24O_{13} - 2O_{14} - 8O_{15} + 4O_{16} - 16O_{17} + 2O_{18} - 12O_{19} + 4O_{20} + 2O_{21} - 24O_{22})$
$\tilde{O}_{14}$	$\frac{1}{4m_n^2}(-3O_1 + 2O_2) + \frac{1}{16m_n^4}(-4O_8 + 8O_9 - 4O_{10} - 4O_{11} - 6O_{12} + 4O_{13})$
$\tilde{O}_{15}$	$\frac{1}{4m_n^2}(-3O_1 + 2O_2) + \frac{1}{16m_n^4}(-O_8 - 12O_9 + 2O_{10} + 8O_{11} + 18O_{12} - 12O_{13} - 3O_{14} - 4O_{15} - 6O_{16} + 4O_{17} - 3O_{18} - 6O_{19} + 2O_{20} - 3O_{21} + 4O_{22})$
$\tilde{O}_{16}$	$\frac{1}{4m_n^2}(3O_4 - 2O_5) + \frac{1}{16m_n^4}(6O_{12} - 4O_{13} + 4O_{14} - 8O_{15} + 4O_{16} + 4O_{17} + 3O_{18} - 18O_{19} - 2O_{20} + 3O_{21} + 12O_{22})$
$\tilde{O}_{17}$	$\frac{1}{4m_n^2}(-6O_4 + 4O_5) + \frac{1}{16m_n^4}(-6O_8 - 8O_9 - 12O_{10} + 8O_{11} + 36O_{12} - 24O_{13} - 2O_{14} - 24O_{15} + 4O_{16} + 16O_{17} + 6O_{18} - 36O_{19} - 4O_{20} + 6O_{21} + 24O_{22})$
$\tilde{O}_{18}$	$\frac{1}{16m_n^4}(O_{18} + 2O_{19} + 2O_{20} + O_{21} + 4O_{22})$
$\tilde{O}_{19}$	$\frac{1}{16m_n^4}(4O_{18} - 8O_{19} + 8O_{20} + 4O_{21} - 16O_{22})$
$\tilde{O}_{20}$	$\frac{1}{16m_n^4}(O_8 + 4O_9 + 2O_{10} + 4O_{11} - 8O_{12} - 16O_{13} - 4O_{14} - 8O_{16} + 16O_{17} - 4O_{18} + 8O_{19} - 8O_{20} - 4O_{21} + 16O_{22})$
$\tilde{O}_{21}$	$\frac{1}{16m_n^4}(-O_8 - 4O_9 - 2O_{10} - 4O_{11} + 4O_{12} + 8O_{13})$
$\tilde{O}_{22}$	$\frac{1}{16m_n^4}(O_{14} + 4O_{15} + 2O_{16} + 4O_{17} + O_{18} + 2O_{19} + 2O_{20} + O_{21} + 4O_{22})$
$\tilde{O}_{23}$	$\frac{1}{16m_n^4}(-O_8 - 4O_9 - 2O_{10} - 4O_{11} + 8O_{12} + 16O_{13} + 16O_{16} - 16O_{17} + 16O_{21} + 16O_{22})$
$\tilde{O}_{24}$	$\frac{1}{16m_n^4}(O_8 + 4O_9 + 2O_{10} + 4O_{11})$
$\tilde{O}_{25}$	$\frac{1}{16m_n^4}(O_8 + 4O_9 + 2O_{10} + 4O_{11})$
$\tilde{O}_{26}$	$\frac{1}{16m_n^4}(-O_{14} - 4O_{15} - 2O_{16} - 4O_{17})$
$\tilde{O}_{27}$	$\frac{1}{16m_n^4}(2O_{14} + 8O_{15} + 4O_{16} + 8O_{17})$
$\tilde{O}_{28}$	$\frac{1}{16m_n^4}(3O_{18} + 6O_{19} - 2O_{20} + 3O_{21} - 4O_{22})$
$\tilde{O}_{29}$	$\frac{1}{16m_n^4}(12O_{18} - 24O_{19} - 8O_{20} + 12O_{21} + 16O_{22})$
$\tilde{O}_{30}$	$\frac{1}{16m_n^4}(-3O_8 - 4O_9 - 6O_{10} + 4O_{11} + 24O_{12} - 16O_{13} + 12O_{14} - 32O_{15} + 24O_{16} + 16O_{17} + 12O_{18} - 24O_{19} - 8O_{20} + 12O_{21} + 16O_{22})$
$\tilde{O}_{31}$	$\frac{1}{16m_n^4}(-O_8 - 4O_9 - 2O_{10} - 4O_{11} + 4O_{12} + 8O_{13})$
$\tilde{O}_{32}$	$\frac{1}{16m_n^4}(3O_{14} + 4O_{15} + 6O_{16} - 4O_{17} + 3O_{18} + 6O_{19} - 2O_{20} + 3O_{21} - 4O_{22})$
$\tilde{O}_{33}$	$\frac{1}{16m_n^4}(3O_8 + 4O_9 + 6O_{10} - 4O_{11})$
$\tilde{O}_{34}$	$\frac{1}{16m_n^4}(3O_8 + 4O_9 + 6O_{10} - 4O_{11})$
$\tilde{O}_{35}$	$\frac{1}{16m_n^4}(-3O_{14} - 4O_{15} - 6O_{16} + 4O_{17})$
$\tilde{O}_{36}$	$\frac{1}{16m_n^4}(6O_{14} + 8O_{15} + 12O_{16} - 8O_{17})$
$\tilde{O}_{37}$	$\frac{1}{16m_n^4}(9O_8 - 12O_9 + 18O_{10} + 4O_{11})$
$\tilde{O}_{38}$	$\frac{1}{16m_n^4}(9O_8 - 12O_9 + 18O_{10} + 4O_{11})$
$\tilde{O}_{39}$	$\frac{1}{16m_n^4}(-9O_{14} + 12O_{15} - 18O_{16} - 4O_{17})$
$\tilde{O}_{40}$	$\frac{1}{16m_n^4}(18O_{14} - 24O_{15} + 36O_{16} + 8O_{17})$

4 - Two-pion exchange contributions to the nucleon-nucleon interaction in covariant baryon chiral perturbation theory

Apart from the nucleon-nucleon contact Lagrangians, the contributions from the TPE are also necessary for our goals. In this chapter, employing the covariant baryon chiral perturbation theory, we calculate the leading and next-to-leading order TPE contributions to NN interaction up to order $O(q^3)$. We compare the so-obtained NN phase shifts with $2 \leq L \leq 6$ and mixing angles with $2 \leq J \leq 6$ with those obtained in the nonrelativistic baryon chiral perturbation theory, which allows us to check the relativistic corrections to the medium-range part of NN interactions. We show that the contributions of relativistic TPE are more moderate than those of the nonrelativistic TPE. The relativistic corrections play an important role in F-waves especially the $^3\mathrm{F}_2$ partial wave. Moreover, the relativistic results seem to converge faster than the nonrelativistic results in almost all the partial waves studied in the present work, consistent with the studies performed in the one-baryon sector.

The chapter is organized as follows. In Sec. 4.1, the chiral Lagrangians needed for computing the two-pion exchange contributions are briefly discussed. The TPE T-matrix up to the third order is presented in Sec. 4.2. In sec. 4.3, we compare the so-obtained NN phase shifts with the Nijmegen partial wave analysis and those of Ref. [61]. A short summary and outlook is given in the last section.

4.1 . Chiral Lagrangian

In order to calculate the contributions of two-pion exchanges, we need the following LO and NLO πN Lagrangians,

$$\mathcal{L} = \mathcal{L}^{(1)}_{\pi N} + \mathcal{L}^{(2)}_{\pi N}, \tag{4.1}$$

where the superscript refers to the respective chiral order, and they read [112, 116], respectively,

$$\mathcal{L}^{(1)}_{\pi N} = \bar{N}\left(\mathrm{i}D\!\!\!/ - m_n + \frac{g_A}{2}u\!\!\!/\gamma_5\right)N, \tag{4.2}$$

$$\mathcal{L}^{(2)}_{\pi N} = c_1\langle\chi_+\rangle\bar{N}N - \frac{c_2}{4m_n^2}\langle u^\mu u^\nu\rangle\left(\bar{N}D_\mu D_\nu N + h.c.\right) + \frac{c_3}{2}\langle u^2\rangle\bar{N}N - \frac{c_4}{4}\bar{N}\gamma^\mu\gamma^\nu\left[u_\mu, u_\nu\right]N, \tag{4.3}$$

where the nucleon field $N = (p, n)^T$, and the covariant derivative D_μ is defined as $D_\mu = \partial_\mu + \Gamma_\mu$ with

$$\Gamma_\mu = \frac{1}{2}\left(u^\dagger\partial_\mu u + u\partial_\mu u^\dagger\right), \qquad u = \exp\left(\frac{\mathrm{i}\Phi}{2f_\pi}\right).$$

The pion field Φ is a 2×2 matrix of the following form,

$$\Phi = \begin{pmatrix} \pi^0 & \sqrt{2}\pi^+ \\ \sqrt{2}\pi^- & -\pi^0 \end{pmatrix},$$

and the axial current type quantity u_μ is defined as,

$$u_\mu = \mathrm{i}\left(u^\dagger \partial_\mu u - u \partial_\mu u^\dagger\right),$$

where $\chi_+ = u^\dagger \chi u + u \chi u^\dagger$ with $\chi = \mathcal{M} = diag\left(m_\pi^2, m_\pi^2\right)$. The following values for the relevant LECs and masses are adopted in the numerical calculation : The pion decay constant $f_\pi = 92.4$ MeV, the axial coupling constant $g_A = 1.29$ [67] [1], the nucleon mass $m_n = 939$ MeV, the pion mass $m_\pi = 139$ MeV [103], and the low-energy constants $c_1 = -1.39$, $c_2 = 4.01$, $c_3 = -6.61$, $c_4 = 3.92$, all in units of GeV^{-1}, taken from Ref. [116] . The values of $c_{1,2,3,4}$ employed in this work are different from the standard values (of HB ChPT) due to the different renormalization schemes adopted. In Ref. [116], the pion-nucleon scattering is studied in the EOMS scheme, which is also the scheme we adopted in this work, while previous calculations are mainly based on the HB scheme. Therefore, we took the values of $c_{1,2,3,4}$ from Ref. [116] for self-consistency. We cannot use the HB values of $c_{1,2,3,4}$ because then the description of pion-nucleon scattering would be ruined. One should note that the complete $\mathcal{L}_{\pi N}^{(2)}$ contains more terms than what are relevant here.

4.2 . Two-pion exchange contributions

4.2.1 . Leading order ($O(q^2)$) results

The two-pion exchange T-matrix is evaluated in the center-of-mass frame and in the isospin limit $m_u = m_d$. The leading order TPE diagrams are shown in Fig. 4.1. They contribute to order $O(q^2)$. All of them can be calculated directly in the EOMS scheme [100, 101], which is just the conventional dimensional regularization scheme with further removal of PCB terms. There is no so-called pinch singularity [57, 58, 61] in this case due to the appearance of the finite nucleon mass. Note that only direct diagrams need to be computed in the NN T-matrix because of the Pauli exclusion principle [61]. In principle, the box diagram includes contributions from irreducible TPE and iterated OPE. As a matter of fact, we have calculated the iterated OPE by inserting the relativistic OPE potential [75] into the Lippmann-Schwinger equation and found that the result is numerically identical to that in Ref. [61]. For this reason, the contributions from iterated OPE are not presented explicitly.

1. This choice is made in order to be consistent with Refs. [64, 65, 66, 67, 48, 68, 50]. Using the more standard value $g_A = 1.267$ yields almost the same results.

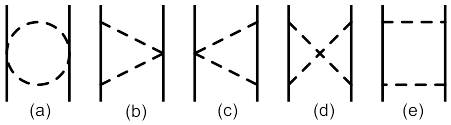

Figure 4.1 – Two-pion exchange diagrams at $O(q^2)$. The pion nucleon vertices refer to vertices from $\mathcal{L}^{(1)}_{\pi N}$

.

Table 4.1 – Products of isospin and coupling factors of two-pion exchange diagrams at $O(q^2)$

	football	triangle L	triangle R	box	crossed
$I=1$	$\frac{1}{8}$	$\frac{1}{8}g_A^2$	$\frac{1}{8}g_A^2$	$\frac{1}{16}g_A^4$	$\frac{5}{16}g_A^4$
$I=0$	$-\frac{3}{8}$	$-\frac{3}{8}g_A^2$	$-\frac{3}{8}g_A^2$	$\frac{9}{16}g_A^4$	$-\frac{3}{16}g_A^4$

The complete TPE contributions to the on-shell NN T-matrix are decomposed into the scalar integrals A_0, B_0, C_0 and D_0 multiplied with some polynomials and fermion bilinears using FeynCalc [117, 118, 119] and then calculated numerically with the help of OneLOop [120, 121]. The procedure to remove the PCB terms is rather standard and has been discussed in detail in Refs. [100, 101, 102, 122]. At the end, the total TPE contributions to the on-shell NN T-matrix at $O(q^2)$ take the following form,

$$\mathcal{T}^{(2)}_{NN} = \frac{1}{16\pi^2 f_\pi^4} \sum_i N_i \mathcal{T}^{(2)}_i, \tag{4.4}$$

where i refers to the i-th Feynman diagram contributing at this order, N_i denotes the product of isospin and coupling factors which is summarized in Table 4.1, $\mathcal{T}^{(2)}_i$ refers to the T-matrix from each Feynman diagram and

$$\mathcal{T}^{(2)}_i = \mathcal{T}'^{(2)}_i - \mathcal{T}''^{(2)}_i, \tag{4.5}$$

where $\mathcal{T}'^{(2)}_i$ denotes the total contribution to T-matrix and $\mathcal{T}''^{(2)}_i$ is the contribution from the PCB term. The total contributions to T-matrix for the football, triangle,

cross and box diagrams read explicitly

$$\mathcal{T}'^{(2)}_{\text{Football}} = -\frac{1}{18}\mathcal{B}_2\left[3\left(4m_\pi^2 - t\right)B_0\left(t, m_\pi^2, m_\pi^2\right) + 6\mathsf{A}_0\left(m_\pi^2\right) + 12m_\pi^2 - 2t\right], \tag{4.6}$$

$$\begin{aligned}
\mathcal{T}'^{(2)}_{\text{TrigL}} &= 4m_n^2\left\{\mathcal{B}_3 m_n\left[2\left(2f_1 + f_2 + f_3\right) + C_0\left(\mathsf{A}\right)\right] + 2\mathcal{B}_2 f_4\right\} + 2\mathcal{B}_2 f_5,\\
\mathcal{T}'^{(2)}_{\text{TrigR}} &= \mathcal{T}'^{(2)}_{\text{TrigL}}(\mathcal{B}_3 \mapsto \mathcal{B}_4),\\
\mathcal{T}'^{(2)}_{\text{Cross}} &= -\left\{2m_n^2\left\{m_n\left[2\left(\mathcal{B}_3 + \mathcal{B}_4\right)\left(f_2 + f_3\right) + 4\left(4\mathcal{B}_1 m_n + \mathcal{B}_3 + \mathcal{B}_4\right)f_1\right.\right.\right.\\
&\quad + \left(4\mathcal{B}_1 m_n + \mathcal{B}_3\right)C_0\left(\mathsf{A}\right) + \left(4\mathcal{B}_1 m_n + \mathcal{B}_4\right)C_0\left(\mathsf{B}\right)\Big] + 4\left\{\mathcal{B}_2 f_4 + m_n^2\left[\left(\mathcal{B}_3 + \mathcal{B}_4\right)\right.\right.\\
&\quad \left.\left.\left.\times D_{22} m_n + D_{23}\left(2\mathcal{B}_1 m_n^2 + \mathcal{B}_5\right) + 2\mathcal{B}_2 D_{00}\right]\right\} + 2\mathcal{B}_1 B_0\left(t, m_\pi^2, m_\pi^2\right)\right\} + \mathcal{B}_2 f_5\Big\},\\
V'^{(2)}_{\text{Box}} &= -\left\{2m_n^2\left\{m_n\left[-2\left(\mathcal{B}_3 + \mathcal{B}_4\right)\left(f_2 + f_3\right) + 4\left(4\mathcal{B}_1 m_n - \mathcal{B}_3 - \mathcal{B}_4\right)f_1\right.\right.\right.\\
&\quad + \left(4\mathcal{B}_1 m_n - \mathcal{B}_3\right)C_0\left(\mathsf{A}\right) + \left(4\mathcal{B}_1 m_n - \mathcal{B}_4\right)C_0\left(\mathsf{B}\right)\Big] - 4\left\{\mathcal{B}_2 f_4 + m_n^2\left[\left(\mathcal{B}_3 + \mathcal{B}_4\right)\right.\right.\\
&\quad \left.\left.\left.\times D_{22} m_n - D_{23}\left(2\mathcal{B}_1 m_n^2 + \mathcal{B}_5\right) + 2\mathcal{B}_2 D_{00}\right]\right\} + 2\mathcal{B}_1 B_0\left(t, m_\pi^2, m_\pi^2\right)\right\} - \mathcal{B}_2 f_5\Big\},
\end{aligned}$$

with

$$\begin{aligned}
f_1 &= \mathsf{PaVe}\left(1, \left\{m_n^2, t, m_n^2\right\}, \left\{m_n^2, m_\pi^2, m_\pi^2\right\}\right),\\
f_2 &= \mathsf{PaVe}\left(1, 1, \left\{m_n^2, t, m_n^2\right\}, \left\{m_n^2, m_\pi^2, m_\pi^2\right\}\right),\\
f_3 &= \mathsf{PaVe}\left(1, 2, \left\{m_n^2, t, m_n^2\right\}, \left\{m_n^2, m_\pi^2, m_\pi^2\right\}\right),\\
f_4 &= \mathsf{PaVe}\left(0, 0, \left\{m_n^2, t, m_n^2\right\}, \left\{m_n^2, m_\pi^2, m_\pi^2\right\}\right),\\
f_5 &= \mathsf{PaVe}\left(0, 0, \{t\}, \left\{m_\pi^2, m_\pi^2\right\}\right),\\
C_0(\mathsf{A}) &= C_0\left(m_n^2, m_n^2, t, m_\pi^2, m_n^2, m_\pi^2\right),\\
C_0(\mathsf{B}) &= C_0\left(m_n^2, t, m_n^2, m_n^2, m_\pi^2, m_\pi^2\right),
\end{aligned} \tag{4.7}$$

where D_{ij} and PaVe are the library functions of FeynCalc [117, 118, 119] and can be simplified to the scalar integrals A_0, B_0, C_0, D_0, and $\mathcal{B}_{1-5}$ denote the following fermion bilinears,

$$\begin{aligned}
\mathcal{B}_1 &= \bar{u}(\boldsymbol{p}')u(\boldsymbol{p})\bar{u}(-\boldsymbol{p}')u(-\boldsymbol{p}),\\
\mathcal{B}_2 &= \bar{u}(\boldsymbol{p}')\gamma^\mu u(\boldsymbol{p})\bar{u}(-\boldsymbol{p}')\gamma_\mu u(-\boldsymbol{p}),\\
\mathcal{B}_3 &= \bar{u}(\boldsymbol{p}')(\not{p}_2 + \not{p}_4)u(\boldsymbol{p})\bar{u}(-\boldsymbol{p}')u(-\boldsymbol{p}),\\
\mathcal{B}_4 &= \bar{u}(\boldsymbol{p}')u(\boldsymbol{p})\bar{u}(-\boldsymbol{p}')(\not{p}_1 + \not{p}_3)u(-\boldsymbol{p}),\\
\mathcal{B}_5 &= \bar{u}(\boldsymbol{p}')(\not{p}_2 + \not{p}_4)u(\boldsymbol{p})\bar{u}(-\boldsymbol{p}')\not{p}_1 u(-\boldsymbol{p}),
\end{aligned} \tag{4.8}$$

where $\boldsymbol{p}, \boldsymbol{p}'$are incoming and outgoing three momentum, $p_1^\mu = (E, \boldsymbol{p})$, $p_2^\mu = (E, -\boldsymbol{p})$, $p_3^\mu = (E', \boldsymbol{p}')$, $p_4^\mu = (E', -\boldsymbol{p}')$, $E = \sqrt{\boldsymbol{p}^2 + m_n^2}$, $E' = \sqrt{\boldsymbol{p}'^2 + m_n^2}$, $t = (p_1 - p_3)^2$, $u(\boldsymbol{p})$ and $\bar{u}(\boldsymbol{p})$ are Dirac spinors as defined in chapter 3. To obtain the T-matrix from the PCB terms, it is convenient to project the T-matrix from

momentum space to helicity space so that the T-matrix become scalar without the Pauli matrix and can easily be expanded in powers of small parameters. The detailed procedure to do this projection is explained later. However, because of their complexity, we do not show the explicit expressions of $\mathcal{T}'$ in helicity space here. One thing to be noted is that the above bilinears are all parity even. This can be easily shown by utilizing momentum conservation and the Dirac equation, e.g.,

$$\begin{aligned}\mathcal{B}_5 &= \bar{u}(\boldsymbol{p}')\left(\not{p}_2+\not{p}_4\right)u(\boldsymbol{p})\bar{u}(-\boldsymbol{p}')\not{p}_1 u(-\boldsymbol{p}) \\ &= \bar{u}(\boldsymbol{p}')\left(\not{p}_2+\not{p}_4\right)u(\boldsymbol{p})\bar{u}(-\boldsymbol{p}')\frac{1}{2}\left(\not{p}_1+\not{p}_3+\not{p}_4-\not{p}_2\right)u(-\boldsymbol{p}) \\ &= \frac{1}{2}\bar{u}(\boldsymbol{p}')\left(\not{p}_2+\not{p}_4\right)u(\boldsymbol{p})\bar{u}(-\boldsymbol{p}')\left(\not{p}_1+\not{p}_3\right)u(-\boldsymbol{p}) \\ &\xrightarrow{\text{Parity}} \mathcal{B}_5.\end{aligned}$$

The T-matrices from the PCB terms in helicity space read,

$$\begin{aligned}\mathcal{T}''^{(2)}_{\text{Football}} &= 0, \\ \mathcal{T}''^{(2)}_{\text{TrigL}} &= 4H_1 m_n^2 \ln\left(\frac{\mu}{m_n}\right), \\ \mathcal{T}''^{(2)}_{\text{TrigR}} &= \mathcal{T}''_{\text{TrigL}}, \\ \mathcal{T}''^{(2)}_{\text{Cross}} &= -4H_1 m_n^2\left[3\ln\left(\frac{\mu}{m_n}\right)-1\right], \\ \mathcal{T}''^{(2)}_{\text{Box}} &= -4H_1 m_n^2\left[\ln\left(\frac{\mu}{m_n}\right)+1\right],\end{aligned} \tag{4.9}$$

where μ refers to the renormalization scale and is set to 1 GeV in our numerical study unless otherwise stated, H_1 is,

$$H_1 = \left[|\bar{\lambda}_1+\lambda_1|\cos\left(\frac{\theta}{2}\right)+|\bar{\lambda}_1-\lambda_1|\sin\left(\frac{\theta}{2}\right)\right]\left[|\bar{\lambda}_2+\lambda_2|\cos\left(\frac{\theta}{2}\right)-|\bar{\lambda}_2-\lambda_2|\sin\left(\frac{\theta}{2}\right)\right], \tag{4.10}$$

where $\lambda_{1,2}, \bar{\lambda}_{1,2}$ denote the helicities of incoming, outgoing particles respectively and θ refers to the scattering angle.

4.2.2 . Next-to-leading order ($O(q^3)$) results

The next-to-leading order TPE diagrams are shown in Fig. 4.2. These diagrams are the same as the corresponding diagrams shown in Fig. 4.1 with the replacement of the πN vertices $\mathcal{L}^{(1)}_{\pi N}$ with $\mathcal{L}^{(2)}_{\pi N}$. Note that there is no box diagram or cross diagram at this order because there is no πNN vertex at order $O(q^2)$.

The next-to-leading order TPE contributions to T-matrix read,

$$\mathcal{T}^{(3)}_{NN} = \mathcal{T}^{(3)}_{\text{FootballL}} + \mathcal{T}^{(3)}_{\text{FootballR}} + \mathcal{T}^{(3)}_{\text{TrigL}} + \mathcal{T}^{(3)}_{\text{TrigR}}, \tag{4.11}$$

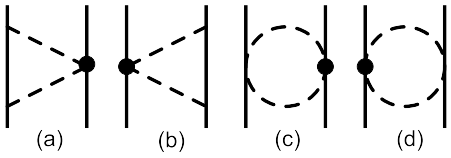

Figure 4.2 – Two-pion exchange diagrams at $O(q^3)$. The black dots denote vertices from $\mathcal{L}^{(2)}_{\pi N}$

.

where the notation is the same as that stated above. The products of isospin and coupling factors have been included in the T-matrix at this order for simplicity.

$$\mathcal{T}^{(3)\prime}_{\text{FootballL}} = \frac{(4I-3)c_4}{72}\left(2\mathcal{B}_2 m_n - \mathcal{B}_4\right)\left[3\left(t-4m_\pi^2\right)B_0\left(t,m_\pi^2,m_\pi^2\right) - 6A_0\left(m_\pi^2\right) + 2\left(t-6m_\pi^2\right)\right], \tag{4.12}$$

$$\begin{aligned}
\mathcal{T}^{(3)\prime}_{\text{FootballR}} &= \mathcal{T}^{(3)\prime}_{\text{FootballL}}(\mathcal{B}_4 \to \mathcal{B}_3),\\
\mathcal{T}^{(3)\prime}_{\text{TrigL}} &= 6c_1 m_n m_\pi^2 \mathcal{B}_1\left[2m_n^2\left(2f_1 + C_0(\mathsf{A})\right) + B_0(t,m_\pi^2,m_\pi^2)\right] + \ldots \quad ,\\
\mathcal{T}^{(3)\prime}_{\text{TrigR}} &= 6c_1 m_n m_\pi^2 \mathcal{B}_1\left[2m_n^2\left(2f_1 + C_0(\mathsf{A})\right) + B_0(t,m_\pi^2,m_\pi^2)\right] + \ldots \quad .
\end{aligned}$$

The T-matrices from PCB terms in helicity space read,

$$\begin{aligned}
\mathcal{T}^{(3)\prime\prime}_{\text{FootballL}} &= 0, \qquad (4.13)\\
\mathcal{T}^{(3)\prime\prime}_{\text{FootballR}} &= 0,\\
\mathcal{T}^{(3)\prime\prime}_{\text{TrigL}} &= 6c_1 H_1 m_n m_\pi^2\left[2\ln\left(\frac{\mu}{m_n}\right)+1\right] + \ldots \quad ,\\
\mathcal{T}^{(3)\prime\prime}_{\text{TrigR}} &= 6c_1 H_1 m_n m_\pi^2\left[2\ln\left(\frac{\mu}{m_n}\right)+1\right] + \ldots \quad .
\end{aligned}$$

where $I = 0, 1$ refers to the isospin. The full expressions of the T-matrix from the triangle diagrams at this order are not given explicitly due to their complexity [2].

In order to compute the phase shifts, we need to transform the T-matrix into LSJ basis where L is the total orbital angular momentum, S is the total spin, and J is the total angular momentum. The procedure for the partial wave projection is rather standard [123, 124]. Here we refer to Ref. [124] for more details. At first, we compute the T-matrix directly in momentum space. Then, we transfer it to helicity basis. Next, it is rotated to the total angular momentum space $|JM\rangle$ using the Wigner d-functions. Last, it is projected to LSJ basis. In order to compute

2. They could be obtained as a Mathematica notebook from the authors upon request.

the phase shifts and mixing angle, we follow the procedure of Ref. [125],

$$\delta_{LSJ} = -\frac{m_n^2|\boldsymbol{p}|}{16\pi^2 E}\ \mathrm{Re}\langle LSJ|\mathcal{T}_{NN}|LSJ\rangle, \tag{4.14}$$
$$\epsilon_J = \frac{m_n^2|\boldsymbol{p}|}{16\pi^2 E}\ \mathrm{Re}\langle J-1,1,J|\mathcal{T}_{NN}|J+1,1,J\rangle.$$

Note that the kinematical prefactors here differ from those of Ref.[61] due to a different sign convention for the NN T-matrix and a different normalization of the matrix elements obtained by partial wave projection.

4.3 . Results and discussions

In this section, the phase shifts with $2 \leq L \leq 6$ and mixing angles with $2 \leq J \leq 6$ in the relativistic framework are presented and compared with those of the nonrelativistic results of Ref. [61]. But before showing the phase shifts, the choice of the LECs $c_{1,2,3,4}$ needs to be clarified. As we stated above, the values of $c_{1,2,3,4}$ adopted in this work are larger than those of Ref. [126] because of different renomalization schemes. In Ref. [116], the four LECs are determined by fitting to πN scattering phase shifts in the EOMS approach at order $O(q^3)$, while in Ref. [126], they are fixed from a fit to nine πN observables in the HB scheme at one-loop order $O(q^3)$. For the sake of self-consistency, we thereby took the values of $c_{1,2,3,4}$ from Ref. [116] for the EOMS case and those of Ref. [126] for the HB case. Otherwise the descriptions of πN scattering in both schemes will be ruined. As a matter of fact, we have performed the nonrelativistic calculation with $c_{1,2,3,4}$ fixed at the values of Ref. [116] and found that the corresponding results are worse than those of Ref. [61].

4.3.1 . D-wave

The D-wave phase shifts and mixing angle ϵ_2 are shown in Fig. 4.3. The black dots refer to the Nijmegen partial wave phase shifts [34]. The Green dashed lines refer to the contributions from relativistic OPE [75], the blue dash dotted lines represent the contributions from the leading order TPE, the red curves contain the next-to-leading order TPE, while the black curves are their nonrelativistic counterparts [61] with g_A fixed at 1.29. The bands are generated by varying μ from 0.5 GeV to 1.5 GeV. The relativistic OPE is independent of μ since it contributes at tree level. The relativistic leading order TPE is also independent of μ for partial waves with $L \geq 2$. Nonetheless, the next-to-leading order relativistic TPE depends considerably on μ for the $^3\mathrm{D}_1$, $^1\mathrm{D}_2$ and $^3\mathrm{D}_2$ partial waves and shows little dependence on μ for the $^3\mathrm{D}_3$ partial wave and mixing angle ϵ_2. On the other hand, the nonrelativistic results are independent of μ [61]. For all the cases the chiral NN phase shifts are in good agreement with data up to $T_{\mathrm{lab}} = 50$ MeV, and the relativistic results show the same tendency as their nonrelativistic counterparts, but the TPE contributions are more moderate, so for all the D-waves the relativistic

results are in better agreement with the Nijmegen phase shifts perhaps with the exception of $^3\mathrm{D}_1$ for $T_{\mathrm{lab}} \geq 150$ MeV, where both descriptions show a much stronger u-turn shape, inconsistent with data. The nonrelativistic result for $^3\mathrm{D}_1$ is in fair agreement with data up to $T_{\mathrm{lab}} = 200$ MeV due to the cancellation of irreducible TPE and iterated OPE [61], while in the relativistic case, the contribution of the next-to-leading order TPE is somehow a little bit larger than the nonrelativistic counterparts so that the curve shifts somewhat upwards. The mixing angle ϵ_2 in the relativistic method is in better agreement with data due to the moderate contribution from the irreducible parts of TPE. Although the relativistic corrections are sizeable in D-wave and improve the description of data, the still relatively large discrepancy indicates the need of short-range contributions, namely the contact terms controlled by LECs.

A few words are in order for the convergence pattern. For the coupled channels, because of the cancellation of the irreducible part and the iterated part in the leading order TPE, the contribution of the next-to-leading order TPE is very large compared with that of the leading order TPE. But for the singlet channel $^1\mathrm{D}_2$, contrast to our expectation, the iterated part contributes negligibly to the phase shifts while the next-to-leading order TPE contributes a lot. Moreover, the contribution of the next-to-leading order TPE seems to be larger than the contribution of OPE. All in all, although the relativistic results are quantitatively better than the nonrelativistic results, pion-exchange contributions alone are not enough to explain the D-wave data, as concluded in Ref. [61].

4.3.2 . F-wave

The F-wave phase shifts and mixing angle ϵ_3 are depicted in Fig. 4.4. The relativistic chiral phase shifts only show moderate dependence on μ for the $^3\mathrm{F}_2$ partial wave and the variation of μ yields indistinguishable difference for the others. As in the D-wave case, the relativistic TPE is moderate so that overall the phase shifts are in better agreement with data. For the $^1\mathrm{F}_3$ partial wave, the relativistic results are almost identical to data up to $T_{\mathrm{lab}} = 200$ MeV. For the $^3\mathrm{F}_3$ partial wave, the relativistic phase shifts are slightly better than the nonrelativistic ones. For the $^3\mathrm{F}_4$ partial wave, the two results are almost identical. However, for the $^3\mathrm{F}_2$ partial wave, the contributions from the next-to-leading order TPE are very small due to the cancellation of the contributions from c_3 and c_4 which leads to a fair agreement with data for $T_{\mathrm{lab}} \leq 210$ MeV. In addition, the fact that the contributions of leading order relativistic TPE are relatively small indicates a good convergence at least up to $O(q^2)$. The contributions of the next-to-leading order TPE are a bit large for the $^1\mathrm{F}_3$, $^3\mathrm{F}_3$ and $^3\mathrm{F}_4$ partial waves when $T_{\mathrm{lab}} \geq 150$ MeV because of the large contribution from c_3, while the contributions of the next-to-leading order TPE are still larger than the leading order case for the mixing angle ϵ_3 due to the relatively large contribution from c_4. This may not be too surprising because for this energy, the momentum transfer q is already about $3.85m_\pi \approx 530$ MeV and therefore may not be regarded as a good low energy scale.

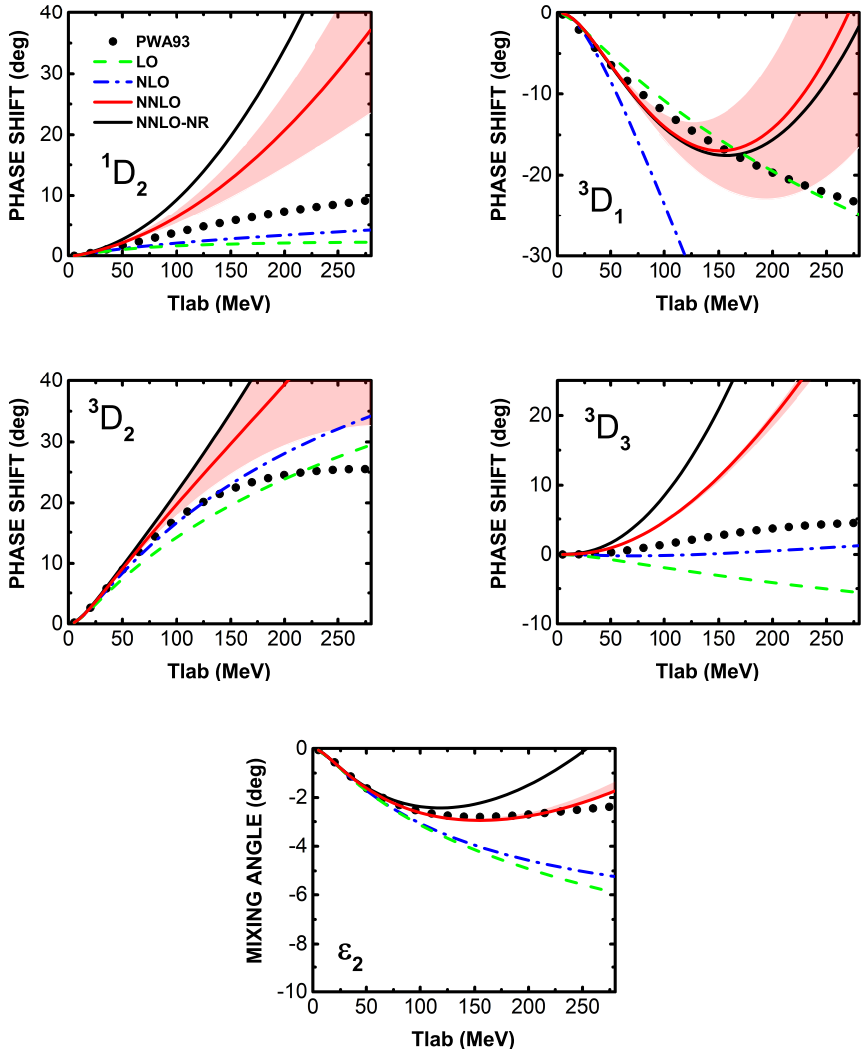

Figure 4.3 – D-wave phase shifts and mixing angle ϵ_2 as a function of T_{lab}. The black dots refer to the Nijmegen partial wave phase shifts. The green dashed curves correspond to the contributions from relativistic OPE, the blue dash dotted curves represent the contributions of leading order TPE, the red solid curves contain the next-to-leading order TPE while the black curves are their nonrelativistic counterpartswith g_A fixed at 1.29. The bands are generated by varying μ from 0.5 GeV to 1.5 GeV.

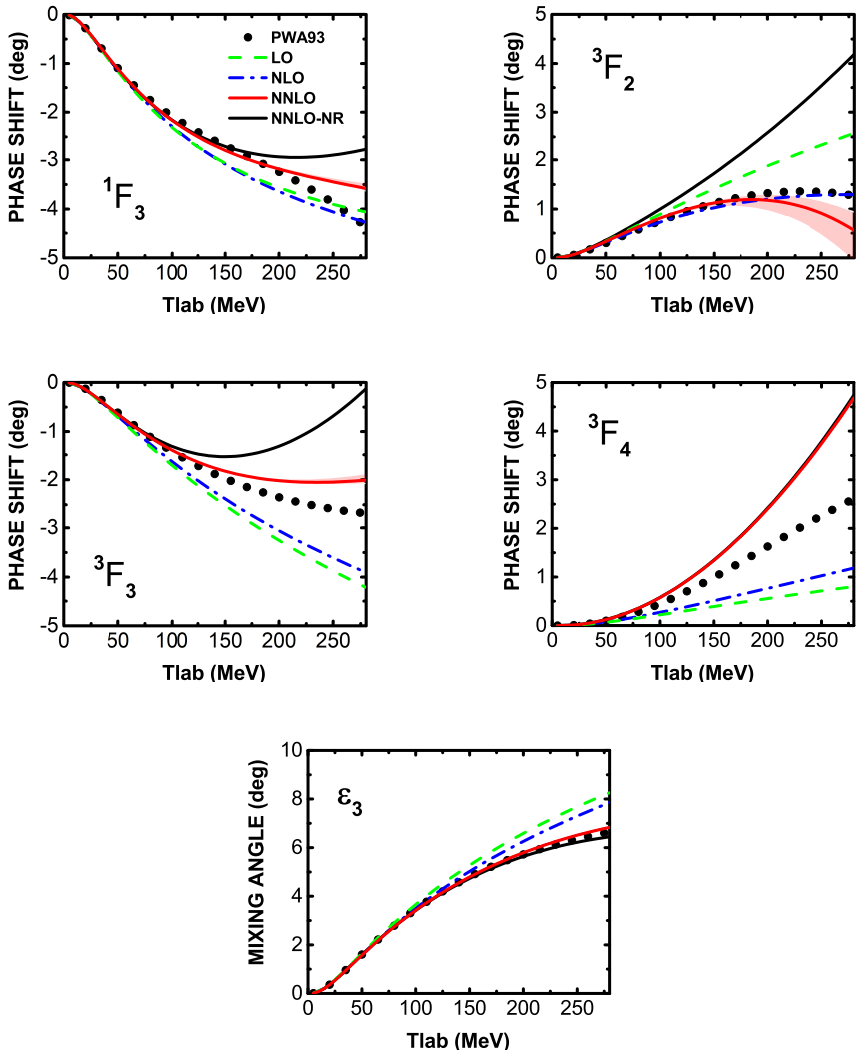

Figure 4.4 – Same as Fig. 4.3, but for F-wave phase shifts and mixing angle ϵ_3.

4.3.3 . G-wave

The G-wave phase shifts and mixing angle ϵ_4 are depicted in Fig. 4.5. Again, the variation of μ affects little the phase shifts for all the partial waves and for all the cases the relativistic phase shifts are in better agreement with data. For the $^1\mathrm{G}_4$, $^3\mathrm{G}_4$, $^3\mathrm{G}_3$ partial waves and mixing angle ϵ_4, the relativistic results are almost identical to data up to $T_{\mathrm{lab}} = 280$ MeV. For the $^3\mathrm{G}_5$ partial waves, the relativistic phase shift is also in perfect agreement with data up to $T_{\mathrm{lab}} = 250$ MeV. Although the descriptions of phase shifts are much improved with the inclusion of the next-to-leading order TPE, the contributions from the next-to-leading order TPE are still relatively large compared with the leading order TPE for the $^1\mathrm{G}_4$, $^3\mathrm{G}_4$, $^3\mathrm{G}_5$ partial waves and mixing angle ϵ_4 because of the same reasons as explained in the F wave case.

4.3.4 . H-wave

The H-wave phase shifts and mixing angle ϵ_5 are depicted in Fig. 4.6. For the H wave, the results are independent of μ and although the TPE contributions are much smaller, the relativistic corrections still improve the description of data. For the $^1\mathrm{H}_5$ and $^3\mathrm{H}_5$, the relativistic and nonrelativistic phase shifts are almost indistinguishable. For the $^3\mathrm{H}_4$ partial wave, the relativistic results are slightly better. Only for $^3\mathrm{H}_6$, the contribution of the next-to-leading order TPE seems to be a bit large when $T_{\mathrm{lab}} \geq 150$ MeV. Moreover, the contributions from the next-to-leading order TPE are still larger than those from the leading order for the $^1\mathrm{H}_5$, $^3\mathrm{H}_5$, $^3\mathrm{H}_6$ partial waves and mixing angle ϵ_5 as explained above.

4.3.5 . I-wave

The I-wave phase shifts and mixing angle ϵ_6 are depicted in Fig. 4.7. The results again are independent of μ and the relativistic phase shifts are nearly identical to the nonrelativistic phase shifts and are in perfect agreement with data for this partial wave due to the negligible contribution of TPE. Notice that for the $^3\mathrm{I}_7$ partial wave, the Nijmegen partial wave phase shifts [34] are larger than those in Ref. [127]. As expected, the contributions from the next-to-leading order TPE are larger than those from the leading order for the $^1\mathrm{I}_6$, $^3\mathrm{I}_6$, $^1\mathrm{I}_7$ partial waves and mixing angle ϵ_6.

4.4 . Summary and outlook

Based on the covariant πN Lagrangians, we calculated the relativistic TPE T-matrix up to $O(q^3)$. With this T-matrix, we further calculated the chiral NN phase shifts with $2 \leq L \leq 6$ and mixing angles with $2 \leq J \leq 6$ and then compared our results with those of the nonrelativistic expansion. We found that for all the partial waves the contributions of relativistic TPE are more moderate than their nonrelativistic counterparts and therefore the obtained NN phase shifts are in better agreement with the Nijmegen partial wave analysis than the nonrelativis-

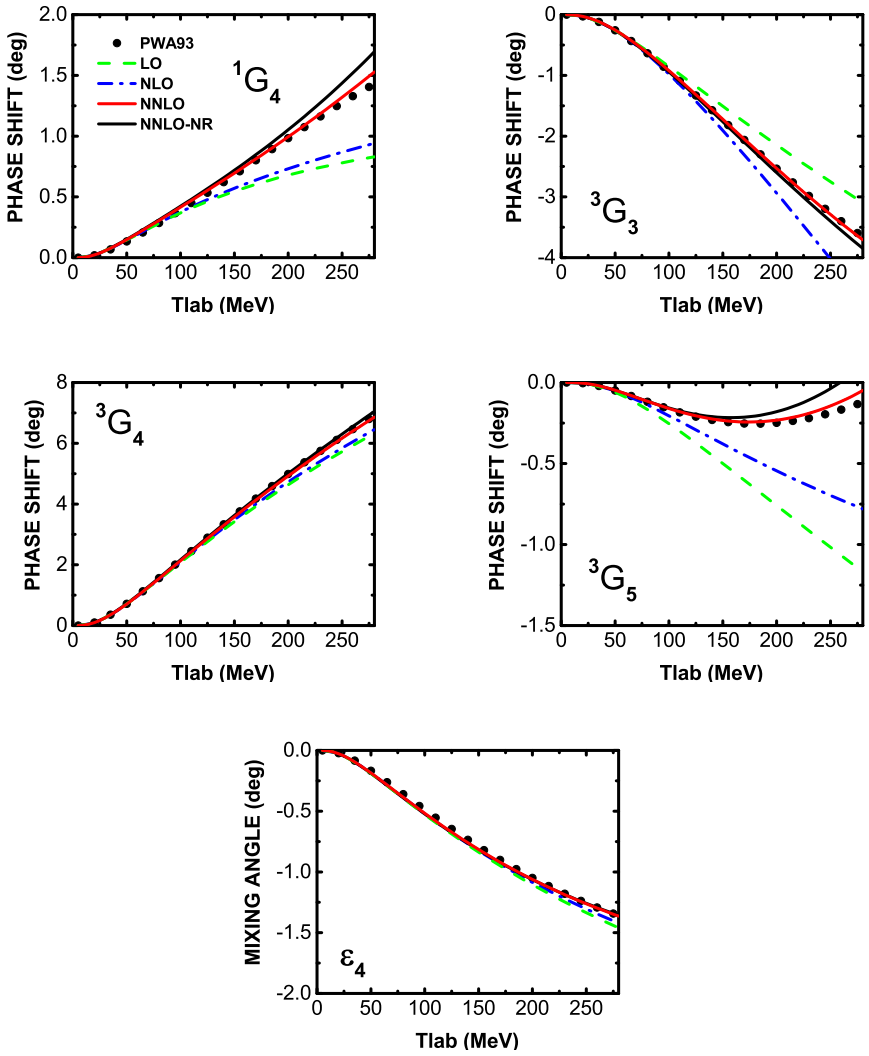

Figure 4.5 – Same as Fig. 4.3, but for G-wave phase shifts and mixing angle ϵ_4.

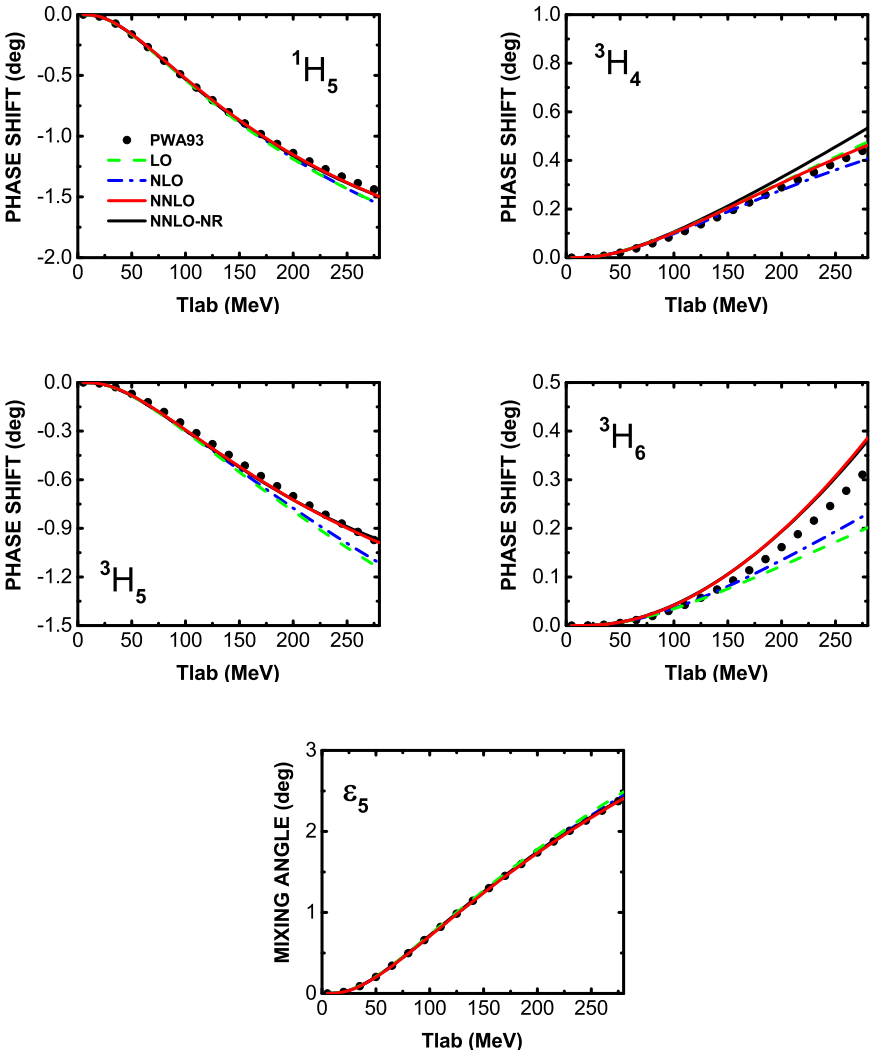

Figure 4.6 – Same as Fig. 4.3, but for H-wave phase shifts and mixing angle ϵ_5.

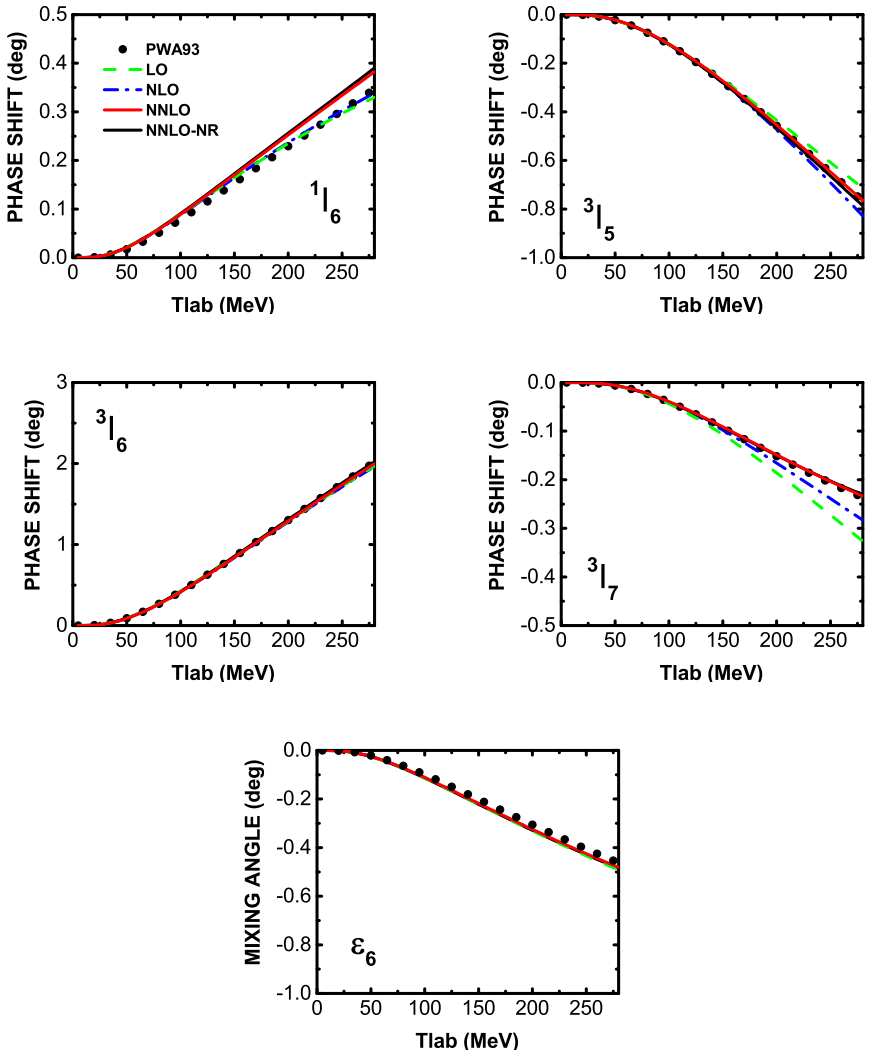

Figure 4.7 – Same as Fig. 4.3, but for I-wave phase shifts and mixing angle ϵ_6.

tic results [61] especially for the F partial waves. Moreover, we showed that the large discrepancies between the nonrelativistic phase shifts and data in the $^3\mathrm{F}_2$ partial wave can be eliminated by including the relativistic corrections. But for the $^3\mathrm{F}_4$ partial wave, the relativistic corrections are insignificant. We found that the contributions of relativistic TPE at the next-to-leading order, similar to their nonrelativistic counterparts, are a bit large for the ^1J_J, ^3J_J, $^3(J-1)_J$ partial waves and mixing angles when $T_{\mathrm{lab}} \geq 150$ MeV because of the large contributions from c_3 and c_4, which indicates that the perturbation theory up to $\mathcal{O}(q^3)$ may not work well in this energy region.

To summarize, although relativistic corrections are found to improve the description of data as expected, they are not significant enough to alter the results of Ref. [61] at least at a qualitative level, thus supporting all the existing studies using the nonrelativistic two-pion exchange contributions of Ref. [61] as inputs. On the other hand, given the covariant nature of the two-pion exchanges presented in this work, they can be easily utilized in the recent series of works [75, 128, 129, 130, 131, 87, 132, 93] which need such two-pion exchanges as inputs and their relevance in such settings remain to be explored.

5 - Two-pion exchange contributions to the nucleon-nucleon interaction with the intermediate Roper resonance

The discussions in chapter 3 and chapter 4 are based on the EFT that includes only ground state of nucleon. The role of nucleon excitations also deserves some discussion. As mentioned in chapter 1, the contributions from $\Delta(1232)$ to the NN interactions have been comprehensively studied before, while the studies on the Roper resonance ($N(1440)$) are rather few. In this chapter, we study the contribution to the nucleon-nucleon (NN) scattering T-matrix from the two-pion exchange potential (TPEP) with the intermediate roper resonance in the heavy baryon chiral perturbation theory up to next-to-leading order. The resulting phase shifts with $L \geq 2$ are compared to those obtained without the contribution of the intermediate roper resonance. We show that the contribution of the roper resonance is sizeable for D-waves and slightly improves the description of phase shifts for all the partial waves. We also discuss the role of the roper resonance in the nucleon-nucleon interaction in the framework of resonance saturation. A similar calculation could also be done in the covariant framework as in chapter 4 for covariant chiral nuclear forces. But as an exploratory study, it is useful to start with the non-relativistic formalism.

This chapter is organized as follows. In Sec. 5.1, we provide the effective Lagrangian relevant to our study and calculate the leading TPE potential with intermediate Roper resonance. The isoscalar and isovector TPE potentials in momentum space and the resulting NN scattering phase shifts for $L \geq 2$ are shown and discussed in Sec. 5.2. A short summary and outlook is given in Sec. 5.3.

5.1 . Roper contributions to the nucleon-nucleon scattering

In this section, we derive the long-range components of the leading TPE potential with intermediate Roper resonances. After the relevant terms in the Lagrangian are presented in Sec. 5.1.1, the triangle and box (planar and crossed) diagrams with one and two Ropers are examined in Sec. 5.1.2.

5.1.1 . Effective Lagrangian

The Roper has the same quantum numbers (spin $S = 1/2$ and isospin $I = 1/2$) as the nucleon and therefore both can be represented by isospinor spinor fields, which we denote R and N, respectively. Since we are interested in the nonrelativistic regime where antibaryon contributions contribute only short-range effects, we can use heavy particle fields [56, 133], each with two components representing particle spin states. The inert nucleon mass is removed through a phase

redefinition, leaving behind the Roper-nucleon mass difference $\rho \equiv m_R - m_N$. The baryon covariant velocity is denoted v_π and covariant spin operator is $S_\mu = i\gamma_5\sigma_{\mu\nu}v^\nu/2$. We will work in the baryons' rest frame, where $v_\mu = (1,0,0,0)$ and $S_\mu = (0,\vec{\sigma}/2)$ in terms of the Pauli spin matrices $\vec{\sigma}$. The contributions from antibaryons are represented by contact interactions.

In addition, we focus on momenta comparable to the pion mass, where the isospin triplet $\boldsymbol{\pi}$ of pseudoscalar pions need to be considered explicitly. Pions are pseudo-Goldstone bosons of spontaneous chiral SU(2)$\times$ SU(2) symmetry breaking, characterized by the pion decay constant $f_\pi \simeq 92$ MeV. Chiral symmetry is realized nonlinearly [134], for example through the use of a field [106, 107] $U(x) = u^2(x) = \exp\left(i\boldsymbol{\pi}\cdot\boldsymbol{\tau}/f_\pi\right)$, where $\boldsymbol{\tau}$ are the Pauli matrices in isospin space. Chiral symmetry is implemented easily through chiral-covariant derivatives

$$u_\mu = i\left(u^\dagger\partial_\mu u - u\partial_\mu u^\dagger\right), \tag{5.1}$$

$$D_\mu\Psi = \partial_\mu\Psi + \frac{1}{2}[u^\dagger\partial_\mu u + u\partial_\mu u^\dagger,\,\Psi], \tag{5.2}$$

for the pion field and a spin-1/2 field Ψ, respectively.

In order to calculate the leading TPE potential with the Roper resonance in HBχPT, we need the leading terms in the effective chiral Lagrangian including pions, nucleon and Roper [135],

$$\begin{aligned}\mathcal{L}^{(0)} =& \frac{f_\pi^2}{4}\mathrm{Tr}\left[(\partial_\mu U)(\partial^\mu U^\dagger) + m_\pi^2(U+U^\dagger)\right] + \bar{N}\left(iv\cdot D + g_A S\cdot u\right)N \\ &+ \bar{R}\left(iv\cdot D - \rho\right)R + g_A'\left(\bar{R}S\cdot uN + \text{H.c.}\right),\end{aligned} \tag{5.3}$$

where g_A and g_A' are the axial-vector coupling of the pion to the nucleon and the transition nucleon-Roper coupling, respectively. Subleading terms include more derivatives, powers of the pion and Roper-nucleon mass difference. With naive dimensional analysis [136], which incorporates naturalness in a perturbative context [137], these terms are suppressed by powers of $M_{\rm QCD} \sim \Lambda_\chi \equiv 4\pi f_\pi$. Also among the higher-order terms one finds also isospin-breaking terms proportional to the quark-mass difference and the fine-structure constant.

5.1.2 . Two-pion exchange potential with intermediate Ropers

The nucleon propagator from the Lagrangian (5.3) is static. Two-nucleon reducible diagrams — that is, those that can be split by cutting only intermediate nucleon lines — have a pinch singularity and are infrared divergent, which requires [58] a resummation in the nucleon propagator of the recoil term proportional to m_N^{-1} appearing in the Lagrangian with an additional derivative, $\mathcal{L}^{(1)}$. These diagrams are then finite but enhanced [110] by a factor of $4\pi m_N/p$, where p is the characteristic momentum of the process. The two-nucleon potential is defined as the sum of two-nucleon irreducible diagrams. Being free of the infrared divergence, contributions to the potential can be estimated [58] with the same power counting

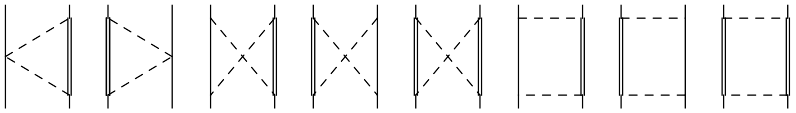

Figure 5.1 – Leading two-pion-exchange contributions to NN interactions with an intermediate Roper resonance. Solid, double, and dashed lines represent nucleons, Ropers,and pions, respectively. Propagators and interactions are from the Lagrangian $\mathcal{L}^{(0)}$, Eq. (5.3).

of χPT [138]. Neglecting isospin-breaking corrections, the potential is a perturbative expansion in $Q/M_{\rm QCD}$, where Q represents the low-energy scales : p, m_π, δ, and in our case ρ as well.

The leading contributions to the NN potential from intermediate Roper resonances and nucleons arise from the Feynman diagrams shown in Fig. 5.1. These are all the one-loop diagrams one can build with the propagators and interactions from the leading Lagrangian in Eq. (5.3) involving nucleons, Ropers and pions. They represent contributions in Roper-full χEFT of $\mathcal{O}(Q^2/M_{\rm QCD}^2)$ relative to OPE. Being free of pinch singularities, nucleons are static with recoil corrections expected at next order. The Roper decay width, arising from a one-loop correction to the Roper propagator, enters two orders down in the chiral expansion. The triangle diagrams arise from the Weinberg-Tomozawa vertex contained in the nucleon chiral-covariant derivative and are proportional to $g_A'^2$. The planar- and crossed-box diagrams are proportional to $g_A^2 g_A'^2$ or $g_A'^4$ depending on whether they contain one or two intermediate Ropers. Note that there is always at least one resonance in intermediate states and no subtraction of iterated OPE is needed.

The inclusion of Roper also implies that one needs to consider explicit contributions from the Delta isobar, since the latter's mass is smaller than the Roper's. At the order we consider here, there are also box diagrams involving one Roper and one Delta in intermediate states, which are proportional to $h_A^2 g_A'^2$, where h_A is the axial-vector nucleon-Delta coupling analog to g_A'. These diagrams are independent of the diagrams considered here and their evaluation is left for a subsequent publication.

As with any other loop diagrams, those in Fig. 5.1 require regularization. They contain short-range components that do not vanish when the regulator is removed. This regulator dependence can be eliminated by an appropriate dependence on the regulator parameter of the bare strengths of two-nucleon contact interactions. The asymptotic form of the potential is obtained at distances much larger than the inverse of the momentum cutoff, see for example Refs. [60, 139] for nucleon and Delta intermediate states. However, the same result is most cleanly obtained with dimensional regularization and minimal subtraction,which we employ in the following. The calculation is completely analogous to that in Refs. [61, 62].

We consider the diagrams in Fig. 5.1 in the center-of-mass frame and denote the

initial and final momenta by $\vec{p}$ and $\vec{p}\,'$, respectively, with $\vec{q}=\vec{p}-\vec{p}\,'$ the transferred momentum. Representing the the spin and isospin operators of nucleons i by $\vec{\sigma}_i$ and $\boldsymbol{\tau}_i$, the corresponding potential takes the conventional form,

$$V = V_C + W_C\,\boldsymbol{\tau}_1\cdot\boldsymbol{\tau}_2 + [V_S + W_S\,\boldsymbol{\tau}_1\cdot\boldsymbol{\tau}_2]\vec{\sigma}_1\cdot\vec{\sigma}_2 + [V_T + W_T\,\boldsymbol{\tau}_1\cdot\boldsymbol{\tau}_2]\,\vec{\sigma}_1\cdot\vec{q}\,\vec{\sigma}_2\cdot\vec{q}, \quad (5.4)$$

where the subscripts C, S, and T refer to the central, spin-spin, and tensor components respectively, with V denoting the isoscalar potential and W the isovector potential.

The explicit expressions are

— Roper resonance in triangle diagrams :

$$\begin{aligned} W_C =& \frac{g_A'^2}{192\pi^2 f_\pi^4}\left[18\rho^2 - 2m_\pi^2 - \frac{13}{6}q^2 - \left(36\rho^2 - 18m_\pi^2 - 5q^2\right)\log\frac{m_\pi}{\mu} - 24\,h\rho\,\cosh^{-1}\frac{\rho}{m_\pi}\right. \\ & \left. - \left(12\rho^2 - 8m_\pi^2 - 5q^2\right)\frac{\omega(q)}{q}\tanh^{-1}\frac{q}{\omega(q)} - 6\left(2\rho^2 - 2m_\pi^2 - q^2\right)f_1(q)\right]. \end{aligned} \quad (5.5)$$

— Single Roper resonance in planar-box diagrams :

$$V_C = -\frac{3}{2}W_C \quad (5.6)$$

$$\begin{aligned} =& \frac{g_A^2 g_A'^2}{256\pi^2 f_\pi^4}\left[30\rho^2 - 32m_\pi^2 - \frac{67}{6}q^2 - \left(60\rho^2 - 90m_\pi^2 - 23q^2\right)\log\frac{m_\pi}{\mu} - 6\pi\frac{m_\pi}{\rho}\omega^2(q)\right. \\ & - 12\left(4\rho^2 - \omega^2(q)\right)\frac{h}{\rho}\cosh^{-1}\frac{\rho}{m_\pi} - \left(12\rho^2 - 20m_\pi^2 - 11q^2\right)\frac{\omega(q)}{q}\tanh^{-1}\frac{q}{\omega(q)} \\ & \left. -12\left(\rho^2 - 2m_\pi^2 - q^2 + \frac{\left(2m_\pi^2 + q^2\right)^2}{2\rho^2}\right)f_1(q)\right], \end{aligned} \quad (5.7)$$

$$V_T = -\frac{3}{2}W_T = -\frac{1}{q^2}V_S = \frac{3}{2q^2}W_S \quad (5.8)$$

$$\begin{aligned} =& \frac{3g_A^2 g_A'^2}{128\pi^2 f_\pi^4}\left[-2 + 2\log\frac{m_\pi}{\mu} - \frac{\pi m_\pi}{2\rho} + \frac{h}{\rho}\cosh^{-1}\frac{\rho}{m_\pi} + \frac{\omega(q)}{q}\tanh^{-1}\frac{q}{\omega(q)}\right. \\ & \left. + \left(1 - \frac{\omega^2(q)}{2\rho^2}\right)f_1(q)\right]. \end{aligned} \quad (5.9)$$

— Single Roper resonance in crossed-box diagrams :

$$V_C = \frac{3}{2} W_C \tag{5.10}$$

$$\begin{aligned} =& \frac{g_A^2 g_A'^2}{256\pi^2 f_\pi^4} \left[-30\rho^2 + 32 m_\pi^2 + \frac{67}{6} q^2 + \left(60\rho^2 - 90 m_\pi^2 - 23 q^2\right) \log \frac{m_\pi}{\mu} - 6\pi \frac{m_\pi}{\rho} \omega^2(q) \right. \\ & + 12 \left(4\rho^2 - \omega^2(q)\right) \frac{h}{\rho} \cosh^{-1} \frac{\rho}{m_\pi} + \left(12\rho^2 - 20 m_\pi^2 - 11 q^2\right) \frac{\omega(q)}{q} \tanh^{-1} \frac{q}{\omega(q)} \\ & \left. + 12 \left(\rho^2 - 2 m_\pi^2 - q^2\right) f_1(q) \right], \end{aligned} \tag{5.11}$$

$$V_T = \frac{3}{2} W_T = -\frac{1}{q^2} V_S = -\frac{3}{2q^2} W_S \tag{5.12}$$

$$= \frac{3 g_A g_A'^2}{128\pi^2 f_\pi^4} \left[2 - 2 \log \frac{m_\pi}{\mu} - \frac{\pi m_\pi}{2\rho} - \frac{h}{\rho} \cosh^{-1} \frac{\rho}{m_\pi} - \frac{\omega(q)}{q} \tanh^{-1} \frac{q}{\omega(q)} - f_1(q) \right]. \tag{5.13}$$

— Double Roper resonance in planar-box diagrams :

$$V_C = -\frac{3}{2} W_C \tag{5.14}$$

$$\begin{aligned} =& \frac{g_A'^4}{512\pi^2 f_\pi^4} \left[30\rho^2 - 32 m_\pi^2 - \frac{67}{6} q^2 - \left(60\rho^2 - 90 m_\pi^2 - 23 q^2\right) \log \frac{m_\pi}{\mu} \right. \\ & - 12 \left(4h^2 - q^2\right) \frac{h}{\rho} \cosh^{-1} \frac{\rho}{m_\pi} - \left(12\rho^2 - 20 m_\pi^2 - 11 q^2\right) \frac{\omega(q)}{q} \tanh^{-1} \frac{q}{\omega(q)} \\ & \left. - 3 \frac{\left(2h^2 - q^2\right)^2}{\rho^2} f_1(q) \right], \end{aligned} \tag{5.15}$$

$$V_T = -\frac{3}{2} W_T = -\frac{1}{q^2} V_S = \frac{3}{2q^2} W_S \tag{5.16}$$

$$= \frac{3 g_A'^4}{128\pi^2 f_\pi^4} \left[-1 + \log \frac{m_\pi}{\mu} + \frac{h}{2\rho} \cosh^{-1} \frac{\rho}{m_\pi} + \frac{\omega(q)}{2q} \tanh^{-1} \frac{q}{\omega(q)} + \frac{4h^2 - q^2}{8\rho^2} f_1(q) \right]. \tag{5.17}$$

— Double Roper resonance in crossed-box diagrams :

$$V_C = \frac{3}{2} W_C \tag{5.18}$$

$$\begin{aligned} =& \frac{g_A'^4}{512\pi^2 f_\pi^4} \left\{ -42\rho^2 - 16m_\pi^2 - \frac{5}{6}q^2 + \left(180\rho^2 - 90m_\pi^2 - 23q^2\right) \log \frac{m_\pi}{\mu} \right. \\ & + 12\left(12h^2 - q^2\right) \frac{\rho}{h} \cosh^{-1} \frac{\rho}{m_\pi} + \left(36\rho^2 - 20m_\pi^2 - 11q^2\right) \frac{\omega(q)}{q} \tanh^{-1} \frac{q}{\omega(q)} \\ & \left. +24\left(2h^2 - q^2\right) \left[f_1(q) + \frac{2h^2 - q^2}{8\rho^2} f_2(q) \right] \right\}, \end{aligned} \tag{5.19}$$

$$V_T = \frac{3}{2} W_T = -\frac{1}{q^2} V_S = -\frac{3}{2q^2} W_S \tag{5.20}$$

$$\begin{aligned} =& \frac{3g_A'^4}{128\pi^2 f_\pi^4} \left[\frac{1}{2} - \log \frac{m_\pi}{\mu} - \frac{\rho}{2h} \cosh^{-1} \frac{\rho}{m_\pi} - \frac{\omega(q)}{2q} \tanh^{-1} \frac{q}{\omega(q)} \right. \\ & \left. - f_1(q) - \frac{4h^2 - q^2}{8\rho^2} f_2(q) \right]. \end{aligned} \tag{5.21}$$

In the above equations, μ is the renormalization scale and the quantities h, ω, f_1, and f_2 are defined as

$$h = \sqrt{\rho^2 - m_\pi^2}, \tag{5.22}$$

$$\omega(q) = \sqrt{4m_\pi^2 + q^2} \tag{5.23}$$

$$f_1(q) = \int_0^1 \mathrm{d}x\, F(q;x)\, \cot^{-1} F(q;x), \tag{5.24}$$

$$f_2(q) = \int_0^1 \mathrm{d}x\, F^2(q;x) \left[F(q;x)\, \cot^{-1} F(q;x) - 1 \right], \tag{5.25}$$

$$f_2(q) = \int_0^1 \mathrm{d}x\, F^3(q;x)\, \cot^{-1} F(q;x) + \frac{4\rho^2 \tan^{-1}\left(\frac{q}{\sqrt{4h^2 - q^2}}\right)}{q\sqrt{4h^2 - q^2}}, \tag{5.26}$$

$$F(q;x) = \left[\frac{q^2}{\rho^2} x(1-x) + \frac{m_\pi^2}{\rho^2} - 1 \right]^{-1/2}. \tag{5.27}$$

It is necessary to check the consistency between the TPE potentials with and without explicit Roper contributions. For such a purpose, we set the Roper-nucleon mass splitting $\rho = 0$ and compare the resulting potential to that in Ref. [61]. We find that they are identical with the exception of the potentials provided by the planar-box diagrams. The difference lies in the pinch singularity, which represents iterated OPE and is subtracted from the planar-box diagrams in the nucleon-only potential.

There are several cancellations among terms in planar and crossed boxes, as can be expected in general since only the sum of all diagrams with a given dependence

on parameters like g_A and g'_A is invariant under field redefinitions. When we add all diagrams we obtain :

$$V_C = -\frac{3g_A'^2}{512\pi^2 f_\pi^4}\left\{8\pi g_A^2\frac{m_\pi}{\rho}w(q)^2 + 4g_A'^2\left[w(q)^2+\rho^2\right] - 40g_A'^2\rho^2\log\frac{m_\pi}{\mu}\right. \tag{5.28}$$
$$+4g_A'^2\left[\frac{q^2\rho}{h} - \left(w(q)^2+8\rho^2\right)\frac{h}{\rho}\right]\cosh^{-1}\frac{\rho}{m_\pi} - 8g_A'^2\rho^2\frac{w(q)}{q}\tanh^{-1}\frac{q}{w(q)}$$
$$\left.+\left[4g_A^2\frac{\left(2{m_\pi}^2+q^2\right)^2}{\rho^2} + g_A'^2\frac{(2h^2+q^2)^2-8\rho^2(2h^2-q^2)}{\rho^2}\right]f_1(q) - g_A'^2\frac{\left(2h^2-q^2\right)^2}{\rho^2}f_2(q)\right\}$$

$$W_C = \frac{g_A'^2}{384\pi^2 f_\pi^4}\left\{-12\rho^2\left(5g_A^2+3g_A'^2-3\right) + 4m_\pi^2\left(16g_A^2+2g_A'^2-1\right) + \frac{q^2}{6}\left(134g_A^2+31g_A'^2-26\right)\right. \tag{5.29}$$
$$+\left[24\rho^2\left(5g_A^2+5g_A'^2-3\right) - 18m_\pi^2\left(10g_A^2+5g_A'^2-2\right) - q^2\left(46g_A^2+23g_A'^2-10\right)\right]\log\frac{m_\pi}{\mu}$$
$$+\frac{6}{\rho\, h}\left[-4g_A^2h^2w(q)^2 + 4\left(4g_A^2+3g_A'^2-2\right)h^2\rho^2 + g_A'^2\left(4h^4-h^2q^2-q^2\rho^2\right)\right]\cosh^{-1}\frac{\rho}{m_\pi}$$
$$+\left[24\rho^2\left(g_A^2+g_A'^2-1\right) - 4m_\pi^2\left(10g_A^2+5g_A'^2-4\right) - q^2\left(22g_A^2+11g_A'^2-10\right)\right]\frac{w(q)}{q}\tanh^{-1}\frac{q}{w(q)}$$
$$+3\left\{2g_A^2\frac{\left(2h^2-q^2\right)^2}{\rho^2} + g_A'^2\frac{\left(2h^2-q^2\right)^2+4\rho^2\left(h^2-2q^2\right)}{2\rho^2} - 4\left(2h^2-q^2\right)\right\}f_1(q)$$
$$\left.+\frac{3g_A'^2}{2}\frac{(2h^2-q^2)^2}{\rho^2}f_2(q)\right\},$$

$$V_T = -\frac{1}{q^2}V_S \tag{5.30}$$
$$=\frac{-3g_A'^2}{256\pi^2 f_\pi^4}\left\{g_A'^2 + g_A^2\frac{2\pi\, m_\pi}{\rho} + g_A'^2\frac{m_\pi^2}{\rho\, h}\cosh^{-1}\frac{\rho}{m_\pi} + \left[g_A^2\frac{w(q)^2}{\rho^2} + g_A'^2\left(1+\frac{w(q)^2}{4\rho^2}\right)\right]f_1(q)\right. \tag{5.31}$$
$$\left.+g_A'^2\frac{4h^2-q^2}{\rho^2}f_2(q)\right\},$$

$$W_T = -\frac{1}{q^2}W_S \tag{5.32}$$
$$=\frac{g_A'^2}{128\pi^2 f_\pi^4}\left[8g_A^2+3g_A'^2-4\left(2g_A^2+g_A'^2\right)\log\frac{m_\pi}{\mu} - \left(\frac{4g_A^2h^2-g_A'^2m_\pi^2}{\rho\, h}\right)\cosh^{-1}\frac{\rho}{m_\pi}\right. \tag{5.33}$$
$$-2\left(2g_A^2+g_A'^2\right)\frac{w(q)}{q}\tanh^{-1}\frac{q}{w(q)} + \left(g_A^2\frac{q^2-4h}{\rho^2} + g_A'^2\frac{w(q)^2-12\rho^2}{4\rho^2}\right)f_1(q)$$
$$\left.+g_A'^2\frac{q^2-4h^2}{4\rho^2}f_2(q)\right].$$

The form of the potential and its effects on observables are considered in the next section.

5.2 . Numerical Results and Discussion

The Roper TPE potential is determined in terms of one-baryon LECs. After we discuss their values, we present plots of the potential and its effects on phase shifts for high partial waves.

5.2.1 . Values of LECs

In order to calculate the NN scattering phase shifts, we have to fix all the relevant LECs. The leading order nucleon axial-vector coupling g_A is fixed at 1.29, the pion decay constant $f_\pi = 92.4$ MeV, the renormalization scale $\mu = 1$ GeV, the pion mass $m_\pi = 139$ MeV, and the nucleon mass $m_N = 939$ MeV. As for the nucleon-roper coupling g'_A and the mass splitting ρ, we adopt the N^{2}LO EFT values listed in Table I of Ref. [135]. That is $g'_A = 1.06$ and $\rho = 690$ MeV. Alternative numerical studies with g'_A and ρ of the N^{3}LO EFT and N^{2}LO GW listed in Table I of Ref. [135] have also been performed and the results are found to be qualitatively consistent with those otained with the N^{2}LO EFT LECs with an insignificant difference at large laboratory energies.

5.2.2 . The potential as function of momentum transfer

The various components of the OPE potential, the TPEP with and without intermediate roper contributions in momentum space up to NLO are shown in Fig. 5.2 [1]. Note that the potential of the tensor part is multiplied with a momentum-dependent factor q^2 to rescale the magnitude [2]. In EFT-$\not{R}$, the first contribution to the isoscalar central force V_C arise at N^{2}LO, while in EFT-R, it emerges at NLO. The NLO-R contribution to V_C is strongly repulsive, but the strength decreases with the transfer momentum q. For the isovector central force W_C, it receives the first contribution at NLO in both EFT-$\not{R}$ and EFT-R. Moreover, the contribution to W_C in both EFTs is repulsive with different tendency and strength. In EFT-R, similar to V_C, W_C not only decreases with q, but also holds almost the same slope as V_C. As a matter of fact, W_C in EFT-R is nearly 1/2 of V_C. Contrary to this, in EFT-$\not{R}$, W_C increases with q, but the strength is much weaker than that in EFT-R. Since $U_C = V_C + (4I-3)W_C$ [61], one would naturally expect that for $I = 0$, $U_C(R)$ and $U_C(\not{R})$ are both attractive and converge at small q, and then $U_c(\not{R})$ decreases with q, while $U_c(R)$ increases with q gently because of the cancellation of $V_C(R)$ and $W_C(R)$. However, for $I = 1$, this behavior interchanges, i.e., $U_C(R)$ retains the features of $V_C(R), W_C(R)$ and its strength is approximately 100GeV^{-2} larger than that of $U_C(\not{R})$ for the q region plotted here. Nevertheless, the contributions to the T-matrix elements in the LSJ basis from

1. The TPEP with and without intermediate roper contributions are denoted as EFT-R and EFT-$\not{R}$.

2. Another reason to redefine the tensor force in such a form is that the contribution to the T-matrix in the LSJ basis from the tensor force is either multiplied with q^2 or multiplied with p^2, and q^2 is proportional to p^2 for given scattering angle.

$U_C(R)$,$U_C(\not{R})$ are of similar magnitude because U_C is always multiplied with the Legendre Polynomial $P_{J/J\pm1}(z)$ in the projection of T-matrix, and the contribution from a constant term equals to zero after the integration over z. Therefore, for $I = 1$, if one shifts $U_C(R)$ downwards about 100 GeV$^-2$, the behaviors of $U_C(R)$ and $U_C(\not{R})$ are similar with different sign and thus their contributions to the T-matrix are comparable. For the redefined isoscalar tensor force q^2V_T, both EFTs contribute at NLO and the EFT-$\not{R}$ potential is nearly twice as strong as the EFT-R potential with a different sign. For the redefined isovector tensor force, the contribution from TPEP with the intermediate roper resonance emerges at NLO and is insignificant for the isospin triplet. However, for the isospin singlet, W_S is comparable to V_S because its contribution to the T-matrix is multiplied with a factor of 3. Hence, the contribution from the tensor force in EFT-$\not{R}$ to the T-matrix is also nearly twice as that in EFT-R for $I = 1$, while the contribution from the tensor force in both EFTs are comparable for $I = 0$. Notice that the isoscalar tensor force in EFT-R provides additional attraction (in comparion with that in EFT-$\not{R}$) thus results in a better convergence and description of the phase shifts at NLO. Because the football and triangle diagrams do not contribute to the tensor and spin-spin force, and $(V/W)_T = -\frac{1}{q^2}(V/W)_S$ in the box diagram, the behaviours of the spin-spin force in both EFTs are the same as those of the tensor force.

5.2.3 . Phase shifts in high partial waves

The NN scattering phase shifts can be obtained by using the "Stapp"- or "bar"- phase shift parameterization [140] of S matrix, which is related to the on-shell T-matrix. In order to obtain the on-shell T-matrix, one need to insert the potential into a scattering equation such as the Lippmann-Schwinger equation. However, for relatively small phase shifts e.g. $|\delta| < 10^\circ$, which is common for partial waves with $L, J \geq 2$, the difference between the phase shifts obtained in the scattering equation and the perturbation theory is insignificant due to the minor difference between δ and $\sin(\delta)\cos(\delta)$. Therefore, in this work, we only calculate the perturbative phase shifts and mixing angles. Their expressions are given as follows :

$$
\begin{aligned}
T &= V, \\
\delta_{LSJ} &= -\frac{M^2 p}{4\pi E}\mathrm{Re}\,\langle LSJ|\,T\,|LSJ\rangle\,, \\
\epsilon_J &= \frac{M^2 p}{4\pi E}\mathrm{Re}\,\langle J-1,1,J|\,T\,|J+1,1,J\rangle\,.
\end{aligned}
\tag{5.34}
$$

where M is the nucleon mass and $E = \sqrt{M^2 + p^2}$ refers to the center of mass energy. On-shell, the transferred momentum $q = |\vec{q}| = 2p\sin\theta/2 = p\sqrt{2(1-\cos\theta)}$ with θ the scattering angle. The explicit partial wave projections of the T-matrix can be found in Ref. [61]. Note that the kinematical prefactors differ from those of Ref. [61] due to a different sign convention for the T matrix.

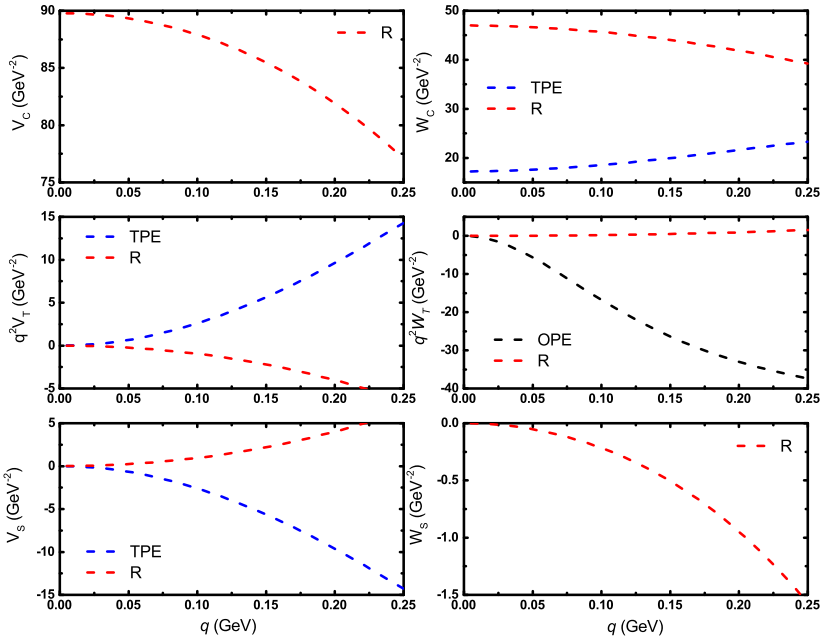

Figure 5.2 – Isoscalar (left panel) and isovector (right panel) NN potentials at NLO. The black line refers to the contribution from the one-pion exchange, the blue lines denote the contributions from the two-pion exchange without intermediate roper contributions and the red lines refer to the potential provided solely by the intermediate roper resonance. The tensor potential is rescaled with a momentum-dependent factor q^2. Notice that in EFT-$\not{R}$, the TPEP only contributes to W_C, V_T and V_S.

Next, we turn to the NN scattering phase shifts for $L \geq 2$. The results for the D-,F-,G wave phase shifts and for the mixing angles $\epsilon_{2,3,4}$ are shown in Figures 5.3 à 5.5. For all the partial waves the consideration of the roper resonance leads to a better description of the phase shifts. For most partial waves the descriptions are reasonably good with the exception of ${}^3D_1$,${}^3D_3$,${}^3F_4$ and ${}^3G_5$, which implies that higher order corrections or the inclusion of the Δ isobar are needed.

Then we discuss the D-wave phase shifts one by one. For the ${}^1D_2$ partial wave, according to the Pauli exclusion principle, the potentials for $I = 1$ would contribute to this channel. Moreover, since the contribution to the T-matrix from the central and tensor forces in form of $(U_C - q^2 U_T)P_J(z)$ and the $q^2 U_T$ term can be shifted, their contributions to the T-matrix almost cancel each other as shown in Fig. 5.2. The spin-spin force nearly saturates this channel. Based on the previous discussion, the spin-spin force in EFT-$\not{R}$ is nearly twice as large as that in EFT-R for $I = 1$, so that the contribution to the phase shifts from TPEP without

the roper resonance is also nearly twice as large as that from the TPEP with it, which is in good agreement with the results shown in Fig. 5.3. For the mixing angle ϵ_2, the potentials for $I = 0$ would contribute to it. Because only the tensor force contributes to the T-matrix in this channel, so the contribution from TPEP with/without the intermediate roper resonance should be comparable according to Fig. 5.2. However, one can observe from Fig. 5.3 that the contribution from the TPEP with the roper resonance is about one third of that from the TPEP without the roper resonance. The reason is that, the tensor potential shown in Fig. 5.2 is a function of q, while the contribution to the T-matrix from the tensor force is a function of p and z. The different behavior of the tensor force as a function of the two basis leads to the disagreement in the mixing angle ϵ_2. The situation is a bit more ambiguous for the triplet channel because of the more complex structure in the projection formulas. So one can observe from Fig. 5.3 that for the ${}^3D_2$ partial wave, the contribution from EFT-R is slightly larger than that from EFT-$\not{R}$, while for the ${}^3D_3$ partial wave, the contribution from EFT-$\not{R}$ is again nearly twice as large as that from EFT-R. The ${}^3D_1$ partial wave is a bit special. In EFT-R, the contribution from the central force is almost cancelled by those from the spin-spin and tensor forces, so the phase shifts retain the shape even the intermediate roper resonance is considered.

As for the F-and G-waves, the contributions from the NLO TPEP without the intermediate roper resonance are insignificant and thus the contributions from the TPEP with the intermediate roper resonance are also insignificant. Nevertheless, the inclusion of the roper resonance still shifts the theoretical phase shifts towards the data.

Now we consider the role of the roper resonance in the framework of resonance saturation. It has long been noted that the N^{2}LO TPEP is somehow comparable or even larger than the NLO TPEP in the HB formalism [61]. And the N^{2}LO TPEP contribution is mainly from the terms that contain LECs c_3 and c_4, whose values can be understood in resonance saturation [126]. Therefore, in some sense, the role of the nucleon excitations to the NN scattering can be visualized simply by comparing their contributions to c_3 and c_4. The values of c_3 and c_4 are dominated by the Δ saturation [126], thus the Δ-isobar is expected to be crucial in the NN interaction. Previous studies [62, 76] showed that the NLO TPEP with the intermediate Δ is equivalent to the N^{2}LO TPEP without the intermediate Δ to some extent, which corroborates the above conjecture. Contrary to the Δ saturation, the contribution to the values of the two LECs from the roper saturation is minor [126]. Hence, from this point of view, the roper resonance may not as important as the Δ in the NN scattering. As a result, we can observe from Figures 5.3 à 5.5 that the contributions from the roper resonance are sizeable for D-waves, but become insignificant as the orbit angular momentum increases.

5.3 . Summary and outlook

We calculated the NN TPEP with intermediate roper resonance in the HBχPT up to NLO. The isoscalar and isovector TPEP with the intermediate roper resonance are compared with the conventional TPEP. We found that for the isospin singlet, the central, spin-spin and tensor forces with the intermediate roper are comparable to those without it. For the isospin triplet, the central force with the intermediate roper resonance is significantly larger than that without it. Nevertheless, the huge difference is suppressed by the Legendre Polynomial when projected to the LSJ basis. As for the tensor and spin-spin forces, the potentials with the intermediate roper resonance are nearly one half of those without it. With the obtained potential, we further evaluated the T-matrix and obtained the perturbative phase shifts for D-,F- and G-waves. We found that for all the partial waves, the description of the phase shifts is improved by the inclusion of the intermediate roper resonance. Moreover, the contributions from the roper resonance are found to be sizeable for D-waves.

Although the obtained phase shifts are in reasonable agreement with the phase shifts data, there are still visible discrepancies for the ${}^3D_1$, ${}^3D_3$, ${}^3F_4$ and ${}^3G_5$ partial waves. Since the present study is only up to NLO and does not include the contribution from Δ, a complete Δ- and roper-full EFT up to N^{2}LO is then awaited to address these questions.

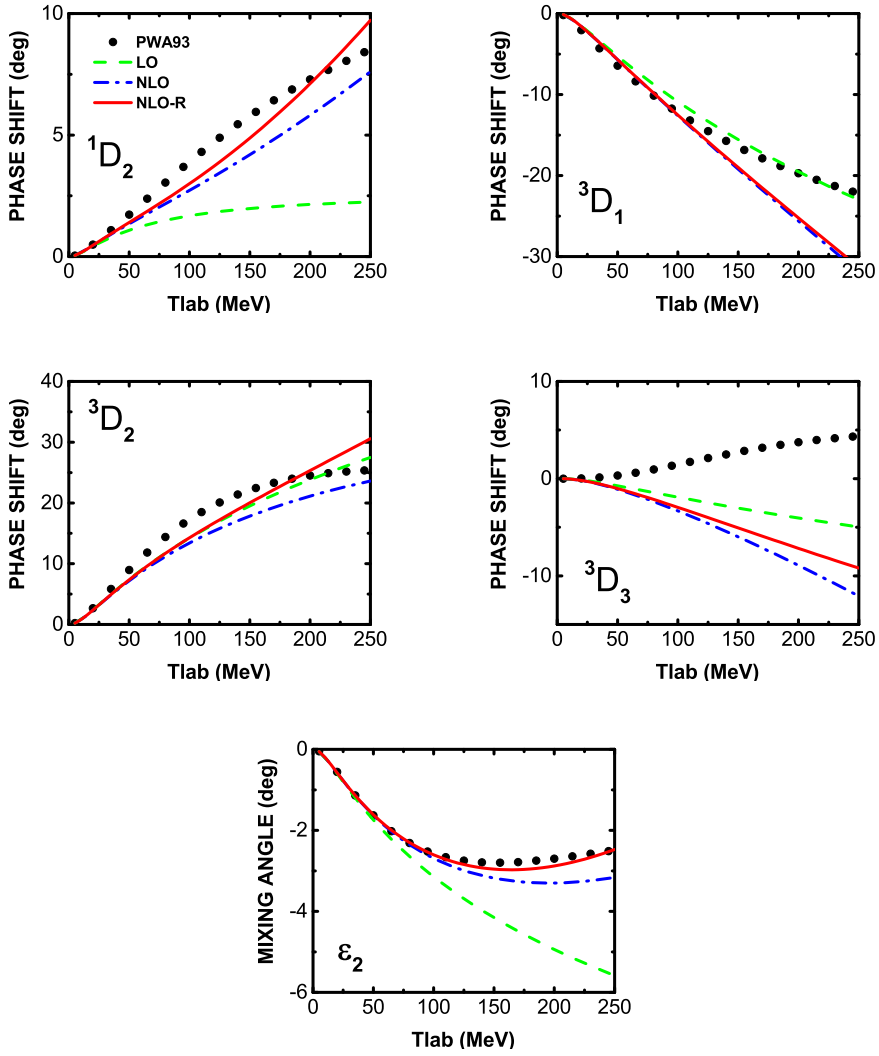

Figure 5.3 – D-wave phase shifts and mixing angle ϵ_2 as a function of T_{lab}. The black dots refer to the Nijmegen partial wave phase shifts. The green dashed curves correspond to the contributions from the OPE, the blue dash dotted curves represent the contributions from TPEP, the red solid curves represent the sum of the OPE and TPE contributions with that from the intermediate roper resonance.

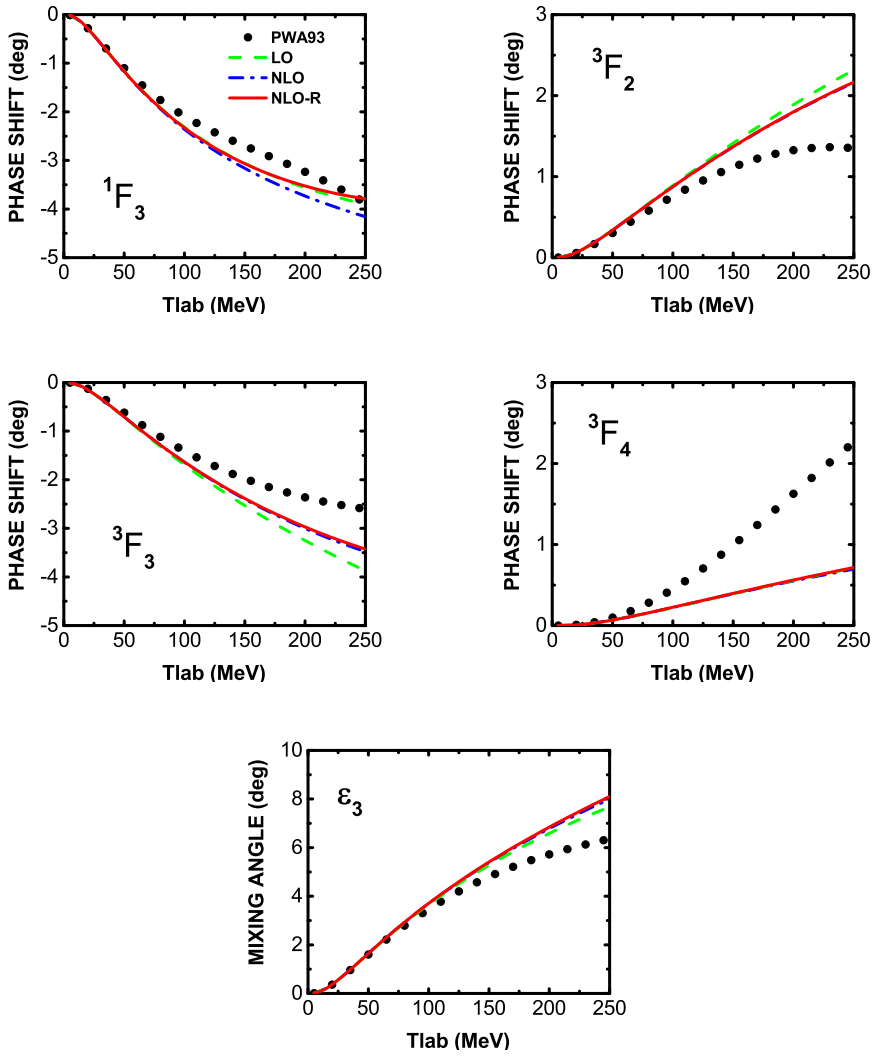

Figure 5.4 – Same as Fig. 5.3, but for F-wave phase shifts and mixing angle ϵ_3.

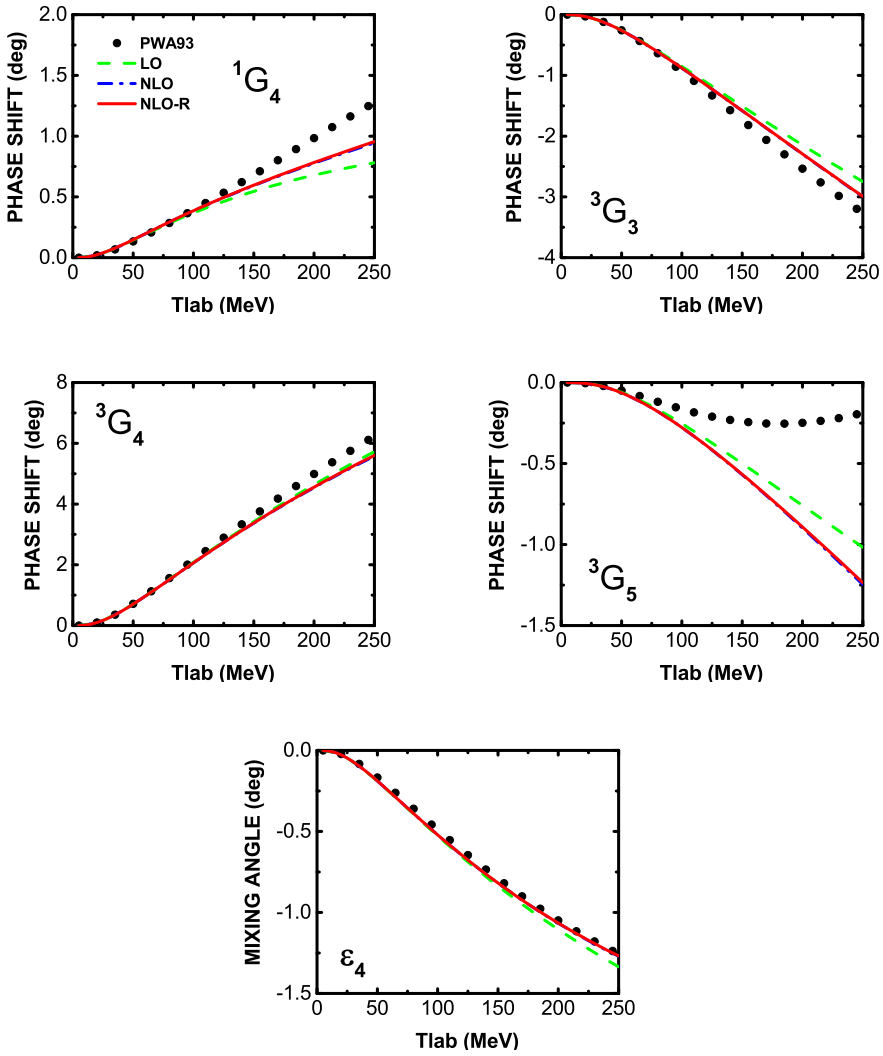

Figure 5.5 – Same as Fig. 5.3, but for G-wave phase shifts and mixing angle ϵ_4.

6 - Summary and outlook

In this thesis, the key input to construct a high-precision covariant nuclear force is obtained in covariant EFT, and the role of the Roper resonance in the nucleon-nucleon interaction is quantified in HBEFT.

First, we briefly introduced the principle of effective field theory. Special attention was paid to chiral symmetry and its explicit and spontaneous breaking in the underlying QCD. The chiral effective field theory, which is the low-energy approximation of QCD that includes explicit pion fields, also incorporates the same symmetries and their breaking patterns. The general way to construct the chiral Lagrangian and the power counting rule was then introduced.

Aiming to construct the high-precision covariant nuclear force, we proposed a covariant power counting rule and presented the steps to construct the covariant nucleon-nucleon contact Lagrangian up to order $\mathcal{O}(q^4)$. The constructed Lagrangians contain $4 + 13 + 23$ terms at $\mathcal{O}(q^0), \mathcal{O}(q^2), \mathcal{O}(q^4)$, respectively, which can be reduced to the well-known non-relativistic $2 + 7 + 15$ terms by performing the non-relativistic reduction. In addition to this, we calculated the TPE contributions to the nucleon-nucleon interaction in covariant χPT and compared our results with the conventional non-relativistic results. Since the calculations are parameter free, the importance of relativistic effects could be explored. As a result, an overall better description of the NN phase shifts, especially for the F wave, and a faster convergence have been observed in the calculations based on the covariant formalism. Both works are key inputs to constructing a high-precision covariant chiral nuclear force, and future applications are awaited.

Apart from the works in covariant EFT, we also studied the role of Roper resonance $N(1440)$, which is the second excitation of a nucleon, in the nucleon-nucleon interaction based on HBEFT. Although contributions from $\Delta(1232)$ had been fully studied before [59, 60, 62, 76, 77, 78, 79, 80, 81, 82, 83, 84, 85, 86], the role of the Roper has never been discussed in the nucleon-nucleon sector. We showed that the contributions of the Roper resonance are sizeable for D waves and improve the description of phase shifts for all partial waves slightly. Such behavior was then discussed in the framework of resonance saturation.

Our results suggest a number of further developments :

— The NN contact terms constructed in Chapter 3 do not include either isospin-breaking terms or external fields, which implies that these Lagrangians are not enough for analyses of differences between proton-proton and neutron-neutron scattering, where isospin breaking enters. Therefore, for a subsequent study, external fields have to be considered in covariant Lagrangians for a better interpretation of NN scattering.

— As shown in Chapter 4, similar to the non-relativistic TPE, the covariant TPE also encounters a convergence problem, suggesting the necessity to

include nucleon excitations. The study performed in Chapter 5 shows that the contributions from the Roper resonance indeed improve the convergence behavior, especially for the D waves. Still, they are not enough to solve the convergence problem. The explicit inclusion of the $\Delta(1232)$ in calculations involving the nucleon and the Roper resonance might provide additional contributions at this order to improve convergence.

— Covariant many-body calculations for finite nuclei, e.g., the Relativistic Brueckner-Hartree-Fock (RBHF) theory, based on the bare nucleon-nucleon potential require massive computing resources. A potential solution is to soften the bare nuclear force to a low-momentum nucleon-nucleon interaction based on the RG method. In addition, RG invariance is one of the bases of an EFT. So a systematic study of the RG invariance of covariant chiral nuclear forces is important. The work in this thesis can provide a foundation for RG studies in covariant chiral nuclear forces.

— Existing relativistic nuclear many-body calculations are mainly based on the CD-Bonn potential. Chiral nuclear forces based on the work in this thesis might provide more insight than phenomenological nuclear forces into studies of nuclear matter and properties of finite nuclei.

— Combing covariant chiral nuclear forces and nuclear many-body theories, one can obtain optimal covariant microscopic potentials and then study nucleon-nucleus scattering with covariant ab initio methods.

7 - Résumé substantiel en français

La force nucléaire est l'ingrédient le plus essentiel de la physique nucléaire, et la compréhension microscopique de cette force a longtemps été le sujet central de la physique nucléaire. En 1932, la découverte du neutron par Chadwick [1] a ouvert les portes aux études de la force nucléaire. Depuis lors, la compréhension de la nature des interactions entre nucléons a toujours été l'un des problèmes les plus importants de la physique nucléaire. La première tentative a été faite par Yukawa [2]. En 1935, Yukawa a proposé que les interactions entre nucléons puissent être médiées par des particules dont la masse est environ 200 fois celle d'un électron, appelées mésons, et sa théorie est la célèbre théorie de l'échange de mésons. Bien qu'il ait été prouvé que la théorie de Yuakwa n'était pas suffisante pour décrire la force nucléaire, l'idée principale de la théorie de l'échange de mésons, selon laquelle la force nucléaire est médiée par des mésons, est toujours instructive aujourd'hui. Au cours des années suivantes, certains physiciens ont suggéré que d'autres mésons devraient également être pris en compte [3, 4]. Cependant, en raison des structures d'opérateurs compliquées qu'elles comportent, ces théories ne sont pas largement utilisées. En fait, à cette époque, la plupart des physiciens pensaient que la nature de la force nucléaire serait finalement exprimée sous une forme simple comme la force de Coulomb et la gravité. Mais les expériences ont prouvé que cette idée était fausse. La force nucléaire s'est alors avérée presque impossible à décrire par une théorie simple [5].

Le principal problème de la théorie de Yukawa est que des mésons beaucoup plus lourds devraient être inclus afin de décrire le comportement de la force nucléaire dans sa partie centrale ($r \lesssim 1$ fm). Sur la base des travaux pionniers de Yuwaka, Taketani, Nakamura et Sasaki ont proposé une nouvelle théorie de la force nucléaire [6]. L'idée principale est de diviser la force nucléaire en trois parties en fonction de l'étendue de la force. L'échange d'un pion (OPE) représente la partie à longue portée ($r \gtrsim 3$ fm) de la force nucléaire, l'échange de deux pions est responsable de la partie à moyenne portée ($1 \lesssim r \lesssim 3$ fm) de la force nucléaire, tandis que l'échange de plusieurs pions contribue à la partie à courte portée ($r \lesssim 1$ fm) de la force nucléaire. Ce concept est instructif car c'est la première fois que l'on se rend compte que la force nucléaire se compose de différents comportements à différents niveaux de force. Cependant, les difficultés à dériver le potentiel d'échange multi-pions limitent son application ultérieure.

Une autre façon de construire la force nucléaire est apparue dans les années 1950∼60 : phénoménologique, basée sur les données abondantes de la diffusion nucléon-nucléon (NN). La forme générale de la partie à courte portée de ces forces est généralement obtenue par diverses analyses d'invariance. Par exemple, le potentiel de Paris est exprimé en termes d'invariants non relativistes habituels avec cinq composantes pour chaque état isospin [7]. En même temps, la partie à longue

portée est obtenue en considérant la théorie de la dispersion. Dans les années 1970, les forces nucléaires phénoménologiques largement utilisées comprenaient le potentiel de Hamada Johnston [8], le potentiel de Reid [9], et le potentiel de Paris [7]. Ces forces nucléaires phénoménologiques sont en accord général avec les données de diffusion nucléon-nucléon. Cependant, leurs formes sont quelque peu arbitraires et elles contiennent de nombreux paramètres ajustables.

Dans les années 1970, la théorie de l'échange de mésons a connu une percée grâce à la découverte de mésons lourds. La théorie correspondante est connue sous le nom de modèle d'échange d'un boson (OBE) [10, 11, 12]. Selon le modèle OBE, la partie à longue portée de la force nucléaire est toujours dominée par l'échange d'un pion, la partie à moyenne portée de la force nucléaire peut être dérivée par l'échange de mésons de masses $500 \sim 550$ MeV, tandis que la partie à courte portée de la force nucléaire peut être obtenue par l'échange de mésons plus lourds, dont les masses sont d'environ $720 \sim 1000$ MeV. En utilisant le modèle OBE, une forte interaction répulsive est obtenue dans la partie centrale de la force nucléaire, ce qui explique l'apparition d'un noyau répulsif. Comme le potentiel OBE contient certaines constantes de couplage, qui sont fixées par les données expérimentales, la théorie est encore semi-phénoménologique.

En dehors de ces modèles, dans les années 1980, Oka, Faessler et Shimizu [13, 14, 15] ont proposé d'étudier la force nucléaire dans des modèles de quark. C'est la première fois que le noyau répulsif de la force nucléaire peut être bien expliqué par l'échange effectif d'un gluon. Bien que ces premiers modèles de quarks expliquent bien la partie à courte portée de la force nucléaire, la nature attractive de la partie à moyenne et longue portée de la force nucléaire ne peut être décrite au niveau des quarks. L'échange de mésons doit être inclus dans ces théories pour générer ces parties de la force nucléaire, et ces théories mixtes sont connues sous le nom de modèles mixtes quark-méson. Après des années d'améliorations, les modèles de quark bien connus comprennent le modèle de quark chiral à canal couplé [16], le modèle de quark constituant [17, 18], le modèle de quark chiral [19, 20], modèle d'écran couleur de délocalisation de quark [21, 22, 23, 24, 25], et modèle de quark SU(6) [26, 27, 28, 29].

Une force nucléaire de haute précision est nécessaire pour obtenir des calculs précis de la structure et des réactions nucléaires. C'est pourquoi diverses forces nucléaires phénoménologiques de haute précision ont été proposées à la fin des années 1990. Ces forces peuvent être classées en deux catégories : celles basées sur l'invariance sous parité, la conjugaison de charge, l'inversion temporelle et la conjugaison hermitienne, comme le potentiel Reid93 [34] et le potentiel AV18 [31], et celles basées sur le modèle OBE, comme le potentiel Nijmegen [30] et le potentiel CD-Bonn [33]. Les données de diffusion nucléon-nucléon et les propriétés du deutéron peuvent être bien expliquées par ces modèles de haute précision. Par exemple, le potentiel CD-Bonn a pu décrire environ 6000 données de diffusion de pp et np au-dessous de 300 MeV avec χ^2/datum ≈ 1, bien plus précis que toute

autre force nucléaire et analyse d'ondes partielles jusqu'alors. Le coût d'une telle précision est d'environ 30 à 50 paramètres ajustables introduits dans ces théories. Néanmoins, ces forces nucléaires de haute précision servent effectivement d'entrées de haute qualité pour les calculs de structure et de réaction nucléaires.

Les nombreuses applications des forces nucléaires phénoménologiques de haute précision mentionnées ci-dessus ne satisfont pas les physiciens, car elles sont toutes phénoménologiques. La force nucléaire idéale devrait non seulement être de haute précision mais aussi indépendante du modèle. Depuis les années 1970, on sait que la chromodynamique quantique (QCD) est la théorie fondamentale des interactions fortes, décrivant les interactions entre quarks par échange de gluons. De plus, la force nucléaire est considérée comme une interaction forte résiduelle. Cependant, une étude directe de la force nucléaire basée sur la CDQ est impossible en raison de la nature non-perturbative de la CDQ dans le régime de basse énergie. Il y a deux façons possibles de dériver la force nucléaire en QCD : 1) effectuer des simulations de QCD en treillis dans des superordinateurs et 2) développer des théories effectives de QCD à basse énergie. La première a fait des progrès considérables récemment [35, 36, 37, 38, 39, 40, 41, 42, 43, 44, 45, 46, 47], mais les calculs sont effectués dans la région non physique en raison des ressources de calcul massives nécessaires, et les résultats sont contradictoires. Ces dernières années, des efforts considérables ont été faits pour établir la relation entre la force nucléaire et la QCD dans le cadre de la théorie effective des champs (EFT). Les travaux dans cette direction ont fait des réalisations remarquables et des forces nucléaires de haute précision ont été construites à partir de la théorie de perturbation chirale des baryons lourds (HBChPT) plus récemment [48, 49, 50, 51].

En 1979, Weinberg a suggéré qu'une expansion systématique et indépendante du modèle pour la matrice S peut être obtenue en considérant la symétrie chirale approximative SU(2)$_L\times$ SU(2)$_R$ de QCD [52]. La symétrie chirale est spontanément brisée et conduit à l'existence de bosons pseudoscalaires légers, qui sont identifiés comme des pions. Cette théorie a été appliquée pour la première fois dans le secteur $\pi\pi$ [53, 54]. Lorsqu'elle est étendue au secteur à un baryon, elle rencontre le problème dit de rupture du comptage de puissance (PCB) à cause de la grande masse non nulle du nucléon dans la limite chirale [55]. Ce problème peut être résolu dans le cadre du HBChPT [56] en faisant l'hypothèse extrême de la limite non-relativiste, que le transfert de momentum entre nucléons est beaucoup plus petit que la masse du nucléon, ce qui implique une expansion en puissances d'un petit momentum sur la masse du nucléon. Contrairement aux systèmes $\pi\pi$ et πN, un état lié à deux nucléons (deutéron) existe, mettant en évidence la nature non-perturbative de l'interaction NN. Afin de l'accommoder, Weinberg a proposé, dans les années 1990, de calculer le potentiel NN de manière perturbative dans l'expansion chirale, puis de l'itérer à tous les ordres dans une équation de Schrödinger ou de Lippmann-Schwinger pour obtenir l'amplitude [57, 58].

La première application du schéma de Weinberg dans le secteur NN par

Ordóñez, Ray, et van Kolck [59, 60] a donné une description raisonnable des données NN à $\mathcal{O}((Q/\Lambda_\chi)^3)$ avec des Deltas explicites et un régulateur gaussien, où il y a sept interactions indépendantes à courte portée. Les avantages d'un tel régulateur local incluent la conservation de la structure analytique de la matrice T près du seuil du pion et le fait qu'aucune régularisation de la fonction spectrale n'est nécessaire, tandis qu'un inconvénient est qu'il conduit à un mélange de différents canaux d'ondes partielles en raison de la dépendance de $\vec{q}$ sur l'angle de diffusion. Les déphasages périphériques de NN dans la théorie de perturbation chirale Δ-less et Δ-full ont été obtenus par Brockmann, Gerstendorfer, Kaiser et Weise [61, 62]. La force nucléaire chirale sans Δ a été redérivée par Epelbaum, Glöckle, et Meißner [63]. La force nucléaire chirale dite de haute précision avec un régulateur exponentiel non local et super-gaussien a été construite à $\mathcal{O}((Q/\Lambda_\chi)^4)$ par Entem et Machleidt [64]. La description des données NN par cette force nucléaire chirale est comparable à celle des potentiels phénoménologiques de haute précision, mais avec moins de paramètres. Une série de forces nucléaires chirales de haute qualité ont été dérivées depuis lors [64, 65, 66, 67, 48, 68, 49, 50, 51]. Des forces nucléaires chirales de pointe ont été construites à $\mathcal{O}((Q/\Lambda_\chi)^5)$ [48, 49, 50] et $\mathcal{O}((Q/\Lambda_\chi)^6)$ [51].

Cependant, certains problèmes sont ancrés dans les forces nucléaires obtenues dans le comptage de puissance de Weinberg. Par exemple, une description cohérente de la puissance d'analyse de la diffusion neutron-deutéron A_y n'a pas été obtenue même lorsque la force chirale à trois nucléons est considérée [69]. Les solutions possibles sont soit d'inclure des termes de contact sous-jacents de $3N$, ce qui implique une convergence plus lente de χEFT que prévu, soit de réaliser qu'une renormalisation appropriée de la théorie nécessite un nouveau comptage de puissance [71, 72, 73, 74]. En outre, la nature non relativiste de ces forces limite également leurs applications dans les études à plusieurs corps dans un cadre relativiste. Motivée par le besoin d'une meilleure force nucléaire chirale avec une convergence plus rapide et des calculs de structure et de réaction nucléaires dans un cadre relativiste, une force nucléaire chirale relativiste a été proposée en 2018 [75]. Une telle approche permet de conserver la forme complète du champ de nucléons. De plus, le potentiel effectif V, obtenu en calculant les diagrammes de Feynman pertinents, est inséré dans l'équation de Kadyshevsky au lieu de l'équation de Lippmann-Schwinger. Par conséquent, davantage d'effets relativistes sont maintenus dans cette approche par rapport au formalisme HB du début. Par conséquent, on peut observer sur les figures 3 et 4 de la référence que la force nucléaire chirale relativiste d'ordre supérieur est comparable à la force nucléaire chirale non relativiste d'ordre immédiatement supérieur pour la description des déphasages de diffusion des ondes S et P NN avec seulement cinq paramètres, ce qui implique une convergence plus rapide dans la théorie.

Néanmoins, la force nucléaire chirale relativiste d'ordre supérieur est encore loin d'être suffisante pour les calculs de structure et de réaction nucléaires. Les

divergences entre la force nucléaire chirale relativiste d'ordre supérieur et l'analyse du déphasage de diffusion de NN [34] impliquent la nécessité de calculs d'ordre supérieur. Afin d'effectuer des calculs au-delà de l'ordre principal, les contributions pertinentes d'ordre supérieur des sommets de contact et des échanges de deux pions sont nécessaires.

Les forces nucléaires chirales susmentionnées ne contiennent principalement que le nucléon de l'état fondamental, les contributions des états excités du baryon étant reléguées aux LEC d'ordre supérieur. Bien qu'elles soient déjà d'une grande précision, ces forces nucléaires chirales rencontrent encore quelques problèmes, par exemple, la convergence par rapport aux composantes du potentiel TPE. On s'est rendu compte depuis longtemps [61] que la composante formellement sous-jacente de la TPE est comparable ou même plus grande que la TPE présumée principale, ce qui remet en question le comptage de puissance sous-jacent à la χEFT. Les problèmes de convergence des forces nucléaires chirales peuvent être améliorés par l'inclusion explicite des résonances baryoniques. Si les effets d'une résonance sont relégués aux LEC, des contributions non analytiques sont perdues, ce qui limite le domaine d'expansion de la théorie. L'inclusion explicite d'une résonance de basse altitude en tant que degré de liberté de basse énergie n'étend pas seulement la validité de l'EFT mais réorganise également les contributions d'échange de multipions et améliore la convergence ordre par ordre. La plus faible excitation du nucléon est l'isobare Delta, $\Delta(1232)$, dont la masse m_Δ est seulement $\delta \equiv m_\Delta - m_N \simeq 300$ MeV plus élevée que celle du nucléon. Sa contribution au NN [59, 60, 62, 76, 77, 78, 79, 80, 81] et les forces chirales à trois noyaux [82, 83, 84, 85, 86] a attiré une attention croissante. Cependant, le rôle de la deuxième excitation nucléonique, la résonance de Roper $N(1440)$, qui s'est avérée nécessaire pour la description de π. nécessaire pour la description de la diffusion πN dans le canal P_{11}, est jusqu'à présent toujours inconnu dans l'interaction nucléon-nucléon. Comme le système NN peut être considéré comme une extension du système πN, et que la masse m_R du $N(1440)$ est $\rho \equiv m_R - m_\Delta \simeq 500$ MeV plus élevée que celle du nucléon, il est intéressant d'étudier les contributions de la résonance de Roper à la force nucléaire.

Dans cette thèse, nous suivons de près la discussion mentionnée ci-dessus, nous étudions les apports nécessaires à la construction d'une force nucléaire relativiste de haute précision, et nous examinons le rôle de la résonance de Roper dans l'interaction nucléon-nucléon dans la théorie des champs effectifs chiraux (ChEFT) :

— Nous adoptons une version covariante de l'analyse dimensionnelle naïve et construisons le lagrangien de contact à deux nucléons contraint par les symétries de Lorentz, de parité, de conjugaison des charges et de conjugaison hermitienne. En utilisant l'EOM pour éliminer les termes redondants, nous trouvons seulement 4 termes de $\mathcal{O}(q^0)$, 13 termes de $\mathcal{O}(q^2)$, et 23 termes de $\mathcal{O}(q^4)$. Nous avons comparé avec les études précédentes et identifié les différences et le raisonnement qui les sous-tend. De plus, nous avons vérifié

qu'en effectuant des expansions de $1/m_n$, on peut récupérer les Lagrangiens chiraux non-relativistes correspondants, qui ont 24 termes jusqu'à $\mathcal{O}(q^4)$. Le Lagrangien covariant construit dans le présent travail peut être utile pour construire des forces nucléaires covariantes ainsi que pour étudier les corrections relativistes.

Il faut souligner que la complétude et la minimalité de l'ensemble des Lagrangiens covariants dérivés dans le présent travail doivent être comprises par rapport aux règles de comptage de puissance que nous avons choisies et au choix que nous avons fait concernant la façon d'utiliser l'équation du mouvement pour éliminer les termes redondants et limiter le nombre de termes disponibles. Plus précisément, on peut mieux les désigner comme un ensemble économique de Lagrangiens covariants qui peuvent récupérer ceux du baryon lourd. Nous espérons que le présent travail pourra motiver d'autres études dans cette direction.

— Sur la base des lagrangiens covariants πN, nous avons calculé la matrice TPE relativiste T jusqu'à $O(q^3)$. Avec cette matrice T, nous avons ensuite calculé les déphasages chiraux NN avec $2 \leq L \leq 6$ et les angles de mélange avec $2 \leq J \leq 6$, puis nous avons comparé nos résultats avec ceux de l'expansion non relativiste. Nous avons trouvé que pour toutes les ondes partielles, les contributions des TPE relativistes sont plus modérées que leurs homologues non relativistes et que, par conséquent, les déphasages NN obtenus sont en meilleur accord avec l'analyse des ondes partielles de Nijmegen que les résultats non relativistes [61], en particulier pour les ondes partielles F. De plus, nous avons montré que les grandes divergences entre les déphasages non relativistes et les données dans l'onde partielle ${}^3\mathrm{F}_2$ peuvent être éliminées en incluant les corrections relativistes. Mais pour l'onde partielle ${}^3\mathrm{F}_4$, les corrections relativistes sont insignifiantes. Nous avons trouvé que les contributions des TPE relativistes à l'ordre le plus proche, similaires à leurs homologues non relativistes, sont un peu grandes pour les ${}^1J_J$, ${}^3J_J$, ${}^3(J-1)_J$ ondes partielles et angles de mélange lorsque $T_{\mathrm{lab}} \geq 150$ MeV en raison des importantes contributions de c_3 et c_4, ce qui indique que la théorie des perturbations jusqu'à $\mathcal{O}(q^3)$ peut ne pas fonctionner correctement dans cette région d'énergie.

En résumé, bien que les corrections relativistes améliorent la description des données comme prévu, elles ne sont pas assez significatives pour modifier les résultats de la Réf. [61] au moins à un niveau qualitatif, soutenant ainsi toutes les études existantes utilisant les contributions non relativistes de l'échange de deux pions de la Réf. [61] comme entrées. D'autre part, étant donné la nature covariante des échanges de deux pions présentés dans ce travail, ils peuvent être facilement utilisés dans la série récente de travaux [75, 128, 129, 130, 131, 87, 132, 93] qui ont besoin de tels échanges de deux pions comme entrées et leur pertinence dans de tels contextes reste

à explorer.

— Nous avons calculé la TPEP NN avec une résonance de roper intermédiaire dans le HBχPT jusqu'à NLO. La TPEP isoscalaire et isovectrice avec la résonance de roper intermédiaire est comparée à la TPEP conventionnelle. Nous avons trouvé que pour le singlet isospin, les forces centrales, spin-spin et tensorielles avec le roper intermédiaire sont comparables à celles sans lui. Pour le triplet d'isospin, la force centrale avec la résonance du roper intermédiaire est significativement plus grande que celle sans elle. Néanmoins, cette énorme différence est supprimée par le polynôme de Legendre lorsqu'elle est projetée dans la base LSJ. Quant aux forces tensorielles et de spin-spin, les potentiels avec la résonance de roper intermédiaire sont presque la moitié de ceux sans résonance. Avec le potentiel obtenu, nous avons ensuite évalué la matrice T et obtenu les déphasages perturbatifs pour les ondes D, F et G. Nous avons constaté que pour toutes les ondes partielles, la description des déphasages est améliorée par l'inclusion de la résonance intermédiaire de roper. De plus, les contributions de la résonance de roper s'avèrent être importantes pour les ondes D.
  Bien que les déphasages obtenus soient en accord raisonnable avec les données de déphasage, il existe encore des divergences visibles pour les ondes partielles ${}^3D_1$, ${}^3D_3$, ${}^3F_4$ et ${}^3G_5$. Puisque la présente étude ne va que jusqu'à NLO et n'inclut pas la contribution de Δ, une EFT complète de Δ et de roper-ful jusqu'à N^{2}LO est alors attendue pour répondre à ces questions.

Le travail présenté dans cette thèse est un élément essentiel pour la construction de forces nucléaires chirales covariantes de haute précision, ainsi que de la force nucléaire chirale avec des résonances baryoniques explicites.

A - Non-relativistic NN contact Lagrangian up to order $\mathcal{O}(q^4)$

In this Appendix, we list the non-relativistic Lagrangian up to order $\mathcal{O}(q^4)$. Compared to the covariant case, the procedures to construct the non-relativistic chiral Lagrangian is simple and straightforward. The basic requirement for a non-relativistic Lagrangian is that the Lagrangian must be scalar. Because of parity constraints, the non-relativistic Lagrangian must contain an even number of gradient operators. Because the three momentum of the nucleon is the only small expansion parameter in the non-relativistic power counting, to the n th order, one needs to include n gradient operators. Using the criteria listed above, one can easily construct the non-relativistic Lagrangians up to order $\mathcal{O}(q^4)$. They are summarized in Table A.1, where N and $N^\dagger$ donate the nucleon field and its hermitian conjuage, and $\boldsymbol{\nabla}$ refers to the gradient operator. Note that $(N^\dagger \boldsymbol{\nabla} N)(N^\dagger N) = -(N^\dagger N)(N^\dagger \boldsymbol{\nabla} N)$ since we are working in the center-of-mass frame.

Table A.1 – $\mathcal{O}(q^0)$, $\mathcal{O}(q^2)$ and $\mathcal{O}(q^4)$ non-relativistic NN contact Lagrangians. The left (right) arrow on $\boldsymbol{\nabla}$ indicates that the derivative acts on the left (right) nucleon field.

O_S	$(N^\dagger N)(N^\dagger N)$	O_{11}	$(N^\dagger \overrightarrow{\boldsymbol{\nabla}} \cdot \overleftarrow{\boldsymbol{\nabla}} N)(N^\dagger \overrightarrow{\boldsymbol{\nabla}} \cdot \overleftarrow{\boldsymbol{\nabla}} N)$
O_T	$(N^\dagger \boldsymbol{\sigma} N) \cdot (N^\dagger \boldsymbol{\sigma} N)$	O_{12}	$i\,(N^\dagger \boldsymbol{\sigma} \cdot \overrightarrow{\boldsymbol{\nabla}} \times \overleftarrow{\boldsymbol{\nabla}} N)(N^\dagger \overrightarrow{\boldsymbol{\nabla}}^2 N) + \text{h.c.}$
O_1	$(N^\dagger N)(N^\dagger \overrightarrow{\boldsymbol{\nabla}}^2 N) + \text{h.c.}$	O_{13}	$i\,(N^\dagger \boldsymbol{\sigma} \cdot \overrightarrow{\boldsymbol{\nabla}} \times \overleftarrow{\boldsymbol{\nabla}} N)(N^\dagger \overrightarrow{\boldsymbol{\nabla}} \cdot \overleftarrow{\boldsymbol{\nabla}} N)$
O_2	$(N^\dagger N)(N^\dagger \overrightarrow{\boldsymbol{\nabla}} \cdot \overleftarrow{\boldsymbol{\nabla}} N)$	O_{14}	$(N^\dagger \sigma^j N)(N^\dagger \sigma^j \overrightarrow{\boldsymbol{\nabla}}^4 N) + \text{h.c.}$
O_3	$i\,(N^\dagger \boldsymbol{\sigma} N) \cdot (N^\dagger \overrightarrow{\boldsymbol{\nabla}} \times \overleftarrow{\boldsymbol{\nabla}} N)$	O_{15}	$(N^\dagger \sigma^j \overrightarrow{\boldsymbol{\nabla}} \cdot \overleftarrow{\boldsymbol{\nabla}} N)(N^\dagger \sigma^j \overrightarrow{\boldsymbol{\nabla}}^2 N) + \text{h.c.}$
O_4	$(N^\dagger \sigma^j N)(N^\dagger \sigma^j \overrightarrow{\boldsymbol{\nabla}}^2 N) + \text{h.c.}$	O_{16}	$(N^\dagger \sigma^j \overrightarrow{\boldsymbol{\nabla}}^2 N)(N^\dagger \sigma^j \overleftarrow{\boldsymbol{\nabla}}^2 N)$
O_5	$(N^\dagger \sigma^j N)(N^\dagger \sigma^j \overrightarrow{\boldsymbol{\nabla}} \cdot \overleftarrow{\boldsymbol{\nabla}} N)$	O_{17}	$(N^\dagger \sigma^j \overrightarrow{\boldsymbol{\nabla}} \cdot \overleftarrow{\boldsymbol{\nabla}} N)(N^\dagger \sigma^j \overrightarrow{\boldsymbol{\nabla}} \cdot \overleftarrow{\boldsymbol{\nabla}} N)$
O_6	$(N^\dagger \boldsymbol{\sigma} \cdot \overrightarrow{\boldsymbol{\nabla}} N)(N^\dagger \boldsymbol{\sigma} \cdot \overrightarrow{\boldsymbol{\nabla}} N) + \text{h.c.}$	O_{18}	$(N^\dagger \boldsymbol{\sigma} \cdot \overrightarrow{\boldsymbol{\nabla}} N)(N^\dagger \boldsymbol{\sigma} \cdot \overrightarrow{\boldsymbol{\nabla}} \overrightarrow{\boldsymbol{\nabla}}^2 N) + \text{h.c.}$
O_7	$(N^\dagger \boldsymbol{\sigma} \cdot \overrightarrow{\boldsymbol{\nabla}} N)(N^\dagger \boldsymbol{\sigma} \cdot \overleftarrow{\boldsymbol{\nabla}} N)$	O_{19}	$(N^\dagger \boldsymbol{\sigma} \cdot \overrightarrow{\boldsymbol{\nabla}} N)(N^\dagger \boldsymbol{\sigma} \cdot \overleftarrow{\boldsymbol{\nabla}} \overrightarrow{\boldsymbol{\nabla}}^2 N) + \text{h.c.}$
O_8	$(N^\dagger N)(N^\dagger \overrightarrow{\boldsymbol{\nabla}}^4 N) + \text{h.c.}$	O_{20}	$(N^\dagger \boldsymbol{\sigma} \cdot \overrightarrow{\boldsymbol{\nabla}} N)(N^\dagger \boldsymbol{\sigma} \cdot \overrightarrow{\boldsymbol{\nabla}} \overrightarrow{\boldsymbol{\nabla}} \cdot \overleftarrow{\boldsymbol{\nabla}} N) + \text{h.c.}$
O_9	$(N^\dagger \overrightarrow{\boldsymbol{\nabla}}^2 N)(N^\dagger \overrightarrow{\boldsymbol{\nabla}} \cdot \overleftarrow{\boldsymbol{\nabla}} N) + \text{h.c.}$	O_{21}	$(N^\dagger \boldsymbol{\sigma} \cdot \overrightarrow{\boldsymbol{\nabla}} N)(N^\dagger \boldsymbol{\sigma} \cdot \overrightarrow{\boldsymbol{\nabla}} \overleftarrow{\boldsymbol{\nabla}}^2 N) + \text{h.c.}$
O_{10}	$(N^\dagger \overrightarrow{\boldsymbol{\nabla}}^2 N)(N^\dagger \overleftarrow{\boldsymbol{\nabla}}^2 N)$	O_{22}	$(N^\dagger \boldsymbol{\sigma} \cdot \overrightarrow{\boldsymbol{\nabla}} N)(N^\dagger \boldsymbol{\sigma} \cdot \overleftarrow{\boldsymbol{\nabla}} \overrightarrow{\boldsymbol{\nabla}} \cdot \overleftarrow{\boldsymbol{\nabla}} N)$

Bibliographie

[1] CHADWICK J. Possible Existence of a Neutron[J]. Nature, 1932, 129 : 312. DOI : 10.1038/129312a0.

[2] YUKAWA H. On the Interaction of Elementary Particles I[J]. Proc. Phys. Math. Soc. (Jap.), 1935, 17 : 48–57. DOI : 10.1143/PTPS.1.1.

[3] PROCA A. Sur la theorie ondulatoire des electrons positifs et negatifs[J]. J. Phys. Radium, 1936, 7 : 347–353. DOI : 10.1051/jphysrad:0193600708034700.

[4] NICHOLAS K. Quantum theory of Einstein-Bose particles and nuclear interaction[J]. Proc. R. Soc. Lond. A, 1938, 166 : 127–153. DOI : 10.1098/rspa.1938.0084.

[5] KRANE K S. Introductory nuclear physics[M]. [S.l.] : Wiley, 1988.

[6] TAKETANI M, NAKAMURA S, SASAKI M. On the Method of the Theory of Nuclear Forces[J]. Prog. Thero. Phys. (Kyo.), 1951, 6(4) : 581–586. DOI : 10.1143/ptp/6.4.581.

[7] LACOMBE M, LOISEAU B, RICHARD J M, et al. Parametrization of the Paris n n Potential[J]. Phys. Rev. C, 1980, 21 : 861–873. DOI : 10.1103/PhysRevC.21.861.

[8] HAMADA T, JOHNSTON I. A potential model representation of two-nucleon data below 315 mev[J]. Nucl. Phys., 1962, 34(2) : 382–403. DOI : 10.1016/0029-5582(62)90228-6.

[9] REID R V. Local phenomenological nucleon-nucleon potentials[J]. Annals Phys. (N.Y.), 1968, 50(3) : 411–448. DOI : 10.1016/0003-4916(68)90126-7.

[10] DE TOURREIL R, ROUBEN B, SPRUNG D W L. Supersoft Core Nucleon-Nucleon Interaction with pi-, rho- and omega Exchange Contributions[J]. Nucl. Phys. A, 1975, 242 : 445–460. DOI : 10.1016/0375-9474(75)90107-4.

[11] HOLINDE K, MACHLEIDT R. OBEP and eikonal form factor[J]. Nucl. Phys. A, 1976, 256 : 497–508. DOI : 10.1016/0375-9474(76)90386-9.

[12] NAGELS M M, RIJKEN T A, DE SWART J J. A Low-Energy Nucleon-Nucleon Potential from Regge Pole Theory[J]. Phys. Rev. D, 1978, 17 : 768. DOI : 10.1103/PhysRevD.17.768.

[13] OKA M, YAZAKI K. Nuclear Force in a Quark Model[J]. Phys. Lett. B, 1980, 90 : 41–44. DOI : 10.1016/0370-2693(80)90046-5.

[14] FAESSLER A, FERNANDEZ F, LUBECK G, et al. The Quark Model and the Nature of the Repulsive Core of the Nucleon Nucleon Interaction[J]. Phys. Lett. B, 1982, 112 : 201–205. DOI : 10.1016/0370-2693(82)90961-3.

[15] SHIMIZU K. Study of Baryon Baryon Interactions and Nuclear Properties in the Quark Cluster Model[J]. Rept. Prog. Phys., 1989, 52 : 1–56. DOI : 10.1088/0034-4885/52/1/001.

[16] VALCARCE A, GARCILAZO H, FERNANDEZ F, et al. Quark-model study of few-baryon systems[J]. Rept. Prog. Phys., 2005, 68 : 965–1042. DOI : 10.1088/0034-4885/68/5/R01.

[17] STRAUB U, ZHANG Z Y, BRAUER K, et al. Hyperon Nucleon Interaction in the Quark Cluster Model[J]. Nucl. Phys. A, 1988, 483 : 686–710. DOI : 10.1016/0375-9474(88)90092-9.

[18] ZHANG Z Y, FAESSLER A, STRAUB U, et al. The Baryon baryon interaction in a modified quark model[J]. Nucl. Phys. A, 1994, 578 : 573–585. DOI : 10.1016/0375-9474(94)90761-7.

[19] ZHANG Z Y, YU Y W, SHEN P N, et al. Hyperon nucleon interactions in a chiral SU(3) quark model[J]. Nucl. Phys. A, 1997, 625 : 59–70. DOI : 10.1016/S0375-9474(97)00033-X.

[20] DAI L R, ZHANG Z Y, YU Y W, et al. N N interactions in the extended chiral SU(3) quark model[J]. Nucl. Phys. A, 2003, 727 : 321–332. DOI : 10.1016/j.nuclphysa.2003.08.006.

[21] WANG F, WU G H, TENG L J, et al. Quark delocalization, color screening, and nuclear intermediate range attraction[J]. Phys. Rev. Lett., 1992, 69 : 2901–2904. DOI : 10.1103/PhysRevLett.69.2901.

[22] WU G H, TENG L J, PING J L, et al. Quark delocalization, color screening, and N N intermediate range attraction : P waves[J]. Phys. Rev. C, 1996, 53 : 1161–1166. DOI : 10.1103/PhysRevC.53.1161.

[23] PING J L, WANG F, GOLDMAN J T. Effective baryon baryon potentials in the quark delocalization and color screening model[J]. Nucl. Phys. A, 1999, 657 : 95–109. DOI : 10.1016/S0375-9474(99)00321-8.

[24] WU G H, PING J L, TENG L J, et al. Quark delocalization, color screening model and nucleon baryon scattering[J]. Nucl. Phys. A, 2000, 673 : 279–297. DOI : 10.1016/S0375-9474(00)00141-X.

[25] PANG H R, PING J L, WANG F, et al. Phenomenological study of hadron interaction models[J]. Phys. Rev. C, 2002, 65 : 014003. DOI : 10.1103/PhysRevC.65.014003.

[26] FUJIWARA Y, NAKAMOTO C, SUZUKI Y. RGM study of the hyperon - nucleon interaction in the SU(6) quark model. 1 : Analysis of N N and Sigma p systems[J]. Prog. Theor. Phys., 1995, 94 : 215–232. DOI : 10.1143/PTP.94.215.

[27] FUJIWARA Y, NAKAMOTO C, SUZUKI Y. A Unified description of N N and Y N interactions in a quark model with effective meson exchange potentials[J]. Phys. Rev. Lett., 1996, 76 : 2242–2245. DOI : 10.1103/PhysRevLett.76.2242.

[28] FUJIWARA Y, NAKAMOTO C, SUZUKI Y. Effective meson exchange potentials in the SU(6) quark model for N N and Y N interactions[J]. Phys. Rev. C, 1996, 54 : 2180–2200. DOI : 10.1103/PhysRevC.54.2180.

[29] FUJITA T, FUJIWARA Y, NAKAMOTO C, et al. Scattering observables of the N N and Y N interactions in the SU(6) quark model[J]. Prog. Theor. Phys., 1998, 100 : 931–955. DOI : 10.1143/PTP.100.931.

[30] STOKS V G J, KLOMP R A M, TERHEGGEN C P F, et al. Construction of high quality N N potential models[J]. Phys. Rev. C, 1994, 49 : 2950–2962. DOI : 10.1103/PhysRevC.49.2950.

[31] WIRINGA R B, STOKS V G J, SCHIAVILLA R. An Accurate nucleon-nucleon potential with charge independence breaking[J]. Phys. Rev. C, 1995, 51 : 38–51. DOI : 10.1103/PhysRevC.51.38.

[32] MACHLEIDT R, SAMMARRUCA F, SONG Y. Nonlocal nature of the nuclear force and its impact on nuclear structure[J]. Phys. Rev. C, 1996, 53 (4) : R1483–R1487. DOI : 10.1103/PhysRevC.53.R1483.

[33] MACHLEIDT R. The High precision, charge dependent Bonn nucleon-nucleon potential (CD-Bonn)[J]. Phys. Rev. C, 2001, 63 : 024001. DOI : 10.1103/PhysRevC.63.024001.

[34] STOKS V G J, KLOMP R A M, RENTMEESTER M C M, et al. Partial wave analaysis of all nucleon-nucleon scattering data below 350-MeV[J]. Phys. Rev. C, 1993, 48 : 792–815. DOI : 10.1103/PhysRevC.48.792.

[35] LUSCHER M. Two particle states on a torus and their relation to the scattering matrix[J]. Nucl. Phys. B, 1991, 354 : 531–578. DOI : 10.1016/0550-3213(91)90366-6.

[36] ISHII N, AOKI S, HATSUDA T. The Nuclear Force from Lattice QCD[J]. Phys. Rev. Lett., 2007, 99 : 022001. DOI : 10.1103/PhysRevLett.99.022001.

[37] AOKI S, HATSUDA T, ISHII N. Theoretical Foundation of the Nuclear Force in QCD and its applications to Central and Tensor Forces in Quenched Lattice QCD Simulations[J]. Prog. Theor. Phys., 2010, 123 : 89–128. DOI : 10.1143/PTP.123.89.

[38] FUKUGITA M, KURAMASHI Y, OKAWA M, et al. Hadron scattering lengths in lattice QCD[J]. Phys. Rev. D, 1995, 52 : 3003–3023. DOI : 10.1103/PhysRevD.52.3003.

[39] BEANE S R, SAVAGE M J. Nucleon-nucleon interactions on the lattice[J]. Phys. Lett. B, 2002, 535 : 177–180. DOI : 10.1016/S0370-2693(02)01762-8.

[40] BEANE S R, DETMOLD W, ORGINOS K, et al. Nuclear Physics from Lattice QCD[J]. Prog. Part. Nucl. Phys., 2011, 66 : 1–40. DOI : 10.1016/j.ppnp.2010.08.002.

[41] NEMURA H, ISHII N, AOKI S, et al. Hyperon-nucleon force from lattice QCD[J]. Phys. Lett. B, 2009, 673 : 136–141. DOI : 10.1016/j.physletb.2009.02.003.

[42] INOUE T, ISHII N, AOKI S, et al. Baryon-Baryon Interactions in the Flavor SU(3) Limit from Full QCD Simulations on the Lattice[J]. Prog. Theor. Phys., 2010, 124 : 591–603. DOI : 10.1143/PTP.124.591.

[43] IKEDA Y. S-wave meson-baryon potentials with strangeness from Lattice QCD[J]. PoS, 2011, LATTICE2011 : 159. DOI : 10.22323/1.139.0159.

[44] INOUE T, ISHII N, AOKI S, et al. Bound H-dibaryon in Flavor SU(3) Limit of Lattice QCD[J]. Phys. Rev. Lett., 2011, 106 : 162002. DOI : 10.1103/PhysRevLett.106.162002.

[45] KAWANAI T, SASAKI S. Charmonium-nucleon interaction from lattice QCD with a relativistic heavy quark action[J]. PoS, 2010, LATTICE2010 : 156. DOI : 10.22323/1.105.0156.

[46] BEANE S R, OTHERS. Evidence for a Bound H-dibaryon from Lattice QCD[J]. Phys. Rev. Lett., 2011, 106 : 162001. DOI : 10.1103/PhysRevLett.106.162001.

[47] INOUE T, AOKI S, DOI T, et al. Two-Baryon Potentials and H-Dibaryon from 3-flavor Lattice QCD Simulations[J]. Nucl. Phys. A, 2012, 881 : 28–43. DOI : 10.1016/j.nuclphysa.2012.02.008.

[48] EPELBAUM E, KREBS H, MEISSNER U G. Precision nucleon-nucleon potential at fifth order in the chiral expansion[J]. Phys. Rev. Lett., 2015, 115(12) : 122301. DOI : 10.1103/PhysRevLett.115.122301.

[49] REINERT P, KREBS H, EPELBAUM E. Semilocal momentum-space regularized chiral two-nucleon potentials up to fifth order[J]. Eur. Phys. J. A, 2018, 54(5) : 86. DOI : 10.1140/epja/i2018-12516-4.

[50] ENTEM D R, MACHLEIDT R, NOSYK Y. High-quality two-nucleon potentials up to fifth order of the chiral expansion[J]. Phys. Rev. C, 2017, 96(2) : 024004. DOI : 10.1103/PhysRevC.96.024004.

[51] RODRIGUEZ ENTEM D, MACHLEIDT R, NOSYK Y. Nucleon-Nucleon Scattering Up to N^5LO in Chiral Effective Field Theory[J]. Front. in Phys., 2020, 8 : 57. DOI : 10.3389/fphy.2020.00057.

[52] WEINBERG S. Phenomenological lagrangians[J]. Physica A : Statistical Mechanics and its Applications, 1979, 96(1) : 327–340. DOI : 10.1016/0378-4371(79)90223-1.

[53] GASSER J, LEUTWYLER H. Chiral Perturbation Theory to One Loop[J]. Annals Phys., 1984, 158 : 142. DOI : 10.1016/0003-4916(84)90242-2.

[54] GASSER J, LEUTWYLER H. Chiral Perturbation Theory : Expansions in the Mass of the Strange Quark[J]. Nucl. Phys. B, 1985, 250 : 465–516. DOI : 10.1016/0550-3213(85)90492-4.

[55] GASSER J, SAINIO M E, SVARC A. Nucleons with Chiral Loops[J]. Nucl. Phys., 1988, B307 : 779–853. DOI : 10.1016/0550-3213(88)90108-3.

[56] JENKINS E E, MANOHAR A V. Baryon chiral perturbation theory using a heavy fermion Lagrangian[J]. Phys. Lett. B, 1991, 255 : 558–562. DOI : 10.1016/0370-2693(91)90266-S.

[57] WEINBERG S. Nuclear forces from chiral Lagrangians[J]. Phys. Lett. B, 1990, 251 : 288–292. DOI : 10.1016/0370-2693(90)90938-3.

[58] WEINBERG S. Effective chiral Lagrangians for nucleon - pion interactions and nuclear forces[J]. Nucl. Phys. B, 1991, 363 : 3–18. DOI : 10.1016/0550-3213(91)90231-L.

[59] ORDONEZ C, RAY L, VAN KOLCK U. Nucleon-nucleon potential from an effective chiral Lagrangian[J]. Phys. Rev. Lett., 1994, 72 : 1982–1985. DOI : 10.1103/PhysRevLett.72.1982.

[60] ORDONEZ C, RAY L, VAN KOLCK U. The Two nucleon potential from chiral Lagrangians[J]. Phys. Rev. C, 1996, 53 : 2086–2105. DOI : 10.1103/PhysRevC.53.2086.

[61] KAISER N, BROCKMANN R, WEISE W. Peripheral nucleon-nucleon phase shifts and chiral symmetry[J]. Nucl. Phys., 1997, A625 : 758–788. DOI : 10.1016/S0375-9474(97)00586-1.

[62] KAISER N, GERSTENDORFER S, WEISE W. Peripheral NN scattering : Role of delta excitation, correlated two pion and vector meson exchange[J]. Nucl. Phys., 1998, A637 : 395–420. DOI : 10.1016/S0375-9474(98)00234-6.

[63] EPELBAUM E, GLOECKLE W, MEISSNER U G. Nuclear forces from chiral Lagrangians using the method of unitary transformation. 2. The two nucleon system[J]. Nucl. Phys. A, 2000, 671 : 295–331. DOI : 10.1016/S0375-9474(99)00821-0.

[64] ENTEM D R, MACHLEIDT R. Accurate charge dependent nucleon nucleon potential at fourth order of chiral perturbation theory[J]. Phys. Rev. C, 2003, 68 : 041001. DOI : 10.1103/PhysRevC.68.041001.

[65] EPELBAUM E, GLOCKLE W, MEISSNER U G. The Two-nucleon system at next-to-next-to-next-to-leading order[J]. Nucl. Phys., 2005, A747 : 362–424. DOI : 10.1016/j.nuclphysa.2004.09.107.

[66] EPELBAUM E, HAMMER H W, MEISSNER U G. Modern Theory of Nuclear Forces[J]. Rev. Mod. Phys., 2009, 81 : 1773–1825. DOI : 10.1103/RevModPhys.81.1773.

[67] MACHLEIDT R, ENTEM D R. Chiral effective field theory and nuclear forces [J]. Phys. Rept., 2011, 503 : 1–75. DOI : 10.1016/j.physrep.2011.02.001.

[68] ENTEM D R, KAISER N, MACHLEIDT R, et al. Dominant contributions to the nucleon-nucleon interaction at sixth order of chiral perturbation theory [J]. Phys. Rev., 2015, C92(6) : 064001. DOI : 10.1103/PhysRevC.92.064001.

[69] EPELBAUM E, NOGGA A, GLOECKLE W, et al. Three nucleon forces from chiral effective field theory[J]. Phys. Rev. C, 2002, 66 : 064001. DOI : 10.1103/PhysRevC.66.064001.

[70] MELENDEZ J A, FURNSTAHL R J, PHILLIPS D R, et al. Quantifying Correlated Truncation Errors in Effective Field Theory[J]. Phys. Rev. C, 2019, 100(4) : 044001. DOI : 10.1103/PhysRevC.100.044001.

[71] NOGGA A, TIMMERMANS R G E, VAN KOLCK U. Renormalization of one-pion exchange and power counting[J]. Phys. Rev. C, 2005, 72 : 054006. DOI : 10.1103/PhysRevC.72.054006.

[72] BIRSE M C. Power counting with one-pion exchange[J]. Phys. Rev. C, 2006, 74 : 014003. DOI : 10.1103/PhysRevC.74.014003.

[73] VALDERRAMA M P, PHILLIPS D R. Power counting of contact-range currents in effective field theory[J/OL]. Phys. Rev. Lett., 2015, 114 : 082502. https://link.aps.org/doi/10.1103/PhysRevLett.114.082502.

[74] KIEVSKY A, VIVIANI M, GATTOBIGIO M, et al. Implications of efimov physics for the description of three and four nucleons in chiral effective field theory[J/OL]. Phys. Rev. C, 2017, 95 : 024001. https://link.aps.org/doi/10.1103/PhysRevC.95.024001.

[75] REN X L, LI K W, GENG L S, et al. Leading order relativistic chiral nucleon-nucleon interaction[J]. Chin. Phys., 2018, C42(1) : 014103. DOI : 10.1088/1674-1137/42/1/014103.

[76] KREBS H, EPELBAUM E, MEISSNER U G. Nuclear forces with Delta-excitations up to next-to-next-to-leading order. I. Peripheral nucleon-nucleon waves[J]. Eur. Phys. J. A, 2007, 32 : 127–137. DOI : 10.1140/epja/i2007-10372-y.

[77] EPELBAUM E, KREBS H, MEISSNER U G. Isospin-breaking two-nucleon force with explicit Delta-excitations[J]. Phys. Rev. C, 2008, 77 : 034006. DOI : 10.1103/PhysRevC.77.034006.

[78] PIARULLI M, GIRLANDA L, SCHIAVILLA R, et al. Minimally nonlocal nucleon-nucleon potentials with chiral two-pion exchange including Δ resonances[J]. Phys. Rev. C, 2015, 91(2) : 024003. DOI : 10.1103/PhysRevC.91.024003.

[79] EKSTRÖM A, HAGEN G, MORRIS T D, et al. Δ isobars and nuclear saturation[J]. Phys. Rev. C, 2018, 97(2) : 024332. DOI : 10.1103/PhysRevC.97.024332.

[80] STROHMEIER S, KAISER N. Nucleon-Nucleon Scattering with Coupled Nucleon-Delta Channels in Chiral Effective Field Theory[J]. Nucl. Phys. A, 2020, 1002 : 121980. DOI : 10.1016/j.nuclphysa.2020.121980.

[81] NOSYK Y, ENTEM D R, MACHLEIDT R. Nucleon-nucleon potentials from Δ-full chiral effective-field-theory and implications[J]. Phys. Rev. C, 2021, 104(5) : 054001. DOI : 10.1103/PhysRevC.104.054001.

[82] VAN KOLCK U. Few nucleon forces from chiral Lagrangians[J]. Phys. Rev., 1994, C49 : 2932–2941. DOI : 10.1103/PhysRevC.49.2932.

[83] PANDHARIPANDE V R, PHILLIPS D R, VAN KOLCK U. Delta effects in pion-nucleon scattering and the strength of the two-pion-exchange three-nucleon interaction[J]. Phys. Rev. C, 2005, 71 : 064002. DOI : 10.1103/PhysRevC.71.064002.

[84] EPELBAUM E, KREBS H, MEISSNER U G. Delta-excitations and the three-nucleon force[J]. Nucl. Phys. A, 2008, 806 : 65–78. DOI : 10.1016/j.nuclphysa.2008.02.305.

[85] KAISER N. Three-pion exchange nucleon-nucleon potentials with virtual Δ-isobar excitation[J]. Phys. Rev. C, 2015, 92(2) : 024002. DOI : 10.1103/PhysRevC.92.024002.

[86] KREBS H, GASPARYAN A M, EPELBAUM E. Three-nucleon force in chiral EFT with explicit $\Delta(1232)$ degrees of freedom : Longest-range contributions at fourth order[J]. Phys. Rev. C, 2018, 98(1) : 014003. DOI : 10.1103/PhysRevC.98.014003.

[87] XIAO Y, GENG L S, REN X L. Covariant chiral nucleon-nucleon contact Lagrangian up to order $\mathcal{O}(q^4)$[J]. Phys. Rev. C, 2019, 99(2) : 024004. DOI : 10.1103/PhysRevC.99.024004.

[88] XIAO Y, WANG C X, LU J X, et al. Two-pion exchange contributions to the nucleon-nucleon interaction in covariant baryon chiral perturbation theory[J]. Phys. Rev. C, 2020, 102(5) : 054001. DOI : 10.1103/PhysRevC.102.054001.

[89] XIAO Y, GENG L S, VAN KOLCK U. Two-pion exchange contributions to the nucleon-nucleon interaction from the Roper resonance[J]. In preparation, 2022.

[90] XIAO Y, REN X L, LU J X, et al. Octet baryon magnetic moments at next-to-next-to-leading order in covariant chiral perturbation theory[J]. Eur. Phys. J., 2018, C78 : 489. DOI : 10.1140/epjc/s10052-018-5960-4.

[91] LIU M Z, XIAO Y, GENG L S. Magnetic moments of the spin-1/2 doubly charmed baryons in covariant baryon chiral perturbation theory[J]. Phys. Rev. D, 2018, 98(1) : 014040. DOI : 10.1103/PhysRevD.98.014040.

[92] SHI R X, XIAO Y, GENG L S. Magnetic moments of the spin-1/2 singly charmed baryons in covariant baryon chiral perturbation theory[J]. Phys. Rev. D, 2019, 100(5) : 054019. DOI : 10.1103/PhysRevD.100.054019.

[93] BAI Q Q, WANG C X, XIAO Y, et al. Pion-mass dependence of the nucleon-nucleon interaction[J]. Phys. Lett., 2020, B : 135745. DOI : 10.1016/j.physletb.2020.135745.

[94] SONG J, XIAO Y, LIU Z W, et al. $\Lambda_c N$ interaction in leading-order covariant chiral effective field theory[J]. Phys. Rev. C, 2020, 102(6) : 065208. DOI : 10.1103/PhysRevC.102.065208.

[95] WANG C X, LU J X, XIAO Y, et al. Nonperturbative two-pion exchange contributions to the nucleon-nucleon interaction in covariant baryon chiral perturbation theory[J]. Phys. Rev. C, 2022, 105(1) : 014003. DOI : 10.1103/PhysRevC.105.014003.

[96] LU J X, WANG C X, XIAO Y, et al. Accurate Relativistic Chiral Nucleon-Nucleon Interaction up to Next-to-Next-to-Leading Order[J]. Phys. Rev. Lett., 2022, 128(14) : 142002. DOI : 10.1103/PhysRevLett.128.142002.

[97] STEWART I. 8.851 effective field theory[EB/OL]. Massachusetts Institute of Technology : MIT OpenCourseWare, 2013. https://ocw.mit.edu.

[98] BERNARD V, KAISER N, KAMBOR J, et al. Chiral structure of the nucleon[J]. Nucl. Phys. B, 1992, 388 : 315–345. DOI : 10.1016/0550-3213(92)90615-I.

[99] BECHER T, LEUTWYLER H. Baryon chiral perturbation theory in manifestly Lorentz invariant form[J]. Eur. Phys. J., 1999, C9 : 643–671. DOI : 10.1007/PL00021673.

[100] GEGELIA J, JAPARIDZE G. Matching heavy particle approach to relativistic theory[J]. Phys. Rev., 1999, D60 : 114038. DOI : 10.1103/PhysRevD.60.114038.

[101] FUCHS T, GEGELIA J, JAPARIDZE G, et al. Renormalization of relativistic baryon chiral perturbation theory and power counting[J]. Phys. Rev., 2003, D68 : 056005. DOI : 10.1103/PhysRevD.68.056005.

[102] GENG L. Recent developments in SU(3) covariant baryon chiral perturbation theory[J]. Front. Phys. (Beijing), 2013, 8 : 328–348. DOI : 10.1007/s11467-013-0327-7.

[103] ZYLA P A, OTHERS. Review of Particle Physics[J]. PTEP, 2020, 2020(8) : 083C01. DOI : 10.1093/ptep/ptaa104.

[104] ADLER S L. Axial vector vertex in spinor electrodynamics[J]. Phys. Rev., 1969, 177 : 2426–2438. DOI : 10.1103/PhysRev.177.2426.

[105] BELL J S, JACKIW R. A PCAC puzzle : $\pi^0 \to \gamma\gamma$ in the σ model[J]. Nuovo Cim. A, 1969, 60 : 47–61. DOI : 10.1007/BF02823296.

[106] COLEMAN S R, WESS J, ZUMINO B. Structure of phenomenological Lagrangians. 1.[J]. Phys. Rev., 1969, 177 : 2239–2247. DOI : 10.1103/PhysRev.177.2239.

[107] CALLAN C G, Jr., COLEMAN S R, WESS J, et al. Structure of phenomenological Lagrangians. 2.[J]. Phys. Rev., 1969, 177 : 2247–2250. DOI : 10.1103/PhysRev.177.2247.

[108] WEINBERG S. Three body interactions among nucleons and pions[J]. Phys. Lett. B, 1992, 295 : 114–121. DOI : 10.1016/0370-2693(92)90099-P.

[109] FRIAR J L. Dimensional power counting in nuclei[J]. Few Body Syst., 1997, 22 : 161. DOI : 10.1007/s006010050059.

[110] HAMMER H W, KÖNIG S, VAN KOLCK U. Nuclear effective field theory : status and perspectives[J]. Rev. Mod. Phys., 2020, 92(2) : 025004. DOI : 10.1103/RevModPhys.92.025004.

[111] GIRLANDA L, PASTORE S, SCHIAVILLA R, et al. Relativity constraints on the two-nucleon contact interaction[J]. Phys. Rev., 2010, C81 : 034005. DOI : 10.1103/PhysRevC.81.034005.

[112] FETTES N, MEISSNER U G, MOJZIS M, et al. The Chiral effective pion nucleon Lagrangian of order p**4[J]. Annals Phys., 2000, 283 : 273–302. DOI : 10.1006/aphy.2000.6059.

[113] PETSCHAUER S, KAISER N. Relativistic SU(3) chiral baryon-baryon Lagrangian up to order q^2[J]. Nucl. Phys., 2013, A916 : 1–29. DOI : 10.1016/j.nuclphysa.2013.07.010.

[114] GIRLANDA L, VIVIANI M. Relativistic covariance of the 2-nucleon contact interactions[J/OL]. Few-Body Systems, 2011, 49(1) : 51–60. https://doi.org/10.1007/s00601-010-0185-6.

[115] DJUKANOVIC D, GEGELIA J, SCHERER S, et al. N N scattering in higher-derivative formulation of baryon chiral perturbation theory[J]. Few Body Syst., 2007, 41 : 141–155. DOI : 10.1007/s00601-007-0194-2.

[116] CHEN Y H, YAO D L, ZHENG H Q. Analyses of pion-nucleon elastic scattering amplitudes up to $O(p^4)$ in extended-on-mass-shell subtraction scheme [J]. Phys. Rev. D, 2013, 87 : 054019. DOI : 10.1103/PhysRevD.87.054019.

[117] SHTABOVENKO V, MERTIG R, ORELLANA F. FeynCalc 9.3 : New features and improvements[J]. Comput. Phys. Commun., 2020, 256 : 107478. DOI : 10.1016/j.cpc.2020.107478.

[118] SHTABOVENKO V, MERTIG R, ORELLANA F. New Developments in FeynCalc 9.0[J]. Comput. Phys. Commun., 2016, 207 : 432–444. DOI : 10.1016/j.cpc.2016.06.008.

[119] MERTIG R, BOHM M, DENNER A. FEYN CALC : Computer algebraic calculation of Feynman amplitudes[J]. Comput. Phys. Commun., 1991, 64 : 345–359. DOI : 10.1016/0010-4655(91)90130-D.

[120] VAN HAMEREN A, PAPADOPOULOS C G, PITTAU R. Automated one-loop calculations : A Proof of concept[J]. JHEP, 2009, 09 : 106. DOI : 10.1088/1126-6708/2009/09/106.

[121] VAN HAMEREN A. OneLOop : For the evaluation of one-loop scalar functions[J]. Comput. Phys. Commun., 2011, 182 : 2427–2438. DOI : 10.1016/j.cpc.2011.06.011.

[122] LU J X, GENG L S, REN X L, et al. Meson-baryon scattering up to the next-to-next-to-leading order in covariant baryon chiral perturbation theory[J]. Phys. Rev. D, 2019, 99(5) : 054024. DOI : 10.1103/PhysRevD.99.054024.

[123] ERKELENZ K, ALZETTA R, HOLINDE K. Momentum space calculations and helicity formalism in nuclear physics[J]. Nucl. Phys. A, 1971, 176 : 413–432. DOI : 10.1016/0375-9474(71)90279-X.

[124] ERKELENZ K. Current status of the relativistic two nucleon one boson exchange potential[J]. Phys. Rept., 1974, 13 : 191–258. DOI : 10.1016/0370-1573(74)90008-8.

[125] GASSER J, MEISSNER U G. On the phase of epsilon-prime[J]. Phys. Lett. B, 1991, 258 : 219–224. DOI : 10.1016/0370-2693(91)91235-N.

[126] BERNARD V, KAISER N, MEISSNER U G. Aspects of chiral pion - nucleon physics[J]. Nucl. Phys. A, 1997, 615 : 483–500. DOI : 10.1016/S0375-9474(97)00021-3.

[127] ARNDT R A, HYSLOP J S, III, ROPER L D. Nucleon-Nucleon Partial Wave Analysis to 1100-MeV[J]. Phys. Rev. D, 1987, 35 : 128. DOI : 10.1103/PhysRevD.35.128.

[128] LI K W, REN X L, GENG L S, et al. Leading order relativistic hyperon-nucleon interactions in chiral effective field theory[J]. Chin. Phys., 2018, C42(1) : 014105. DOI : 10.1088/1674-1137/42/1/014105.

[129] REN X L, WANG C X, LI K W, et al. Relativistic Chiral Description of the 1 S 0 Nucleon–Nucleon Scattering[J]. Chin. Phys. Lett., 2021, 38(6) : 062101. DOI : 10.1088/0256-307X/38/6/062101.

[130] SONG J, LI K W, GENG L S. Strangeness S=−1 hyperon-nucleon interactions : Chiral effective field theory versus lattice QCD[J]. Phys. Rev. C, 2018, 97(6) : 065201. DOI : 10.1103/PhysRevC.97.065201.

[131] LI K W, HYODO T, GENG L S. Strangeness S=−2 baryon-baryon interactions in relativistic chiral effective field theory[J]. Phys. Rev. C, 2018, 98 (6) : 065203. DOI : 10.1103/PhysRevC.98.065203.

[132] WANG C X, GENG L S, LONG B. Renormalizability of leading order covariant chiral nucleon-nucleon interaction[J]. Chin. Phys. C, 2021, 45(5) : 054101. DOI : 10.1088/1674-1137/abe368.

[133] JENKINS E E, MANOHAR A V. Chiral corrections to the baryon axial currents[J]. Phys. Lett. B, 1991, 259 : 353–358. DOI : 10.1016/0370-2693(91)90840-M.

[134] WEINBERG S. Nonlinear realizations of chiral symmetry[J]. Phys. Rev., 1968, 166 : 1568–1577. DOI : 10.1103/PhysRev.166.1568.

[135] LONG B, VAN KOLCK U. The Role of the Roper in Chiral Perturbation Theory[J]. Nucl. Phys. A, 2011, 870-871 : 72–82. DOI : 10.1016/j.nuclphysa.2011.09.002.

[136] MANOHAR A, GEORGI H. Chiral Quarks and the Nonrelativistic Quark Model[J]. Nucl. Phys. B, 1984, 234 : 189–212. DOI : 10.1016/0550-3213(84)90231-1.

[137] VAN KOLCK U. Naturalness in nuclear effective field theories[J]. Eur. Phys. J. A, 2020, 56(3) : 97. DOI : 10.1140/epja/s10050-020-00092-1.

[138] WEINBERG S. Phenomenological Lagrangians[J]. Physica, 1979, A96(1-2) : 327–340. DOI : 10.1016/0378-4371(79)90223-1.

[139] FRIAR J L. Equivalence of nonstatic two pion exchange nucleon-nucleon potentials[J]. Phys. Rev. C, 1999, 60 : 034002. DOI : 10.1103/PhysRevC.60.034002.

[140] STAPP H P, YPSILANTIS T J, METROPOLIS N. Phase shift analysis of 310-MeV proton proton scattering experiments[J]. Phys. Rev., 1957, 105 : 302–310. DOI : 10.1103/PhysRev.105.302.